



SATURN

MPR - SAT - FE - 70 - 2

JUNE 20, 1970

(NASA-TM-X-64422) SATURN 5 LAUNCH VEHICLE
FLIGHT EVALUATION REPORT: AS-508 APOLLO 13
MISSION (NASA) 242 p

N90-70432

Unclas
00/15 0257075

SATURN V LAUNCH VEHICLE FLIGHT EVALUATION REPORT AS-508 APOLLO 13 MISSION

FF No. 602(C)	(ACCESSION NUMBER)	(THRU)
	242	9-C
	(PAGES)	(CODE)
	TMX-64422	30
	(NASA CR OR TMX OR AD NUMBER)	(CATEGORY)



PREPARED BY
SATURN FLIGHT EVALUATION WORKING GROUP



NATIONAL AERONAUTICS AND SPACE ADMINISTRATION

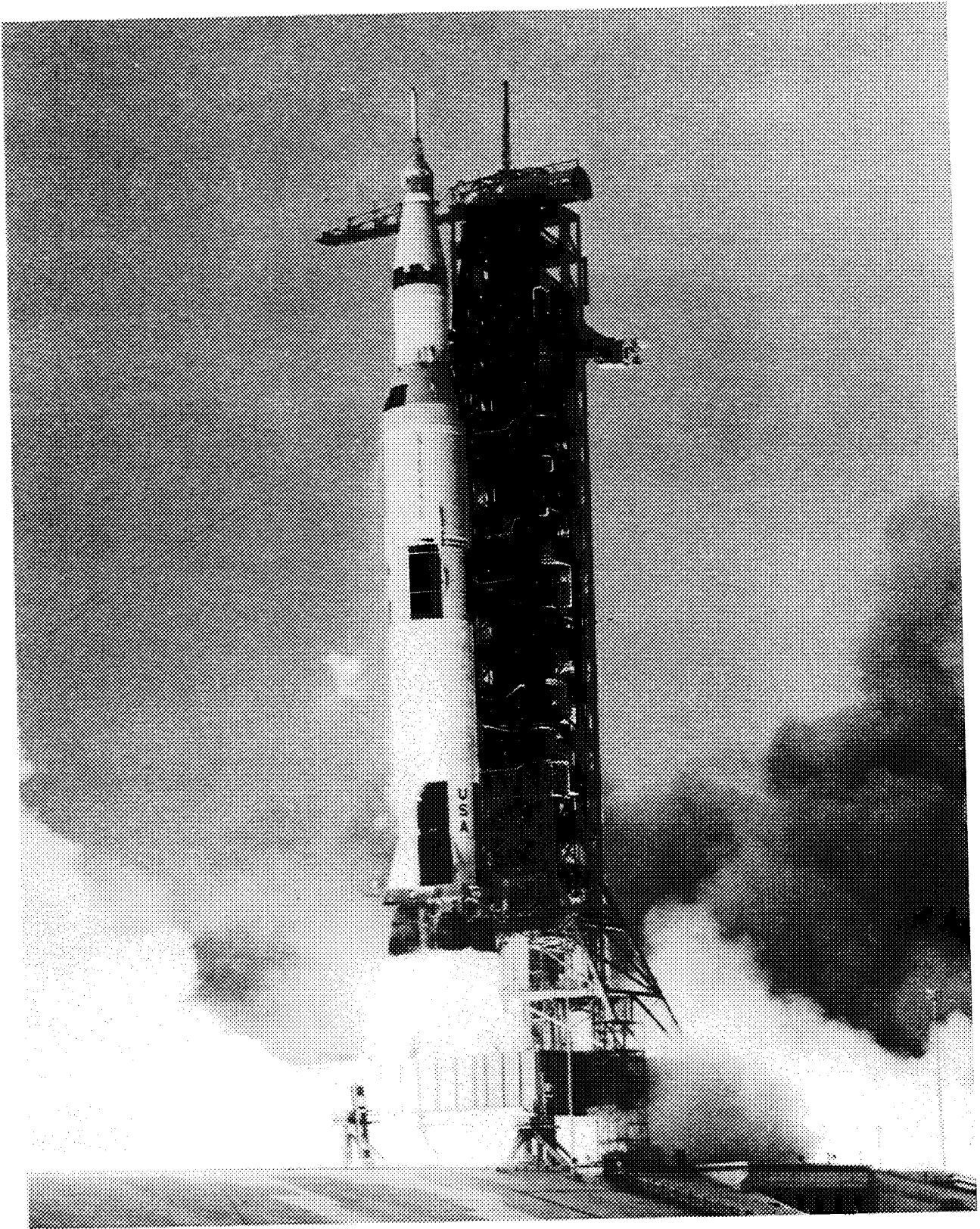
GEORGE C. MARSHALL SPACE FLIGHT CENTER

MPR-SAT-FE-70-2

**SATURN V LAUNCH VEHICLE
FLIGHT EVALUATION REPORT - AS-508
APOLLO 13 MISSION**

PREPARED BY

SATURN FLIGHT EVALUATION WORKING GROUP



AS-508 LAUNCH VEHICLE

MPR-SAT-FE-70-2

SATURN V LAUNCH VEHICLE FLIGHT EVALUATION REPORT - AS-508

APOLLO 13 MISSION

BY

Saturn Flight Evaluation Working Group
George C. Marshall Space Flight Center

ABSTRACT

Saturn V AS-508 (Apollo 13 Mission) was launched at 14:13:00.00 Eastern Standard Time on April 11, 1970, from Kennedy Space Center, Complex 39, Pad A. The vehicle lifted off on schedule on a launch azimuth of 90 degrees east of north and rolled to a flight azimuth of 72.043 degrees east of north. The launch vehicle successfully placed the manned spacecraft in the planned translunar injection coast mode despite a premature S-II center engine cutoff. The S-IVB/IU impacted the lunar surface at 2.5 ± 0.5 degrees south and 27.9 ± 0.1 degrees west at 280,601.0 seconds (77:56:41.0) which was 65.5 ± 7.8 , -4.8 kilometers (35.4 ± 4.2 , -2.6 n mi) from the target of 3 degrees south and 30 degrees west. Impact velocity was 2579 m/s (8461 ft/s).

All Mandatory and Desirable Objectives of this mission for the launch vehicle were accomplished except the precise determination of the lunar impact point. It is expected that this will be accomplished at a later date. No failures, anomalies, or deviations occurred that seriously affected the mission.

Any questions or comments pertaining to the information contained in this report are invited and should be directed to:

Director, George C. Marshall Space Flight Center
Huntsville, Alabama 35812
Attention: Chairman, Saturn Flight Evaluation Working
Group, S&E-CSE-LF (Phone 205-453-2575)

TABLE OF CONTENTS

	Page		Page
TABLE OF CONTENTS	iii	SECTION 4A - LUNAR IMPACT	
LIST OF ILLUSTRATIONS	vi	4A.1 Summary	4A-1
LIST OF TABLES	ix	4A.2 Time Base 8 Maneuvers	4A-1
ACKNOWLEDGEMENT	xi	4A.3 Trajectory Evaluation	4A-5
ABBREVIATIONS	xii	4A.4 Lunar Impact Condition	4A-5
MISSION PLAN	xv	4A.5 Tracking	4A-8
FLIGHT SUMMARY	xviii	SECTION 5 - S-IC PROPULSION	
MISSION OBJECTIVES ACCOMPLISHMENT	xxii	5.1 Summary	5-1
FAILURES, ANOMALIES AND DEVIATIONS	xxiii	5.2 S-IC Ignition Transient Performance	5-1
SECTION 1 - INTRODUCTION		5.3 S-IC Mainstage Performance	5-3
1.1 Purpose	1-1	5.4 S-IC Engine Shutdown Transient Performance	5-7
1.2 Scope	1-1	5.5 S-IC Stage Propellant Management	5-7
SECTION 2 - EVENT TIMES		5.6 S-IC Pressurization Systems	5-8
2.1 Summary of Events	2-1	5.6.1 S-IC Fuel Pressurization System	5-8
2.2 Variable Time and Commanded Switch Selector Events	2-1	5.6.2 S-IC LOX Pressurization System	5-9
SECTION 3 - LAUNCH OPERATIONS		5.7 S-IC Pneumatic Control Pressure System	5-10
3.1 Summary	3-1	5.8 S-IC Purge Systems	5-10
3.2 Prelaunch Milestones	3-1	5.9 S-IC POGO Suppression System	5-10
3.3 Countdown Events	3-1	5.10 S-IC Hydraulic System	5-10
3.4 Propellant Loading	3-1	SECTION 6 - S-II PROPULSION	
3.4.1 RP-1 Loading	3-1	6.1 Summary	6-1
3.4.2 LOX Loading	3-3	6.2 S-II Chilldown and Buildup Transient Performance	6-2
3.4.3 LH ₂ Loading	3-3	6.3 S-II Mainstage Performance	6-3
3.5 Insulation	3-3	6.4 S-II Shutdown Transient Performance	6-6
3.6 Ground Support Equipment	3-4	6.5 S-II Stage Propellant Management	6-8
3.6.1 Ground/Vehicle Interface	3-4	6.6 S-II Pressurization System	6-8
3.6.2 MSFC Furnished Ground Support Equipment	3-4	6.6.1 S-II Fuel Pressurization System	6-8
3.6.3 Camera Coverage	3-5	6.6.2 S-II LOX Pressurization System	6-10
SECTION 4 - TRAJECTORY		6.7 S-II Pneumatic Control Pressure System	6-12
4.1 Summary	4-1	6.8 S-II Helium Injection System	6-14
4.2 Trajectory Evaluation	4-1	6.9 S-II Hydraulic System	6-14
4.2.1 Ascent Phase	4-1		
4.2.2 Parking Orbit Phase	4-8		
4.2.3 Injection Phase	4-10		
4.2.4 Post TLI Phase	4-11		

PRECEDING PAGE BLANK NOT FILMED.

TABLE OF CONTENTS (CONTINUED)

	Page		Page
SECTION 7 - S-IVB PROPULSION			
7.1	Summary	7-1	
7.2	S-IVB Chilldown and Buildup Transient Performance for First Burn	7-2	
7.3	S-IVB Mainstage Performance for First Burn	7-2	
7.4	S-IVB Shutdown Transient Performance for First Burn	7-5	
7.5	S-IVB Parking Orbit Coast Phase Conditioning	7-5	
7.6	S-IVB Chilldown and Restart for Second Burn	7-7	
7.7	S-IVB Mainstage Performance for Second Burn	7-7	
7.8	S-IVB Shutdown Transient Performance for Second Burn	7-11	
7.9	S-IVB Stage Propellant Management	7-11	
7.10	S-IVB Pressurization Systems	7-13	
7.10.1	S-IVB Fuel Pressurization System	7-13	
7.10.2	S-IVB LOX Pressurization System	7-15	
7.11	S-IVB Pneumatic Control System	7-22	
7.12	S-IVB Auxiliary Propulsion System	7-22	
7.13	S-IVB Orbital Safing Operations	7-26	
7.13.1	Fuel Tank Safing	7-27	
7.13.2	LOX Tank Dump and Safing	7-27	
7.13.3	Cold Helium Dump	7-27	
7.13.4	Ambient Helium Dump	7-29	
7.13.5	Stage Pneumatic Control Sphere Safing	7-29	
7.13.6	Engine Start Tank Safing	7-29	
7.13.7	Engine Control Sphere Safing	7-29	
7.14	Hydraulic System	7-29	
SECTION 8 - STRUCTURES			
8.1	Summary	8-1	
8.2	Total Vehicle Structures Evaluation	8-2	
8.2.1	Longitudinal Loads	8-2	
8.2.2	Bending Moments	8-2	
8.2.3	Vehicle Dynamic Characteristics	8-2	
8.3	Vibration Evaluation	8-15	
SECTION 9 - GUIDANCE AND NAVIGATION			
9.1	Summary	9-1	
9.1.1	Performance of the Guidance and Navigation System as Implemented in the Flight Program	9-1	
9.1.2	Instrument Unit Components	9-1	
9.2	Guidance Comparisons	9-1	
9.3	Navigation and Guidance Scheme Evaluation	9-4	
9.4	Guidance System Component Evaluation	9-11	
9.4.1	LVDC and LVDA Performances	9-11	
9.4.2	ST-124M-3 Inertial Platform	9-14	
9.4.3	Ladder Outputs	9-17	
9.4.4	Telemetry Outputs	9-17	
9.4.5	Discrete Outputs	9-17	
9.4.6	Switch Selector Functions	9-17	
SECTION 10 - CONTROL AND SEPARATION			
10.1	Summary	10-1	
10.2	S-IC Control System Evaluation	10-2	
10.3	S-II Control System Evaluation	10-4	
10.4	S-IVB Control System Evaluation	10-7	
10.4.1	Control System Evaluation During First Burn	10-7	
10.4.2	Control System Evaluation During Parking Orbit	10-8	
10.4.3	Control System Evaluation During Second Burn	10-8	
10.4.4	Control System Evaluation After S-IVB Second Burn	10-10	
10.5	Instrument Unit Control Components Evaluation	10-16	
10.6	Separation	10-17	
SECTION 11 - ELECTRICAL NETWORKS AND EMERGENCY DETECTION SYSTEM			
11.1	Summary	11-1	
11.2	S-IC Stage Electrical System	11-1	
11.3	S-II Stage Electrical System	11-2	
11.4	S-IVB Stage Electrical System	11-3	
11.5	Instrument Unit Electrical System	11-8	
11.6	Saturn V Emergency Detection System (EDS)	11-13	
SECTION 12 - VEHICLE PRESSURE AND ACOUSTIC ENVIRONMENT			
12.1	Summary	12-1	
12.2	Base Pressures	12-1	
12.2.1	S-IC Base Pressures	12-1	
12.3	Acoustic Environment	12-5	
12.3.1	External Acoustics	12-5	
SECTION 13 - VEHICLE THERMAL ENVIRONMENT			
13.1	Summary	13-1	
13.2	S-IC Base Heating	13-1	
13.3	S-II Base Heating	13-1	
13.4	Vehicle Aeroheating Thermal Environment	13-6	
SECTION 14 - ENVIRONMENTAL CONTROL SYSTEMS			
14.1	Summary	14-1	
14.2	S-IC Environmental Control	14-1	
14.3	S-II Environmental Control	14-2	
14.4	IU Environmental Control	14-3	
14.4.1	Thermal Conditioning System	14-3	
14.4.2	ST-124M-3 Gas Bearing System	14-7	

TABLE OF CONTENTS (CONTINUED)

	Page
SECTION 15 - DATA SYSTEMS	
15.1 Summary	15-1
15.2 Vehicle Measurements Evaluation	15-1
15.3 Airborne VHF Telemetry Systems Evaluation	15-2
15.4 C-Band Radar System Evaluation	15-2
15.5 Secure Range Safety Command Systems Evaluation	15-6
15.6 Command and Communication System Evaluation	15-8
15.7 Ground Engineering Cameras	15-8
SECTION 16 - MASS CHARACTERISTICS	
16.1 Summary	16-1
16.2 Mass Evaluation	16-1
SECTION 17 - SPACECRAFT SUMMARY	
17-1	
APPENDIX A - ATMOSPHERE	
A.1 Summary	A-1
A.2 General Atmospheric Conditions at Launch Time	A-1
A.3 Surface Observations at Launch Time	A-1
A.4 Upper Air Measurements	A-1
A.4.1 Wind Speed	A-3
A.4.2 Wind Direction	A-6
A.4.3 Pitch Wind Component	A-6
A.4.4 Yaw Wind Component	A-6
A.4.5 Component Wind Shears	A-6
A.4.6 Extreme Wind Data in the High Dynamic Region	A-6
A.5 Thermodynamic Data	A-6
A.5.1 Temperature	A-6
A.5.2 Atmospheric Pressure	A-15
A.5.3 Atmospheric Density	A-15
A.5.4 Optical Index of Refraction	A-15
A.6 Comparison of Selected Atmospheric Data for Saturn V Launches	A-15
APPENDIX B - AS-508 SIGNIFICANT CONFIGURATION CHANGES	
B.1 Introduction	B-1

LIST OF ILLUSTRATIONS

Figure	Page	Figure	Page
2-1	Range Time to Vehicle Time Conversion	2-2	
4-1	Ascent Trajectory Position Comparison	4-2	
4-2	Ascent Trajectory Space-Fixed Velocity and Flight Path Angle Comparisons	4-3	
4-3	Ascent Trajectory Acceleration Comparison	4-3	
4-4	Dynamic Pressure and Mach Number Comparisons	4-4	
4-5	Ground Track	4-9	
4-6	Injection Phase Space-Fixed Velocity and Flight Path Angle Comparisons	4-10	
4-7	Injection Phase Acceleration Comparison	4-11	
4A-1	S-IVB/IU Unscheduled Velocity Change	4A-3	
4A-2	Accumulated Longitudinal Velocity Change During Time Base 8	4A-4	
4A-3	Lunar Impact Trajectory Radius and Space-Fixed Velocity Profiles	4A-6	
4A-4	Comparison of Projected Lunar Impact Points	4A-7	
4A-5	Summary of CCS Tracking Data Used for Post-TLI Orbit Determination	4A-10	
5-1	S-IC LOX Start Box Requirements	5-2	
5-2	S-IC Engines Thrust Buildup	5-3	
5-3	S-IC Stage Propulsion Performance	5-4	
5-4	F-1 LOX Pump Bearing Jet Pressure, Engine No. 2	5-6	
5-5	S-IC Stage Fuel Ullage Pressure	5-8	
5-6	S-IC Stage LOX Tank Ullage Pressure	5-9	
6-1	S-II Engine Start Tank Performance	6-2	
6-2	S-II Engine Pump Inlet Start Requirements	6-4	
6-3	S-II Steady State Operation	6-5	
6-4	S-II Fuel Tank Ullage Pressure	6-9	
6-5	S-II Fuel Pump Inlet Conditions	6-11	
6-6	S-II LOX Tank Ullage Pressure	6-12	
6-7	S-II LOX Pump Inlet Conditions	6-13	
7-1	S-IVB Start Box and Run Requirements - First Burn	7-3	
7-2	S-IVB Steady State Performance - First Burn	7-4	
7-3	S-IVB CVS Performance - Coast Phase	7-6	
7-4	S-IVB Ullage Conditions During Repressurization Using O ₂ /H ₂ Burner	7-8	
7-5	S-IVB O ₂ /H ₂ Burner Thrust and Pressurant Flowrates	7-9	
7-6	S-IVB Start Box and Run Requirements - Second Burn	7-10	
7-7	S-IVB Steady State Performance - Second Burn	7-12	
7-8	S-IVB LH ₂ Ullage Pressure - First Burn and Parking Orbit	7-14	
7-9	S-IVB LH ₂ Ullage Pressure - Second Burn and Translunar Coast	7-15	
7-10	S-IVB Fuel Pump Inlet Conditions - First Burn	7-16	
7-11	S-IVB Fuel Pump Inlet Conditions - Second Burn	7-17	
7-12	S-IVB LOX Tank Ullage Pressure - First Burn and Parking Orbit	7-18	
7-13	S-IVB LOX Tank Ullage Pressure - Second Burn and Translunar Coast	7-19	
7-14	S-IVB LOX Pump Inlet Conditions - First Burn	7-20	
7-15	S-IVB LOX Pump Inlet Conditions - Second Burn	7-21	
7-16	S-IVB Cold Helium Supply History	7-23	
7-17	APS Helium Bottle Temperature and Regulator Outlet Pressure	7-25	
7-18	S-IVB LOX Dump and Orbital Safing Sequence	7-26	
7-19	S-IVB LOX Dump Parameter Histories	7-28	
8-1	Longitudinal Acceleration at CM and IU During Thrust Buildup and Launch	8-3	
8-2	Longitudinal Load at Time of Maximum Bending Moment, CECO and OECO	8-3	

LIST OF ILLUSTRATIONS (CONTINUED)

Figure	Page	Figure	Page
8-3	Maximum Bending Moment Near Max Q	8-4	
8-4	Comparison of Longitudinal Responses During S-IC Boost	8-5	
8-5	Longitudinal Acceleration at CM and IU at S-IC CECO and OEEO	8-5	
8-6	Comparison of S-II Engine No. 5 Thrust Pad Acceleration With Previous Flights	8-6	
8-7	Comparison of S-II Engine No. 1 Thrust Pad Acceleration With Previous Flights	8-6	
8-8	S-II Pre-CECO Thrust Chamber Pressure Characteristics	8-7	
8-9	Comparison of S-II LOX Sump Acceleration With Previous Flights	8-7	
8-10	S-II Stage Center Engine LOX Feed System	8-9	
8-11	Center Engine LOX Pump Inlet Pressure Shift and Beam Vibration	8-9	
8-12	Center Engine Gain During S-II Oscillations	8-10	
8-13	S-II LOX Ullage Pressure	8-10	
8-14	Comparison of AS-507/AS-508 S-II Engine No. 5 LOX Line Characteristics	8-11	
8-15	S-II Engine Inboard/Outboard Power Ratio	8-11	
8-16	AS-508/AS-507 Longitudinal Acceleration Response Comparison During S-II Oscillations	8-13	
8-17	AS-508/AS-507 Acceleration and Pressure Characteristics From S-II CECO to OEEO (8 to 14 Bandpass Filter)	8-14	
8-18	S-IVB First Burn Spectral Analyses	8-16	
8-19	S-IVB Second Burn Spectral Analyses	8-16	
8-20	S-IVB Aft Interstage Skin and Stringer Vibration	8-17	
9-1	Trajectory and ST-124M-3 Platform Velocity Comparison Boost-to-EPO (Trajectory Minus Guidance)	9-2	
9-2	Trajectory and ST-124M-3 Platform Velocity Comparison Second S-IVB Burn	9-3	
9-3	LH ₂ Continuous Vent Thrust During Parking Orbit	9-8	
9-4	Attitude Commands During Boost to EPO	9-9	
9-5	Attitude Commands During S-IVB Second Burn	9-10	
9-6	Crossrange Velocity Measured by the ST-124M-3 Inertial Platform	9-15	
9-7	ST-124M-3 Accelerometer Pickoff	9-15	
10-1	Pitch and Yaw Plane Dynamics During S-IC Burn	10-3	
10-2	Angle-of-Attack During S-IC Burn	10-5	
10-3	Pitch and Yaw Plane Attitude Errors During S-II Burn	10-6	
10-4	Pitch and Yaw Attitude Errors During S-IVB First Burn	10-7	
10-5	Pitch Attitude Error During Parking Orbit	10-9	
10-6	Pitch and Yaw Attitude Errors During S-IVB Second Burn	10-9	
10-7	Pitch Attitude Error During Translunar Coast	10-11	
10-8	Yaw Rate Gyro Switch	10-14	
10-9	Pitch and Yaw Control System Response to Loss of Attitude Reference	10-15	
11-1	S-IVB Stage Forward No. 1 Battery Voltage and Current	11-4	
11-2	S-IVB Stage Forward No. 2 Battery Voltage and Current	11-5	
11-3	S-IVB Stage Aft No. 1 Battery Voltage and Current	11-6	
11-4	S-IVB Stage Aft No. 2 Battery Voltage and Current	11-7	
11-5	IU Battery 6D10 Voltage, Current and Temperature	11-9	
11-6	IU Battery 6D20 Voltage, Current and Temperature	11-10	
11-7	IU Battery 6D30 Voltage, Current and Temperature	11-11	
11-8	IU Battery 6D40 Voltage, Current and Temperature	11-12	
12-1	S-IC Base Heat Shield Differential Pressure	12-2	
12-2	S-II Base Heat Shield Forward Face Pressure	12-3	
12-3	S-II Thrust Cone Pressure	12-3	
12-4	S-II Heat Shield Aft Face Pressure	12-4	
12-5	AS-508 Acoustic Instrumentation	12-6	
12-6	External Overall Sound Pressure Level At Liftoff	12-6	
12-7	Vehicle External Overall Fluctuating Pressure Level	12-7	
12-8	Vehicle External Fluctuating Pressure Spectral Densities	12-9	
13-1	S-IC Base Heat Shield Total Heating Rate	13-2	

LIST OF ILLUSTRATIONS (CONTINUED)

Figure		Page
13-2	S-IC Base Gas Temperature	13-3
13-3	S-IC Ambient Gas Temperature Under Engine Cocoon	13-4
13-4	S-II Heat Shield Aft Heat Rate	13-5
13-5	S-II Heat Shield Recovery Temperature	13-5
13-6	S-II Heat Shield Aft Radiation Heat Rate	13-7
13-7	Forward Location of Separated Flow on S-IC Stage	13-7
14-1	S-IC Aft Compartment Temperature Near Battery 12K10	14-2
14-2	IU TCS Coolant Control Parameters	14-3
14-3	IU Sublimator Performance During Ascent	14-4
14-4	IU TCS Hydraulic Performance	14-5
14-5	IU TCS GN ₂ Sphere Pressure (D025-601)	14-5
14-6	Selected IU Component Temperatures	14-6
14-7	Comparison of AS-507 and AS-508 IU Temperatures	14-7
14-8	IU Inertial Platform GN ₂ Pressures	14-8
14-9	IU GBS GN ₂ Sphere Pressure (D010-603)	14-9
15-1	VHF Telemetry Coverage Summary	15-5
15-2	C-Band Radar Coverage Summary	15-7
15-3	CCS Coverage Summary	15-10
A-1	Surface Weather Map Approximately 7 Hours Before Launch of AS-508	A-2
A-2	500 Millibar Map Approximately 7 Hours Before Launch of AS-508	A-3
A-3	Scalar Wind Speed at Launch Time of AS-508	A-5
A-4	Wind Direction at Launch Time of AS-508	A-7
A-5	Pitch Wind Velocity Component (W _x) at Launch Time of AS-508	A-8
A-6	Yaw Wind Velocity Component (W _z) at Launch Time of AS-508	A-9
A-7	Pitch (S _x) and Yaw (S _z) Component Wind Shears at Launch Time of AS-508	A-10
A-8	Relative Deviation of Temperature and Pressure From the PRA-63 Reference Atmosphere, AS-508	A-13
A-9	Relative Deviation of Density and Absolute Deviation of the Index of Refraction From the PRA-63 Reference Atmosphere, AS-508	A-14

LIST OF TABLES (CONTINUED)

Table		Page
16-4	Total Vehicle Mass, S-II Burn Phase (Pounds)	16-4
16-5	Total Vehicle Mass, S-IVB First Burn Phase (Kilograms)	16-5
16-6	Total Vehicle Mass, S-IVB First Burn Phase (Pounds)	16-5
16-7	Total Vehicle Mass, S-IVB Second Burn Phase (Kilograms)	16-6
16-8	Total Vehicle Mass, S-IVB Second Burn Phase (Pounds)	16-6
16-9	Flight Sequence Mass Summary	16-7
16-10	Mass Characteristics Comparison	16-9
A-1	Surface Observations at AS-508 Launch Time	A-2
A-2	Solar Radiation at AS-508 Launch Time, Launch Pad 39A	A-4
A-3	Systems Used to Measure Upper Air Wind Data for AS-508	A-4
A-4	Maximum Wind Speed in High Dynamic Pressure Region for Apollo/Saturn 501 through Apollo/Saturn 508 Vehicles	A-11
A-5	Extreme Wind Shear Values in the High Dynamic Pressure Region for Apollo/Saturn 501 through Apollo/Saturn 508 Vehicles	A-12
A-6	Selected Atmospheric Observations for Apollo/Saturn 501 through Apollo/Saturn 508 Vehicle Launches at Kennedy Space Center, Florida	A-15
B-1	S-IC Significant Configuration Changes	B-1
B-2	S-II Significant Configuration Changes	B-2
B-3	S-IVB Significant Configuration Changes	B-2
B-4	IU Significant Configuration Changes	B-3

ACKNOWLEDGEMENT

This report is published by the Saturn Flight Evaluation Working Group, composed of representatives of Marshall Space Flight Center, John F. Kennedy Space Center, and MSFC's prime contractors, and in cooperation with the Manned Spacecraft Center. Significant contributions to the evaluation have been made by:

George C. Marshall Space Flight Center

Science and Engineering

Central Systems Engineering
Aero-Astroynamics Laboratory
Astrionics Laboratory
Computation Laboratory
Astronautics Laboratory

Program Management

John F. Kennedy Space Center

Manned Spacecraft Center

The Boeing Company

McDonnell Douglas Astronautics Company

International Business Machines Company

North American Rockwell/Space Division

North American Rockwell/Rocketdyne Division

ABBREVIATIONS

ACS	Alternating Current Power Supply	ECS	Environmental Control System
AOS	Acquisition of Signal	EDS	Emergency Detection System
APS	Auxiliary Propulsion System	EMR	Engine Mixture Ratio
ARIA	Apollo Range Instrument Aircraft	EPO	Earth Parking Orbit
ASC	Accelerometer Signal Conditioner	ESC	Engine Start Command
BDA	Bermuda	EST	Eastern Standard Time
CCS	Command and Communications System	ETW	Error Time Word
CDDT	Countdown Demonstration Test	EVA	Extra-Vehicular Activity
CECO	Center Engine Cutoff	FCC	Flight Control Computer
CG	Center of Gravity	FM/FM	Frequency Modulation/ Frequency Modulation
CM	Command Module	FRT	Flight Readiness Test
CNV	Cape Kennedy	GBS	Gas Bearing System
CRO	Carnarvon	GFCV	GOX Flow Control Valve
CSM	Command and Service Module	GDS	Goldstone
CVS	Continuous Vent System	GDSX	Goldstone Wing Station
CYI	Grand Canary Island	GG	Gas Generator
DEE	Digital Events Evaluator	GOX	Gaseous Oxygen
DO	Desirable Objective	GRR	Guidance Reference Release
DTS	Data Transmission System	GSE	Ground Support Equipment
EBW	Exploding Bridge Wire	GSCU	Ground Support Cooling Unit
ECO	Engine Cutoff	GWM	Guam
ECP	Engineering Change Proposal	GYM	Guaymas
		HAW	Hawaii
		HDA	Holddown Arm
		HFCV	Helium Flow Control Valve

ABBREVIATIONS (CONTINUED)

HSK	Honeysuckle Creek	MSFN	Manned Space Flight Network
HSKX	Honeysuckle Creek Wing Station	MSS	Mobile Service Structure
IGM	Iterative Guidance Mode	MTF	Mississippi Test Facility
IMU	Inertial Measurement Unit	M/W	Methanol Water
IU	Instrument Unit	NPSP	Net Positive Suction Pressure
KSC	Kennedy Space Center	NPV	Nonpropulsive Vent
LET	Launch Escape Tower	NASA	National Aeronautics and Space Administration
LH ₂	Liquid Hydrogen	OAT	Overall Test
LM	Lunar Module	OCP	Orbital Correction Program
LOI	Lunar Orbit Insertion	OECO	Outboard Engine Cutoff
LOS	Loss of Signal	OMPT	Operational Mass Point Trajectory
LOX	Liquid Oxygen	OT	Operational Trajectory
LV	Launch Vehicle	PAFB	Patrick Air Force Base
LVDA	Launch Vehicle Data Adapter	PCM	Pulse Code Modulation
LVDC	Launch Vehicle Digital Computer	PCM/ FM	Pulse Code Modulation/ Frequency Modulation
LVGSE	Launch Vehicle Ground Support Equipment	PEA	Platform Electronics Assembly
MAD	Madrid	POI	Parking Orbit Insertion
MADX	Madrid Wing Station	PMR	Programed Mixture Ratio
MCC-H	Mission Control Center - Houston	PRA	Patrick Reference Atmosphere
MILA	Merritt Island Launch Area	PTCS	Propellant Tanking Control System
ML	Mobile Launcher	PU	Propellant Utilization
MMH	Monomethyl Hydrazine	RF	Radiofrequency
MO	Mandatory Objective	RFI	Radiofrequency Interference
MOV	Main Oxidizer Valve	RMS	Root Mean Square
MR	Mixture Ratio	RP-1	Designation for S-IC Stage Fuel (kerosene)
MSC	Manned Spacecraft Center		
MSFC	Marshall Space Flight Center		

ABBREVIATIONS (CONTINUED)

SA	Service Arm
SC	Spacecraft
SCFM	Standard Cubic Feet per Minute
SLA	Spacecraft/LM Adapter
SM	Service Module
SPS	Service Propulsion System
SRSCS	Secure Range Safety Command System
SS/FM	Single Sideband/Frequency Modulation
STDV	Start Tank Discharge Valve
SV	Space Vehicle
T_1	Time Base 1
TCS	Thermal Conditioning System
TD&E	Transposition, Docking and Ejection
TEI	Transearth Injection
TEX	Corpus Christi (Texas)
TLI	Translunar Injection
TMR	Triple Module Redundant
TSM	Tail Service Mast
TVC	Thrust Vector Control
UCR	Unsatisfactory Condition Report
USB	Unified S-Band
UT	Universal Time
VA	Volt Amperes
VAN	Vanguard (ship)
VHF	Very High Frequency

MISSION PLAN

The AS-508 flight (Apollo 13 Mission) is the eighth flight in the Apollo/Saturn V flight program, the third lunar landing mission and the first landing planned for the lunar highlands. The primary mission objectives are: a) Perform selenological inspection, survey, and sampling of materials in a preselected region of the Fra Mauro formation; b) deploy and activate the Apollo Lunar Surface Experiments Package (ALSEP III); c) develop man's capability to work in the lunar environment; and d) obtain photographs of candidate exploration sites. The crew consists of James A. Lovell (Mission Commander), John L. Swigert, Jr. (Command Module Pilot), and Fred W. Haise, Jr. (Lunar Module Pilot).

The AS-508 launch vehicle is composed of the S-IC-8, S-II-8, and S-IVB-508 stages, and Instrument Unit-508. The Spacecraft (SC) consists of Spacecraft/Lunar Module Adapter (SLA)-16, Command and Service Module (CSM)-109, and Lunar Module (LM)-7.

Vehicle launch from Complex 39A at Kennedy Space Center (KSC) is along a 90 degree azimuth with a roll to a flight azimuth of approximately 72 degrees measured east of true north. Vehicle mass at ignition is 6,505,746 lbm.

The S-IC stage powered flight is approximately 164 seconds; the S-II stage provides powered flight for approximately 392 seconds. Following S-IVB burn (approximately 144 seconds duration), the S-IVB/IU/SLA/LM/CSM is inserted into a circular 100 n mi altitude (referenced to the earth equatorial radius) Earth Parking Orbit (EPO). Vehicle mass at orbit insertion is 300,263 lbm.

At approximately 10 seconds after EPO insertion, the vehicle is aligned with the local horizontal. Continuous hydrogen venting is initiated shortly after EPO insertion and the Launch Vehicle (LV) and CSM systems are checked in preparation for the Translunar Injection (TLI) burn. During the second or third revolution in EPO, the S-IVB stage is restarted and burns for approximately 356 seconds. This burn injects the S-IVB/IU/SLA/LM/CSM into a free-return, translunar trajectory.

Within 15 minutes after TLI, the vehicle initiates an inertial attitude hold for CSM separation, docking and LM ejection. Following the attitude freeze, the CSM separates from the LV and the SLA panels are jettisoned. The CSM then transposes and docks to the LM. After docking, the CSM/LM is spring ejected from the S-IVB/IU. Following separation of the combined CSM/LM from the S-IVB/IU, the S-IVB/IU will perform a yaw maneuver and an 80 second burn of the S-IVB Auxiliary Propulsion System (APS) ullage engines to propel the S-IVB/IU a safe distance away from the spacecraft. Subsequent to the completion of the S-IVB/IU evasive maneuver, the S-IVB/IU is placed on a trajectory such that it will impact the lunar surface in the vicinity of the Apollo 12 landing site. The impact trajectory is achieved by propulsive venting of liquid hydrogen (LH₂), dumping of liquid oxygen (LOX) and by firing the APS engines. The S-IVB/IU impact will be recorded by the seismograph deployed during the Apollo 12 mission. S-IVB/IU lunar impact is predicted at approximately 77 hours 45 minutes after launch.

During the three day translunar coast, the astronauts will perform star-earth landmark sightings, Inertial Measurement Unit (IMU) alignments, general lunar navigation procedures and possibly four midcourse corrections. One of these maneuvers will transfer the SC into a low-periselenium non-free-return translunar trajectory at approximately 28 hours after TLI. At approximately 77 hours and 25 minutes, a Service Propulsion System (SPS), Lunar Orbit Insertion (LOI) burn of approximately 356 seconds inserts the CSM/LM into a 59 by 170 n mi altitude parking orbit.

Approximately two revolutions after LOI, a 23.1-second SPS burn will adjust the orbit into a 9 by 59 n mi altitude. The LM is entered by astronauts Lovell and Haise and checkout is accomplished. During the twelfth revolution in orbit at 59 hours, the LM separates from the CSM and prepares for the lunar descent. The LM descent propulsion system is used to brake the LM into the proper landing trajectory and maneuver the LM during descent to the lunar surface.

Following lunar landing, two 4.0 hour Extravehicular Activity (EVA) time periods are scheduled during which the astronauts will explore the lunar surface, examine the LM exterior, photograph the lunar terrain, and deploy scientific instruments. The total stay time on the lunar surface is open-ended, with a planned maximum of 35 hours, depending upon the outcome of current lunar surface operations planning and of real-time operational decisions. After the EVA, the astronauts prepare the LM ascent propulsion system for lunar ascent.

The CSM performs a plane change approximately 24 hours before lunar ascent. At approximately 137 hours and 16 minutes, the ascent stage inserts the LM into a 9 by 44 n mi altitude lunar orbit, and rendezvous and docks with the CSM. Following docking, equipment transfer and

decontamination procedures, the LM ascent stage is jettisoned and targeted to impact the lunar surface between Apollo 12 and Apollo 13 landing sites. Seismometer readings will be provided from both sites. Following LM ascent stage deorbit burn, the CSM performs a plane change to photograph future landing sites. Photographing and landmark tracking will be performed during revolutions 40 through 44. Transearth Injection (TEI) is accomplished at the end of revolution 46 at approximately 167 hours and 29 minutes with a 135-second SPS burn.

During the 73-hour transearth coast, the astronauts will perform navigation procedures, star-earth-moon sightings and possibly three midcourse corrections. The Service Module (SM) will separate from the Command Module (CM) 15 minutes before reentry. Splashdown will occur in the Pacific Ocean approximately 241 hours and 3 minutes after liftoff.

After the recovery operations, a biological quarantine is imposed on the crew and CM. An incubation period of 18 days from splashdown (21 days from lunar ascent) is required for the astronauts. The hardware incubation period is the time required to analyze certain lunar samples.

FLIGHT SUMMARY

The sixth manned Saturn V Apollo space vehicle, AS-508 (Apollo 13 Mission) was launched at 14:13:00 Eastern Standard Time on April 11, 1970 from Kennedy Space Center, Complex 39, Pad A. Except for high amplitude, low frequency oscillations which resulted in premature S-II Center Engine Cutoff (CECO), the basic performance of the launch vehicle was satisfactory. The high amplitude oscillations were not transmitted above the S-II stage. Despite the anomaly, this eighth launch of the Saturn V/Apollo successfully performed all the mandatory and desirable launch vehicle objectives. All aspects of the S-IVB/IU lunar impact objective were accomplished successfully except for the precise determination of the impact point. It is expected that the final impact solution will satisfy the mission objective.

The launch countdown support systems performed well. However, several systems experienced component failures and malfunctions that required corrective action. All repairs were accomplished in time to maintain the launch schedule and no unscheduled holds were experienced. Damage to the pad, mobile launcher, and support equipment was minor.

The vehicle was launched on an azimuth 90 degrees east of north. A roll maneuver at 12.6 seconds placed the vehicle on a flight azimuth of 72.043 degrees east of north. Trajectory parameters were close to nominal during S-IC stage and S-II stage burns until early shutdown of the S-II center engine. The premature S-II CECO caused considerable deviations for certain launch vehicle trajectory parameters. Despite these deviations, near nominal trajectory parameters were achieved at parking orbit insertion and at Translunar Injection (TLI) although the events occurred 44.0 and 13.6 seconds later than predicted, respectively at a heading angle 1.230 degrees later than nominal. Command Service Module (CSM) separation occurred 38.9 seconds later than predicted, causing some deviation in trajectory parameters at this time. The earth impact locations for the S-IC and S-II stages were determined by a theoretical free-flight simulation. The analyses for the S-IC and S-II stages showed the surface range for the impact points to be 7.6 kilometers (4.1 n mi) and 8.6 kilometers (4.6 n mi) greater than nominal, respectively.

At 280,599.7 \pm 0.1 seconds (77:56:39.7) vehicle time the S-IVB/IU impacted the lunar surface at approximately 2.5 \pm 0.5 degrees south latitude and 27.9 \pm 0.1 degrees west longitude, which is approximately 65.5 \pm 7.8, -4.8 kilometers (35.4 \pm 4.2, -2.6 n mi) from the target of 3 degrees south latitude and 30 degrees west longitude. Impact velocity was 2579 m/s (8461 ft/s). The mission objectives were to maneuver the S-IVB/IU such that it would have at least a 50 percent probability of impacting the lunar surface within 350 kilometers (189 n mi) of the target, and to determine the actual impact point within 5 kilometers (2.7 n mi) and the time of impact within 1 second. Preliminary results of the seismic experiment indicate that the S-IVB/IU impact signal was 20 to 30 times greater in amplitude and four times longer in duration than the Apollo 12 Lunar Module (LM) impact.

All S-IC propulsion systems performed satisfactorily, as did the hydraulic system. Stage thrust, specific impulse, total propellant consumption rate, and total consumed mixture ratio (averaged from liftoff to OECO) were 0.26, 0.20, 0.06, and 0.24 percent higher than predicted, respectively. Total propellant consumption from holddown arm release to Outboard Engine Cutoff (OECO) was low by 0.06 percent. CECO was commanded by the IU as planned. OECO, initiated by the LOX low level sensors, occurred 0.4 second earlier than predicted.

The S-II propulsion system performance was satisfactory throughout flight except for the premature CECO which occurred 132.4 seconds early due to high amplitude, low frequency oscillations in the propulsion/structural system. OECO occurred 34.5 seconds late as a result of the early CECO. Stage thrust, propellant flowrate, and propellant mixture ratio were 0.19, 0.25, and 0.18 percent lower than predicted, respectively, at the standard time slice 62 seconds after engine start. The specific impulse at this time slice was 0.09 percent higher than predicted. The IU command to shift Engine Mixture Ratio from high to low upon attainment of a pre-programmed stage velocity increase occurred 32.2 seconds later than predicted primarily because of the early CECO. The engine servicing, recirculation, helium injection, valve actuation, and LOX and LH₂ tank pressurization systems all performed satisfactorily. S-II hydraulic system performance was normal throughout flight.

The J-2 engine operated satisfactorily throughout the operational phase of S-IVB first and second burns with normal engine shutdowns. S-IVB first burn duration was 9.3 seconds longer than predicted, primarily due to the performance of lower stages. The engine performance during first burn, as determined from standard altitude reconstruction analysis, differed from the predicted by +0.29 percent for thrust while the specific impulse was near that predicted. The Continuous Vent System (CVS) adequately regulated LH₂ tank ullage pressure at an average level of 19.3 psia during orbit and the Oxygen/Hydrogen burner satisfactorily achieved LH₂ and LOX tank repressurization for restart. Engine restart conditions

were within specified limits. The restart with the propellant utilization valve fully open was successful. S-IVB second burn duration was 4.9 seconds less than predicted. The engine performance during second burn, as determined from the standard altitude reconstruction analysis, differed from the predicted by -0.24 percent for thrust and 0.09 percent for specific impulse. Subsequent to second burn the stage propellant tanks and helium spheres were safed satisfactorily. Sufficient impulse was derived from LOX dump, LH₂ CVS operation and APS ullage burn to achieve a successful lunar impact. An additional velocity change of 7 to 10 ft/s was experienced during the unanticipated APS firings at 70,150 seconds (19:29:10). The S-IVB hydraulic system performance was satisfactory throughout the mission.

The structural loads experienced during S-IC boost phase were well below design values. The maximum Q region bending moment was 69×10^6 lbf-in. at the S-IC LOX tank, which was 25 percent of design value. Thrust cut-off transients experienced by AS-508 were similar to those of previous flights. The maximum dynamic transient at the IU resulting from S-IC CECO was ± 0.20 g longitudinal. At OECO a maximum dynamic longitudinal acceleration of ± 0.28 g and ± 0.85 g was experienced at the IU and Command Module (CM), respectively. The order of magnitude of the thrust cutoff responses are considered normal. During S-IC stage boost phase, 4 to 5 hertz oscillations were detected beginning at 100 seconds. The maximum amplitude measured in the IU at 125 seconds was ± 0.04 g. Oscillations in the 4 to 5 hertz range have been observed on previous flights and are considered to be normal vehicle response to flight environment. AS-508 experienced low frequency (14 to 16 hertz) POGO oscillations during S-II stage boost. Three distinct periods of structural/propulsion coupled oscillations exhibited peaks at 180, 250, and 330 seconds. The third period of oscillations resulted in LOX pump discharge pressure variations of sufficient magnitude to activate the center engine thrust OK pressure switches and shut down the engine 132.4 seconds early. All oscillations decayed to a normal level following CECO. Analysis of flight data indicates that no structural failure occurred as a result of the oscillations. Flight measurements also show that the oscillations were confined to the S-II stage and were not transmitted up the vehicle. The structural loads experienced during the S-IVB stage burn were well below design values. During first burn the S-IVB experienced low amplitude 18 to 20 hertz oscillations. The amplitudes measured on the gimbal block were comparable to previous flights and well within the expected range of values. Similarly, S-IVB second burn produced intermittent low amplitude oscillations in the 12 to 14 hertz frequency range which peaked near second burn cutoff. Three vibration measurements were made on the S-IVB aft interstage. The maximum vibration levels measured occurred at liftoff and during the Mach 1 to Max Q flight period.

The guidance and navigation system performed satisfactorily resulting in accurate parking orbit and TLI parameters. Guidance parameters were modified to compensate for the early S-II CECO, and the S-IVB burn was lengthened to compensate for the additional gravity losses during S-II burn. The Launch Vehicle Digital Computer (LVDC), the Launch Vehicle

Data Adapter (LVDA), and the ST-124M-3 inertial platform functioned satisfactorily. Crossrange velocity, as measured by the inertial platform, exhibited a negative shift of approximately 0.65 m/s (2.13 ft/s) at approximately 3.4 seconds, introducing a 0.5 m/s (1.6 ft/s) velocity error. The velocity shift probably resulted from the accelerometer head momentarily contacting a mechanical stop due to the high vibration levels after liftoff. The effect on navigation accuracy was negligible. A similar crossrange velocity shift was exhibited on AS-506. At 68,948 seconds (19:09:08), the LVDC exhibited a memory failure due to 6D10 battery depletion, and the flight program essentially ceased operation.

Vehicle control system performance was satisfactory during the flight. At Iterative Guidance Mode (IGM) initiation a pitchup transient occurred similar to that experienced on previous flights. All separations were normal. During the CSM separation from the S-IVB/IU and during the Transposition, Docking and Ejection (TD&E) maneuver the control system maintained a fixed inertial attitude to provide a stable docking platform. Following TD&E, S-IVB/IU attitude control was maintained during the evasive maneuver, the maneuver to lunar impact attitude, and the LOX dump and APS burns. An unscheduled decrease in range rate of approximately 2 to 3 m/s (7 to 10 ft/s) was experienced for approximately 60 seconds beginning at 70,150 seconds (19:29:10). This unscheduled maneuver had no adverse effect on lunar targeting.

The launch vehicle electrical systems and emergency detection system performed satisfactorily throughout all phases of flight. Operation of the batteries, power supplies, inverters, exploding bridgewire firing units, and switch selectors was normal. AS-508 was the first flight for which significant data were available to battery depletion.

Vehicle base pressure, base thermal and acoustic environments, in general, were similar to those experienced on earlier flights. The environmental control system performance was satisfactory.

All elements of the data system performed satisfactorily throughout the flight. Measurements from onboard telemetry were 99.9 percent reliable. Telemetry performance was normal and Radiofrequency (RF) propagation was generally good although the usual problems due to flame effects and staging were experienced. Usable VHF data were received to 14,280 seconds (03:58:00). Command systems RF performance for both the secure range safety command systems and the Command and Communications System (CCS) was normal. Usable CCS telemetered data were received to 70,380 seconds (19:33:00). CCS signal carrier was tracked until lunar impact. The only significant problem encountered during the mission was signal interference between the IU CCS and the LM unified S-band during translunar coast. This problem was caused by the necessity to power the LM before S-IVB/IU lunar impact. Good tracking data were received from the C-band radar with Carnarvon reporting final loss of signal at 44,220 seconds (12:17:00). The 67 ground engineering cameras provided good data during the launch.

MISSION OBJECTIVES ACCOMPLISHMENT

Table 1 presents the MSFC Mandatory Objectives and Desirable Objectives as defined in the Saturn V Mission Implementation Plan, "H" Series Missions, Apollo 12, 13, 14, and 15; MSFC Document PM-SAT-8010.5 (Revision C), dated February 9, 1970. An assessment of the degree of accomplishment of each objective is shown. Discussion supporting the assessment can be found in other sections of this report as shown in Table 1.

Table 1. Mission Objectives Accomplishment

NO.	MSFC MANDATORY OBJECTIVES (MO) AND DESIRABLE OBJECTIVES (DO)	DEGREE OF ACCOMPLISHMENT	DISCREPANCIES	PARAGRAPH IN WHICH DISCUSSED
1	Launch on a flight azimuth between 72 and 96 degrees and insert the S-IVB/IU/SC into the planned circular earth parking orbit (MO).	Complete	None	4.1, 9.1.1
2	Restart the S-IVB during either the second or third revolution and inject the S-IVB/IU/SC onto the planned translunar trajectory (MO).	Complete	None	4.2.3, 7.6
3	Provide the required attitude control for the S-IVB/IU/SC during TD&E (MO).	Complete	None	10.4.4
4	Perform an evasive maneuver after ejection of the CSM/LM from the S-IVB/IU (DO).	Complete	None	10.4.4
5	Attempt to impact the S-IVB/IU on the lunar surface within 350 kilometers of 3 degrees South, 30 degrees West (DO).	Complete	None	4A.1
6	Determine actual impact point within 5 kilometers and time of impact within one second (DO).	Probably Complete	Analysis not Complete	4A.1
7	Vent and dump the remaining gases and propellants to save the S-IVB/IU (DO).	Complete	None	7.13

FAILURES, ANOMALIES AND DEVIATIONS

Evaluation of the launch vehicle data revealed no failures, one anomaly and three deviations. The anomaly and the deviations are summarized in the following tables.

Table 2. Summary of Anomaly

ANOMALY IDENTIFICATION					RECOMMENDED CORRECTIVE ACTION			
ITEM	VEHICLE SYSTEM	DESCRIPTION (CAUSE)	EFFECT ON MISSION	OCCURRENCE (RANGE TIME SECONDS)	DESCRIPTION	ACTION STATUS	VEHICLE EFFECTIVITY	PARAGRAPH REFERENCE
1	S-II Structure/Propulsion	High amplitude oscillations in the 14 to 16 hertz range during S-II mainstage were sufficiently severe to cause the center engine to shut down 132 seconds early. (Oscillations of this frequency are an inherent characteristic of the present configuration of the S-II stage, although the high amplitude occurring during AS-508 flight was not expected.)	None	330.6	<p>Addition of an accumulator in the LOX feed line of center engine to lower the natural frequency of the line, and hence decouple the line from the cross-beam mode which should in turn suppress the high amplitude vibrations.</p> <p>Investigation of an additional safety cutoff device is underway. Leading candidate is a structural vibration detection system.</p>	<p>Accumulator presently being installed in AS-509</p> <p>No firm action yet on vibration detection system</p>	AS-509 and Subs	8.2.3 6.3

Table 3. Summary of Deviations

ITEM	VEHICLE SYSTEM	DEVIATION	PROBABLE CAUSE	SIGNIFICANCE	PARAGRAPH REFERENCE
1	S-1C Propulsion	Unexpected shifts in engine No. 2 turbopump bearing jet pressure	Contaminant restrictions within the bearing jets.	Probably none. Several F-1 turbopumps have experienced similar shifts during engine static tests without problems. The occurrence of this type bearing jet pressure discrepancy during flight is not considered detrimental to F-1 engine turbopump reliability. No shifts have occurred since incorporation of an improved cleaning procedure. The only remaining flight engines not incorporating the improved cleaning procedure are engines S/N F2059 and S/N F2061.	5.3
2	S-IVB/IU Control	Unscheduled S-IVB/IU velocity change of 7 to 10 ft/s at 70,150 seconds (19:29:10).	APS firings in pitch and yaw due to Flight Control Computer output resulting from loss of yaw rate feedback and in response to the attitude error signal after loss of attitude control.	The stage would not necessarily have impacted the lunar surface within the prescribed limits if the velocity change had been in a different direction with respect to the flight path. The direction of the resultant velocity increment is unpredictable.	4A, 10.4.4 7.12
3	IU	At approximately 3.4 seconds the crossrange velocity measurement exhibited a shift of 2.13 ft/s, resulting in a velocity error of approximately 1.64 ft/s.	The velocity shift resulted from the accelerometer head momentarily contacting a mechanical stop due to the high vibration levels after liftoff.	This deviation had negligible effect on launch vehicle operation.	9.1.2

SECTION 1

INTRODUCTION

1.1 PURPOSE

This report provides the National Aeronautics and Space Administration (NASA) Headquarters, and other interested agencies, with the launch vehicle evaluation results of the AS-508 flight (Apollo 13 Mission). The basic objective of flight evaluation is to acquire, reduce, analyze, evaluate and report on flight data to the extent required to assure future mission success and vehicle reliability. To accomplish this objective, actual flight failures, anomalies and deviations are identified, their causes determined, and information made available for corrective action.

1.2 SCOPE

This report contains the performance evaluation of the major launch vehicle systems, with special emphasis on failures, anomalies and deviations. Summaries of launch operations and spacecraft performance are included.

The official George C. Marshall Space Flight Center (MSFC) position at this time is represented by this report. It will not be followed by a similar report unless continued analysis or new information should prove the conclusions presented herein to be significantly incorrect. Reports covering major subjects and special subjects will be published as required.

SECTION 2

EVENT TIMES

2.1 SUMMARY OF EVENTS

Range zero time, the basic time reference for this report is 14:13:00 Eastern Standard Time (EST) (19:13:00 Universal Time [UT]) April 11, 1970. Range time is the elapsed time from range zero time and, unless otherwise noted, is the time used throughout this report. All data, except as otherwise defined, presented in "Range Time" are the times at which the data were received at the telemetry ground station, i.e., actual time of occurrence at the vehicle plus telemetry transmission time. The Time-From-Base times are presented as elapsed vehicle time from start of time base. Vehicle time is the Launch Vehicle Digital Computer (LVDC) clock time, and differs from actual time of occurrence by any clock error that may exist. Figure 2-1 shows the conversion between range and vehicle times.

Range times for each time base used in the flight sequence program and the signal for initiating each time base are presented in Table 2-1. Start times of T_0 , T_1 , T_2 and T_3 were nominal. T_4 and T_5 were initiated approximately 34.6 and 44.0 seconds late, respectively, due to variations in the stage burn times. The variations, discussed in Sections 6, 7 and 8, affected the start of all subsequent time bases. Start times of T_6 and T_7 were 18.2 and 13.6 seconds late, respectively. T_8 , which was initiated by the receipt of a ground command, started 239.3 seconds late.

A summary of significant events for AS-508 is given in Table 2-2. The events in Table 2-2 associated with guidance, navigation, and control were nominal and are accurate to within a major computation cycle.

The predicted times for establishing actual minus predicted times in Table 2-2 were taken from 40M33628, "Interface Control Document Definition of Saturn SA-508 Flight Sequence Program", and from the "AS-508 H-2 Mission Launch Vehicle Operational Flight Trajectory", dated December 18, 1969 and updated January 19, 1970, except as noted.

2.2 VARIABLE TIME AND COMMANDED SWITCH SELECTOR EVENTS

Table 2-3 lists the switch selector events which were issued during the flight but were not programmed for specific times. The water coolant valve open and close switch selector commands were issued based on the condition

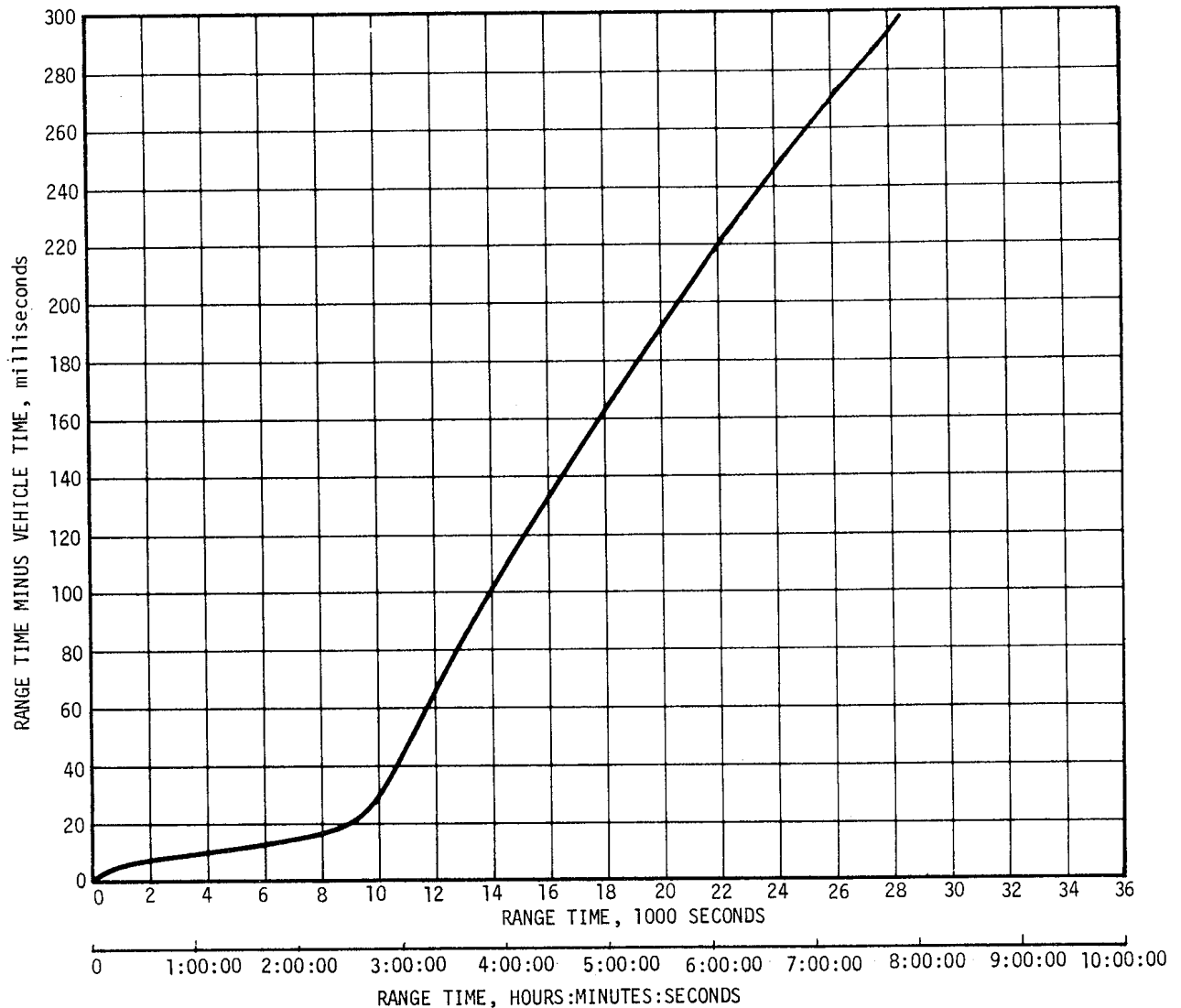


Figure 2-1. Range Time to Vehicle Time Conversion

of two thermal switches in the Environmental Control System (ECS). The outputs of these switches were sampled once every 300 seconds, beginning at 480 seconds, and a switch selector command was issued to open or close the water valve. The valve was opened if the sensed temperature was too high, and was closed if the temperature was too low. Data indicate the water coolant valve responded properly to temperature fluctuations.

The IU command to shift Engine Mixture Ratio (EMR) from high to low occurred 32.2 seconds late, mainly due to the early S-II stage Center Engine Cutoff (CECO), as discussed in paragraph 6.5. This command is issued upon attainment of a preprogrammed velocity increase as sensed by the LVDC. The program logic delays the EMR shift and provides for Translunar Injection capability with one S-II engine out.

Table 2-1. Time Base Summary

TIME BASE	RANGE TIME SEC (HR:MIN:SEC)	SIGNAL START
T ₀	-16.96	Guidance Reference Release
T ₁	0.61	IU Umbilical Disconnect Sensed by LVDC
T ₂	135.33	Downrange Velocity \geq 500 m/s at T ₁ +134.7 seconds as Sensed by LVDC
T ₃	163.64	S-IC OECO Sensed by LVDC
T ₄	592.66	S-II OECO Sensed by LVDC
T ₅	750.05	S-IVB ECO (Velocity) Sensed by LVDC
T ₆	8768.11 (02:26:08.11)	Restart Equation Solution
T ₇	9697.40 (02:41:37.40)	S-IVB ECO (Velocity) Sensed by LVDC
T ₈	15,479.43 (04:17:59.43)	Initiated by Ground Command

Table 2-3 also contains the special sequence of switch selector events which were programed to be initiated by telemetry station acquisition and included the following calibration sequence:

Function	Stage	Time (Sec)
Telemetry Calibrator In-Flight Calibrate ON	IU	Acquisition +60.0
IM Calibrate ON	S-IVB	Acquisition +60.4
TM Calibrate OFF	S-IVB	Acquisition +61.4
Telemetry Calibrator In-Flight Calibrate OFF	IU	Acquisition +65.0

Table 2-2. Significant Event Times Summary

ITEM	EVENT DESCRIPTION	RANGE TIME		TIME FROM BASE	
		ACTUAL SEC	ACT-PRED SEC	ACTUAL SEC	ACT-PRED SEC
1	GUIDANCE REFERENCE RELEASE (GRR)	-17.0	0.0	-17.6	0.1
2	S-IC ENGINE START SEQUENCE COMMAND (GROUND)	-8.9	0.0	-9.5	0.0
3	S-IC ENGINE NO.5 START	-6.7	0.0	-7.3	0.0
4	S-IC ENGINE NO.1 START	-6.3	0.0	-6.9	0.0
5	S-IC ENGINE NO.3 START	-6.2	0.0	-6.8	0.0
6	S-IC ENGINE NO.4 START	-6.0	0.0	-6.6	0.1
7	S-IC ENGINE NO.2 START	-6.0	0.0	-6.6	0.0
8	ALL S-IC ENGINES THRUST OK	-1.4	0.1	-2.0	0.2
9	RANGE ZERO	0.0		-0.6	
10	ALL HCLDDOWN ARMS RELEASED (FIRST MOTION)	0.3	0.0	-0.4	0.0
11	IU UMBILICAL DISCONNECT, START OF TIME BASE 1 (T1)	0.6	-0.1	0.0	0.0
12	BEGIN TOWER CLEARANCE YAW MANEUVER	2.3	0.6	1.7	0.7
13	END YAW MANEUVER	10.0	-0.9	9.4	-0.9
14	BEGIN PITCH AND ROLL MANEUVER	12.6	0.1	12.0	0.1
15	S-IC OUTBOARD ENGINE CANT	20.6	-0.1	20.0	0.0
16	END ROLL MANEUVER	32.1	1.7	31.5	1.8
17	MACH 1	68.4	-0.2	67.8	-0.2
18	MAXIMUM DYNAMIC PRESSURE (MAX Q)	81.3	-4.0	80.7	-3.9
19	S-IC CENTER ENGINE CUTOFF (CECO)	135.18	-0.09	134.57	-0.05
20	START OF TIME BASE 2 (T2)	135.3	-0.1	0.0	0.0
21	END PITCH MANEUVER (TILT ARREST)	163.3	1.3	27.9	1.2
22	S-IC OUTBOARD ENGINE CUTOFF (OECO)	163.60	-0.40	28.27	-0.38
23	START OF TIME BASE 3 (T3)	163.6	-0.4	0.0	0.0

Table 2-2. Significant Event Times Summary (Continued)

ITEM	EVENT DESCRIPTION	RANGE TIME		TIME FROM BASE	
		ACTUAL SEC	ACT-PRED SEC	ACTUAL SEC	ACT-PRED SEC
24	START S-II LH2 TANK HIGH PRESSURE VENT MODE	163.7	-0.4	0.1	0.0
25	S-II LH2 RECIRCULATION PUMPS OFF	163.8	-0.4	0.2	0.0
26	S-II ULLAGE MOTOR IGNITION	164.1	-0.4	0.5	0.0
27	S-IC/S-II SEPARATION COMMAND TO FIRE SEPARATION DEVICES AND RETRO MOTORS	164.3	-0.4	0.7	0.0
28	S-II ENGINE START SEQUENCE COMMAND (ESC)	165.0	-0.4	1.4	0.0
29	S-II ENGINE SOLENOID ACTIVATION (AVERAGE OF FIVE)	165.0	-0.4	1.4	0.0
30	S-II IGNITION-STDV OPEN	166.0	-0.4	2.4	0.0
31	S-II MAINSTAGE	168.0	-0.4	4.4	0.0
32	S-II ULLAGE MOTOR BURN TIME TERMINATION (THRUST REACHES 75%)	168.1	-0.5	4.4	-0.2
33	S-II CHILLDOWN VALVES CLOSE	170.0	-0.4	6.4	0.0
34	S-II HIGH (5.5) EMR ON	170.5	-0.4	6.9	0.0
35	S-II SECOND PLANE SEPARATION COMMAND (JETTISON S-II AFT INTERSTAGE)	194.3	-0.4	30.7	0.0
36	LAUNCH ESCAPE TOWER (LET) JETTISON	201.0	0.6	37.4	1.0
37	ITERATIVE GUIDANCE MODE (IGM) PHASE 1 INITIATED*	204.5	-0.5	40.9	-0.1
38	S-II LCX STEP PRESSURIZATION	263.6	-0.4	100.0	0.0
39	S-II ENGINE #5 SOLENOID DEACTIVATION SIGNAL (K1-205) (CECO)	330.65	-132.36	167.00	-132.00
40	S-II CENTER ENGINE CUTOFF COMMAND	462.6	-0.4	299.0	0.0
41	S-II LH2 STEP PRESSURIZATION	463.6	-0.4	300.0	0.0
42	GUIDANCE SENSED TIME TO BEGIN EMR SHIFT (IGM PHASE 2 INITIATED & START OF ARTIFICIAL TAU MODE)*	534.7	32.2	371.0	32.5

*Time is accurate to major computation cycle dependent upon length of computation cycle.

Table 2-2. Significant Event Times Summary (Continued)

ITEM	EVENT DESCRIPTION	RANGE TIME		TIME FROM BASE	
		ACTUAL SEC	ACT-PRED SEC	ACTUAL SEC	ACT-PRED SEC
43	S-II LOW ENGINE MIXTURE RATIO (EMR) SHIFT (ACTUAL)	537.5	33.7	373.8	34.0
44	END OF ARTIFICIAL TAU MODE*	545.8	32.8	382.2	33.2
45	S-II OUTBOARD ENGINE CUTOFF (OECO)	592.64	34.53	429.00	34.90
46	S-II ENGINE CUTOFF INTERRUPT, START OF TIME BASE 4 (T4) (START OF IGM PHASE 3)	592.7	34.6	0.0	0.0
47	S-IVB ULLAGE MOTOR IGNITION	593.4	34.5	0.8	0.0
48	S-II/S-IVB SEPARATION COMMAND TO FIRE SEPARATION DEVICES AND RETRO MOTORS	593.5	34.5	0.9	0.0
49	S-IVB ENGINE START COMMAND (FIRST ESC)	593.6	34.5	1.0	0.0
50	FUEL CHILLDOWN PUMP OFF	594.8	34.5	2.2	0.0
51	S-IVB IGNITION (STDV OPEN)	596.9	34.8	4.3	0.3
52	S-IVB MAINSTAGE	599.4	34.8	6.8	0.3
53	START OF ARTIFICIAL TAU MODE*	600.2	34.7	7.5	0.1
54	S-IVB ULLAGE CASE JETTISON	605.4	34.5	12.8	0.0
55	END OF ARTIFICIAL TAU MODE*	611.2	36.9	18.5	2.4
56	BEGIN TERMINAL GUIDANCE*	716.9	44.6	124.2	10.1
57	END IGM PHASE 3*	743.2	45.3	150.5	10.7
58	BEGIN CHI FREEZE*	743.2	45.3	150.5	10.7
59	S-IVB VELOCITY CUTOFF COMMAND (FIRST GUIDANCE CUTOFF) (FIRST ECO)	749.83	44.06	-0.22	-0.02
60	S-IVB ENGINE CUTOFF INTERRUPT, START OF TIME BASE 5 (T5)	750.0	44.0	0.0	0.0
61	S-IVB APS ULLAGE ENGINE NO. 1 IGNITION COMMAND	750.3	44.0	0.3	0.0
62	S-IVB APS ULLAGE ENGINE NO. 2 IGNITION COMMAND	750.4	44.0	0.4	0.0
63	LOX TANK PRESSURIZATION OFF	751.2	44.0	1.2	0.0
64	PARKING ORBIT INSERTION	759.8	44.0	9.8	0.0

*Time is accurate to major computation cycle dependent upon length of computation cycle.

Table 2-2. Significant Event Times Summary (Continued)

ITEM	EVENT DESCRIPTION	RANGE TIME		TIME FROM BASE	
		ACTUAL SEC	ACT-PRED SEC	ACTUAL SEC	ACT-PRED SEC
65	BEGIN MANEUVER TO LOCAL HORIZONTAL ATTITUDE*	770.1	43.7	20.1	-0.3
66	S-IVB CONTINUOUS VENT SYSTEM (CVS) ON	809.0	44.0	59.0	0.0
67	S-IVB APS ULLAGE ENGINE NO. 1 CUTOFF COMMAND	837.0	44.0	87.0	0.0
68	S-IVB APS ULLAGE ENGINE NO. 2 CUTOFF COMMAND	837.1	44.0	87.1	0.0
69	BEGIN ORBITAL NAVIGATION *	850.4	44.0	100.3	-0.1
70	BEGIN S-IVB RESTART PREPARATIONS, START OF TIME BASE 6 (T6)	8768.1	18.2	0.0	0.0
71	S-IVB O2/H2 BURNER LH2 ON	8809.4	18.2	41.3	0.0
72	S-IVB O2/H2 BURNER EXCITERS ON	8809.7	18.2	41.6	0.0
73	S-IVB O2/H2 BURNER LOX ON (HELIUM HEATER ON)	8810.1	18.2	42.0	0.0
74	S-IVB CVS OFF	8810.3	18.2	42.2	0.0
75	S-IVB LH2 REPRESSURIZATION CONTROL VALVE ON	8816.2	18.2	48.1	0.0
76	S-IVB LOX REPRESSURIZATION CONTROL VALVE ON	8816.4	18.2	48.3	0.0
77	S-IVB AUX HYDRAULIC PUMP FLIGHT MODE ON	8987.1	18.2	219.0	0.0
78	S-IVB LOX CHILLDOWN PUMP ON	9017.1	18.2	249.0	0.0
79	S-IVB LH2 CHILLDOWN PUMP ON	9022.1	18.2	254.0	0.0
80	S-IVB PREVALVES CLOSED	9027.1	18.2	259.0	0.0
81	S-IVB PU MIXTURE RATIO 4.5 ON	9218.2	18.2	450.1	0.0
82	S-IVB APS ULLAGE ENGINE NO. 1 IGNITION COMMAND	9264.4	18.2	496.3	0.0
83	S-IVB APS ULLAGE ENGINE NO. 2 IGNITION COMMAND	9264.5	18.2	496.4	0.0
84	S-IVB O2/H2 BURNER LH2 OFF (HELIUM HEATER OFF)	9264.9	18.2	496.8	0.0
85	S-IVB O2/H2 BURNER LOX OFF	9269.4	18.2	501.3	0.0

*Time is accurate to major computation cycle dependent upon length of computation cycle.

Table 2-2. Significant Event Times Summary (Continued)

ITEM	EVENT DESCRIPTION	RANGE TIME		TIME FROM BASE	
		ACTUAL SEC	ACT-PRED SEC	ACTUAL SEC	ACT-PRED SEC
86	S-IVB LH2 CHILLDOWN PUMP OFF	9337.5	18.2	569.4	0.0
87	S-IVB LOX CHILLDOWN PUMP OFF	9337.7	18.2	569.6	0.0
88	S-IVB ENGINE RESTART COMMAND (FUEL LEAD INITIATION) (SECOND ESC)	9338.1	18.2	570.0	0.0
89	S-IVB APS ULLAGE ENGINE NO. 1 CUTOFF COMMAND	9341.1	18.2	573.0	0.0
90	S-IVB APS ULLAGE ENGINE NO. 2 CUTOFF COMMAND	9341.2	18.2	573.1	0.0
91	S-IVB SECOND IGNITION (STDV OPEN)	9346.4	18.5	578.3	0.3
92	S-IVB MAINSTAGE	9348.9	18.5	580.8	0.3
93	ENGINE MIXTURE RATIO (EMR) SHIFT	9448.7	18.3	680.6	0.1
94	S-IVB LH2 STEP PRESSURIZATION (SECOND BURN RELAY OFF)	9618.1	18.2	850.0	0.0
95	BEGIN TERMINAL GUIDANCE *	9668.3	14.1	900.2	-4.0
96	BEGIN CHI FREEZE*	9695.7	14.2	927.6	-4.0
97	S-IVB SECOND GUIDANCE CUTOFF COMMAND (SECOND ECO)	9697.17	13.55	-0.23	-0.03
98	S-IVB ENGINE CUTOFF INTERRUPT, START OF TIME BASE 7	9697.4	13.6	0.0	0.0
99	S-IVB CVS ON	9697.9	13.6	0.5	0.0
100	TRANSLUNAR INJECTION	9707.2	13.6	9.8	0.0
101	BEGIN MANEUVER TO LOCAL HORIZONTAL ATTITUDE*	9848.0	13.3	150.6	-0.3
102	BEGIN ORBITAL NAVIGATION*	9848.0	13.3	150.6	-0.3
103	S-IVB CVS OFF	9848.3	13.6	150.9	0.0
104	BEGIN MANEUVER TO TRANSPOSITION AND DOCKING ATTITUDE (TD&E)*	10598.3	14.5	900.9	0.9
105	CSM SEPARATION	11198.9	38.9**	1501.5	25.3
106	CSM DOCK	11948.8	188.8**	2251.4	175.3
107	SC/LV FINAL SEPARATION	14460.8	0.8**	4763.3	-12.8

*Time is accurate to major computation cycle dependent upon length of computation cycle.
 **The predicted time for establishing this actual minus predicted time has been taken from the Apollo 13 Final Flight Plan, Revision B, dated March 16, 1970.

Table 2-2. Significant Event Times Summary (Continued)

ITEM	EVENT DESCRIPTION	RANGE TIME		TIME FROM BASE	
		ACTUAL SEC	ACT-PRED SEC	ACTUAL SEC	ACT-PRED SEC
108	START OF TIME BASE 8 (T8)	15479.4	239.3**	0.0	0.0
109	S-IVB APS ULLAGE ENGINE NO. 1 IGNITION COMMAND	15480.6	239.3**	1.2	0.0
110	S-IVB APS ULLAGE ENGINE NO. 2 IGNITION COMMAND	15480.8	239.3**	1.4	0.0
111	S-IVB APS ULLAGE ENGINE NO. 1 CUTOFF COMMAND	15560.6	239.3**	81.2	0.0
112	S-IVB APS ULLAGE ENGINE NO. 2 CUTOFF COMMAND	15560.8	239.3**	81.4	0.0
113	INITIATE MANEUVER TO LOX DUMP ATTITUDE*	16060.0	240.0**	580.6	0.7
114	S-IVB CVS ON	16479.4	239.3**	1000.0	0.0
115	BEGIN LOX DUMP	16759.4	239.3**	1280.0	0.0
116	S-IVB CVS OFF	16779.4	239.3**	1300.0	0.0
117	END LOX DUMP	16807.4	239.3**	1328.0	0.0
118	H2 NONPROPULSIVE VENT (NPV) ON	16886.4	239.3**	1407.0	0.0
119	INITIATE MANEUVER TO ATTITUDE REQUIRED FOR FINAL S-IVB APS BURN*	20887.8	187.8**	5408.3	-51.5
120	S-IVB APS ULLAGE ENGINE NO. 1 IGNITION COMMAND	21599.5	-0.5**	6120.0	-239.8
121	S-IVB APS ULLAGE ENGINE NO. 2 IGNITION COMMAND	21599.7	-0.5**	6120.2	-239.8
122	S-IVB APS ULLAGE ENGINE NO. 1 CUTOFF COMMAND	21816.5	-19.5**	6337.0	-258.8
123	S-IVB APS ULLAGE ENGINE NO. 2 CUTOFF COMMAND	21816.7	-19.5**	6337.2	-258.8
124	S-IVB/IU LUNAR IMPACT	280601.0 (77:56:41.0) (HRS:MIN:SEC)	701.0**	265121.6 (73:38:41.6) (HRS:MIN:SEC)	461.7

*Time is accurate to major computation cycle dependent upon length of computation cycle.
 **The predicted time for establishing this actual minus predicted time has been taken from the Apollo 13 Final Flight Plan, Revision B, dated March 16, 1970.

Table 2-3. Variable Time and Commanded Switch Selector Events

FUNCTION	STAGE	RANGE TIME (SEC)	TIME FROM BASE (SEC)	REMARKS
High (5.5) Engine Mixture Ratio Off	S-II	535.3	T ₃ +371.6	LVDC Function
Low (4.5) Engine Mixture Ratio On	S-II	535.5	T ₃ +371.8	LVDC Function
Water Coolant Valve Open	IU	781.2	T ₅ +31.1	LVDC Function
Telemetry Calibrator Inflight Calibrate On	IU	1079.0	T ₅ +329.0	Acquisition By Canary Revolution 1
TM Calibrate On	S-IVB	1079.4	T ₅ +329.4	Acquisition By Canary Revolution 1
TM Calibrate Off	S-IVB	1080.4	T ₅ +330.4	Acquisition By Canary Revolution 1
Telemetry Calibrator Inflight Calibrate Off	IU	1084.0	T ₅ +334.0	Acquisition By Canary Revolution 1
Telemetry Calibrator Inflight Calibrate On	IU	3223.0	T ₅ +2473.0	Acquisition By Carnarvon Revolution 1
TM Calibrate On	S-IVB	3223.4	T ₅ +2473.4	Acquisition By Carnarvon Revolution 1
TM Calibrate Off	S-IVB	3224.4	T ₅ +2474.4	Acquisition By Carnarvon Revolution 1
Telemetry Calibrator Inflight Calibrate Off	IU	3228.0	T ₅ +2478.0	Acquisition By Carnarvon Revolution 1
Telemetry Calibrator Inflight Calibrate On	IU	6703.0	T ₅ +5953.0	Acquisition By Canary Revolution 2
TM Calibrate On	S-IVB	6703.4	T ₅ +5953.4	Acquisition By Canary Revolution 2
TM Calibrate Off	S-IVB	6704.4	T ₅ +5954.4	Acquisition By Canary Revolution 2
Telemetry Calibrator Inflight Calibrate Off	IU	6718.0	T ₅ +5958.0	Acquisition By Canary Revolution 2
Water Coolant Valve Closed	IU	8805.4	T ₆ +37.3	LVDC Function
Telemetry Calibrator Inflight Calibrate On	IU	9988.6	T ₇ +291.2	Acquisition By Hawaii Revolution 2
TM Calibrate On	S-IVB	9989.0	T ₇ +291.6	Acquisition By Hawaii Revolution 2
TM Calibrate Off	S-IVB	9989.9	T ₇ +292.6	Acquisition By Hawaii Revolution 2
Telemetry Calibrator Inflight Calibrate Off	IU	9993.6	T ₇ +296.2	Acquisition By Hawaii Revolution 2
Water Coolant Valve Open	IU	12,480.7	T ₇ +2783.3	LVDC Function
Water Coolant Valve Closed	IU	12,780.2	T ₇ +3082.8	LVDC Function
Water Coolant Valve Open	IU	15,180.2	T ₇ +5482.7	LVDC Function
Start of Time Base 8 (T ₈)		15,479.4	T ₈ +0.0	CCS Command
Water Coolant Valve Closed	IU	15,480.9	T ₈ +1.4	LVDC Function
Water Coolant Valve Open	IU	18,180.3	T ₈ +2700.8	LVDC Function
Water Coolant Valve Closed	IU	18,480.8	T ₈ +3001.3	LVDC Function

Table 2-3. Variable Time and Commanded Switch Selector Events (Continued)

FUNCTION	STAGE	RANGE TIME (SEC)	TIME FROM BASE (SEC)	REMARKS
Water Coolant Valve Open	IU	21,180.4	T _g +5700.9	LVDC Function
Water Coolant Valve Closed	IU	21,480.8	T _g +6001.2	LVDC Function
S-IVB Ullage Engine No. 1 On	S-IVB	21,599.5	T _g +6120.0	CCS Command
S-IVB Ullage Engine No. 2 On	S-IVB	21,599.7	T _g +6120.2	CCS Command
S-IVB Ullage Engine No. 1 Off	S-IVB	21,816.5	T _g +6337.0	CCS Command
S-IVB Ullage Engine No. 2 Off	S-IVB	21,816.7	T _g +6337.2	CCS Command

SECTION 3

LAUNCH OPERATIONS

3.1 SUMMARY

The ground systems supporting the AS-508/Apollo 13 countdown and launch performed satisfactorily. System component failures and malfunctions requiring corrective action were corrected during countdown and no unscheduled holds were incurred. Propellant tanking was accomplished satisfactorily. Launch occurred at 14:13:00 Eastern Standard Time (EST), April 11, 1970, from Pad 39A of the Kennedy Space Center, Saturn Complex. Damage to the pad, Launch Umbilical Tower (LUT) and support equipment was considered minimal.

3.2 PRELAUNCH MILESTONES

A chronological summary of prelaunch milestones for the AS-508 launch is contained in Table 3-1.

3.3 COUNTDOWN EVENTS

The AS-508/Apollo 13 terminal countdown was picked up at T-28 hours on April 9, 1970, at 24:00:00 EST. Scheduled holds in the launch countdown sequence were 9 hours 13 minutes duration at T-9 hours and 1 hour duration at T-3 hours 30 minutes. Launch activities were directed from Launch Control Center (LCC) Firing Room 1. Launch occurred on schedule at 14:13:00 EST, April 11, 1970.

3.4 PROPELLANT LOADING

3.4.1 RP-1 Loading

The RP-1 system successfully supported the launch countdown without incident. S-IC stage replenishment was initiated at approximately T-13 hours and level adjust at T-1 hour. The air vent trap (A4120, P/N 76K00072) closed prematurely during replenish operations causing a quantity of fill line gas residuals to be pumped through the S-IC stage fuel tank. This problem also occurred during the Countdown Demonstration Test (CDDT) and is under design investigation.

Table 3-1. AS-508/Apollo 13 Prelaunch Milestones

DATE	ACTIVITY OR EVENT
June 13, 1969	S-IVB-508 Stage Arrival
June 16, 1969	S-IC-8 Stage Arrival
June 18, 1969	S-IC Erection on Mobile Launcher 3
June 26, 1969	Command and Service Module (CSM)-109 Arrival
June 27, 1969	Lunar Module (LM)-7 Ascent Stage Arrival
June 28, 1969	LM-7 Descent Stage Arrival
June 29, 1969	S-II-8 Stage Arrival
July 7, 1969	Instrument Unit (IU)-508 Arrival
July 17, 1969	S-II Erection
July 18, 1969	Spacecraft/Lunar Module Adapter (SLA)-16 Arrival
July 31, 1969	S-IVB Erection
August 1, 1969	IU Erection
August 29, 1969	Launch Vehicle (LV) Electrical System Test
October 21, 1969	LV Propellant Dispersion/Malfunction Overall Test (OAT) Complete
December 4, 1969	LV Service Arm OAT
December 10, 1969	Spacecraft (SC) Erection
December 15, 1969	Space Vehicle (SV)/Mobile Launcher Transfer to Pad 39A
January 19, 1970	SV Electrical Mate
January 20, 1970	SV OAT No. 1 (Plugs In)
February 26, 1970	SV Flight Readiness Test (FRT) Completed
March 16, 1970	RP-1 Loading
March 25, 1970	Countdown Demonstration Test (CDDT) Completed (Wet)
March 26, 1970	CDDT Completed (Dry)
April 9, 1970	SV Terminal Countdown Started
April 11, 1970	SV Launch On Schedule

3.4.2 LOX Loading

The LOX system satisfactorily supported the launch countdown. The fill sequence was nominal beginning with start of S-IVB stage loading at T-8 hours 22 minutes. LOX loading was completed and replenishment initiated on all stages at T-5 hours 41 minutes.

During the countdown, at approximately T-2 hours 5 minutes, the S-IC stage LOX vent valve No. 2 stuck in the open position. A procedure to cycle the vent valves at 15 to 20-minute intervals had been in effect since completion of S-IC fast fill at approximately T-5 hours 41 minutes. LOX vent valve No. 2 had been successfully cycled about 15 minutes prior to sticking. The problem was resolved by closing LOX vent valve No. 1 and applying a GN₂ purge through the sticking LOX vent valve No. 2. After 88 seconds of purge and 13 cycles of the close command switch, the LOX vent valve No. 2 returned to the closed position. The LOX vent valve No. 2 was left in the closed position for the remainder of the countdown, and no further problems developed. An investigation to determine the cause of the problem is underway.

3.4.3 LH₂ Loading

The LH₂ system successfully supported launch countdown. The fill sequence was nominal beginning with start of S-II stage loading at T-5 hours 33 minutes. LH₂ loading was completed and replenishment initiated at T-4 hours 4 minutes.

During S-IVB stage loading, major excursions occurred on the LH₂ fine and the LH₂ coarse mass measurements. As loading progressed the system recovered allowing the countdown to continue normally. The system again operated abnormally beginning at T-3 seconds and lasting through tower clearance. This system was known to be a potential problem from previous testing. An alternate loading procedure had been prepared prior to start of the launch countdown but was not required to complete the countdown.

3.5 INSULATION

The S-II-8 was the first stage to utilize spray-on foam as the external insulation for the LH₂ tank sidewalls and forward skirt. This is discussed further in Appendix B. The performance of the stage insulation, including Ground Support Equipment (GSE) purge and vacuum systems, was satisfactory with no parameters exceeding redline limits. Detailed inspection of the external insulation, using operational television, indicated that the spray-on foam performed satisfactorily. The total heat leak through the insulation to the LH₂ tank was well below the specification value.

3.6 GROUND SUPPORT EQUIPMENT

3.6.1 Ground/Vehicle Interface

In general performance of the ground service systems supporting all stages of the launch vehicle was satisfactory. Overall damage to the pad, LUT, and support equipment from the blast and flame impingement was considered minimal. Detailed discussion of the GSE is contained in KSC Apollo/Saturn V (AS-508) "Ground Support Evaluation Report".

The ground Environmental Control System (ECS) performed satisfactorily throughout countdown and launch, with one exception. With ground ECS flowrate and temperature at maximum values, the S-IC aft flight battery compartment temperature, with specification limits of $80 \pm 15^\circ\text{F}$, dropped to 61°F . The low temperature had been anticipated from CDDT performance and a waiver had been approved permitting limits of 50 to 95°F for the compartment temperature during the AS-508 launch (see paragraph 14.2).

The Holddown Arms and Service Arms (SA) satisfactorily supported the launch and caused no countdown holds or delays. Because of a Digital Events Evaluator (DEE)-6 failure at T-1 second, SA retract times and valve actuation times are not available. However, the SA control panels indicated that all retract and withdrawal firing systems actuated, and that all arms fully retracted and latched.

Overall performance of the Tail Service Mast system was satisfactory. Valve actuation and retract times are not available because of the DEE-6 failure. Television observation and panel lights indicated that all three return valves opened, the masts retracted together and hoods closed within the 4.0 second maximum allowed from aft umbilical plate separation.

3.6.2 MSFC Furnished Ground Support Equipment

The S-IC stage mechanical and electrical Ground Support Equipment performed satisfactorily during launch operations with only one minor system failure encountered. At T-14 hours a gradual increase in GN_2 primary pressure, from 3540 to 3650 psig, was noted on the S-IC pneumatics console. Investigation indicated possible internal leakage in the dome loading regulator (P/N A9927). The regulator was replaced and the system retested satisfactorily. Subsequent analysis of the removed regulator could not confirm the failure. No further action is planned.

At T-1.156 seconds the DEE-6 began displaying erroneous data. This condition existed until 1800 seconds when the problem cleared and the output was normal. Permanent record data from magnetic tape was also erroneous. It is suspected that the problem occurred in the "W" Time Multiplex Communication Channel (I/O Channel) since the only area affected was outputting of data to magnetic tape and printers. The cause of failure is unknown at this time, but is apparently due to launch vibration.

Blast damage to the equipment was considered minimal.

3.6.3 Camera Coverage

Upon review of the film coverage the following conditions were observed:

- a. S-II stage intermediate SA No. 4 umbilical door (station 1772) did not secure upon SA withdrawal from the vehicle.
- b. S-II stage forward SA umbilical cover (between stringer 68 and 69) did not secure upon SA withdrawal from the vehicle. This condition also occurred during the AS-506 and AS-507 launches.

SECTION 4

TRAJECTORY

4.1 SUMMARY

The vehicle was launched on an azimuth 90 degrees east of north. A roll maneuver at 12.6 seconds placed the vehicle on a flight azimuth of 72.043 degrees east of north. The reconstructed trajectory was generated by merging the ascent phase, the parking orbit phase, the injection phase, and the post Translunar Injection (TLI) phase trajectories. The analysis for each phase was conducted separately with appropriate end point constraints to provide trajectory continuity. Available C-Band radar and Unified S-Band (USB) tracking data plus telemetered guidance velocity data were used in the trajectory reconstruction.

The trajectory parameters were close to nominal through S-IC and S-II stage burns until the early shutdown of the S-II center engine. The premature S-II Center Engine Cutoff (CECO) caused considerable deviations for certain trajectory parameters. S-II Outboard Engine Cutoff (OECO) occurred 34.5 seconds late as a result of the early CECO. The S-IVB burn time was extended by the guidance unit so that the vehicle achieved near nominal earth parking orbit insertion conditions 44.07 seconds later than predicted at a heading angle 1.230 degrees greater than nominal. The trajectory parameters at TLI were also close to nominal although the event itself was 13.56 seconds later than nominal. The trajectory parameters at Command Service Module (CSM) separation deviated somewhat from nominal since the event occurred 38.9 seconds later than predicted.

The earth impact locations for the S-IC and S-II stages were determined by a theoretical free-flight simulation. The analysis for the S-IC stage showed the surface range for the impact point to be 7.6 kilometers (4.1 n mi) greater than nominal. The analysis for the S-II stage showed the surface range for the impact point to be 8.6 kilometers (4.6 n mi) greater than nominal.

4.2 TRAJECTORY EVALUATION

4.2.1 Ascent Phase

The ascent phase spans the interval from guidance reference release through parking orbit insertion. The ascent trajectory was established by using

telemetered guidance velocities as generating parameters to fit tracking data from five C-Band stations and two S-Band stations. Approximately 20 percent of the tracking data were eliminated due to inconsistencies. The launch phase portion of the ascent phase, (liftoff to approximately 20 seconds), was established by constraining integrated telemetered guidance accelerometer data to the best estimate trajectory. The launch phase trajectory was initialized from launch camera data.

Actual and nominal altitude, surface range, and crossrange for the ascent phase are presented in Figure 4-1. Actual and nominal space-fixed velocity and flight path angle during ascent are shown in Figure 4-2. Actual and nominal comparisons of total inertial accelerations are shown in Figure 4-3. The maximum acceleration during S-IC burn was 3.83 g. The early shutdown of the S-II center engine resulted in subsequent longer burns of the S-II and S-IVB stages. These extended burn times compensated for the early S-II CECO and the vehicle was inserted into a near nominal parking orbit.

Mach number and dynamic pressure are shown in Figure 4-4. These parameters were calculated using meteorological data measured to an altitude of 80.5 kilometers (43.5 n mi). Above this altitude the measured data were merged into the U. S. Standard Reference Atmosphere.

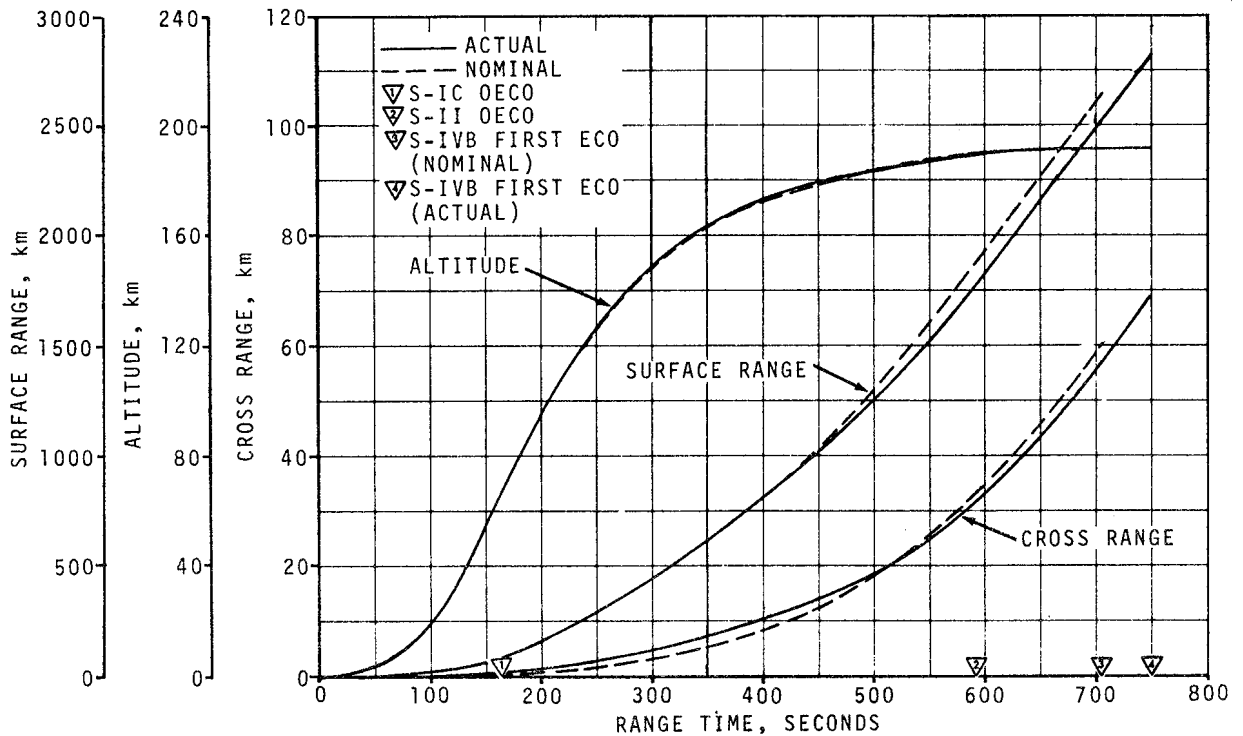


Figure 4-1. Ascent Trajectory Position Comparison

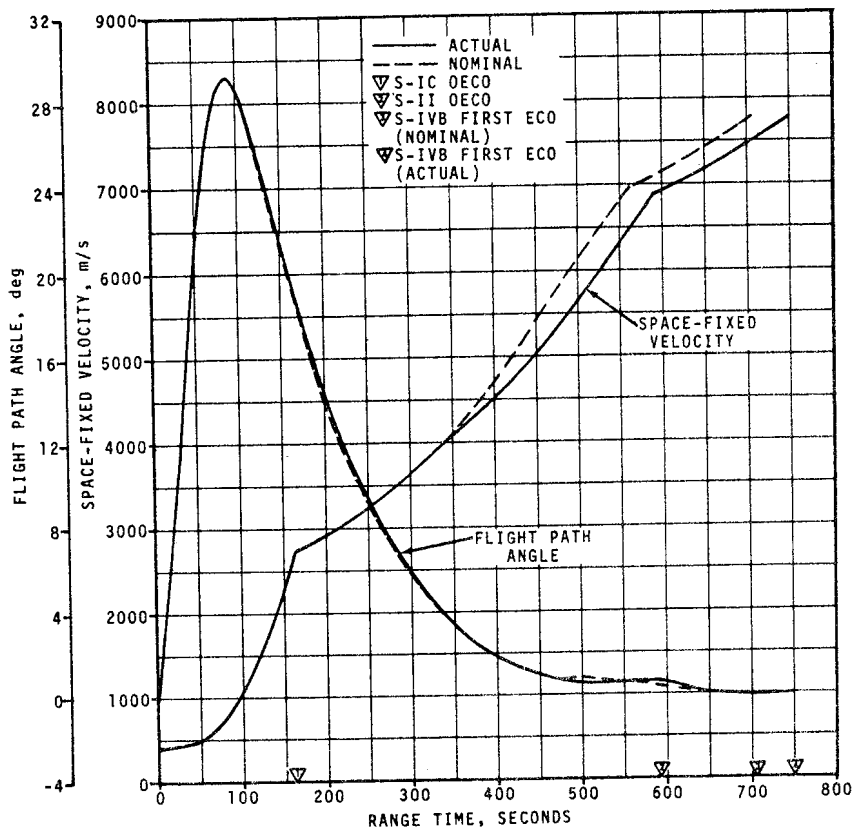


Figure 4-2. Ascent Trajectory Space-Fixed Velocity and Flight Path Angle Comparisons

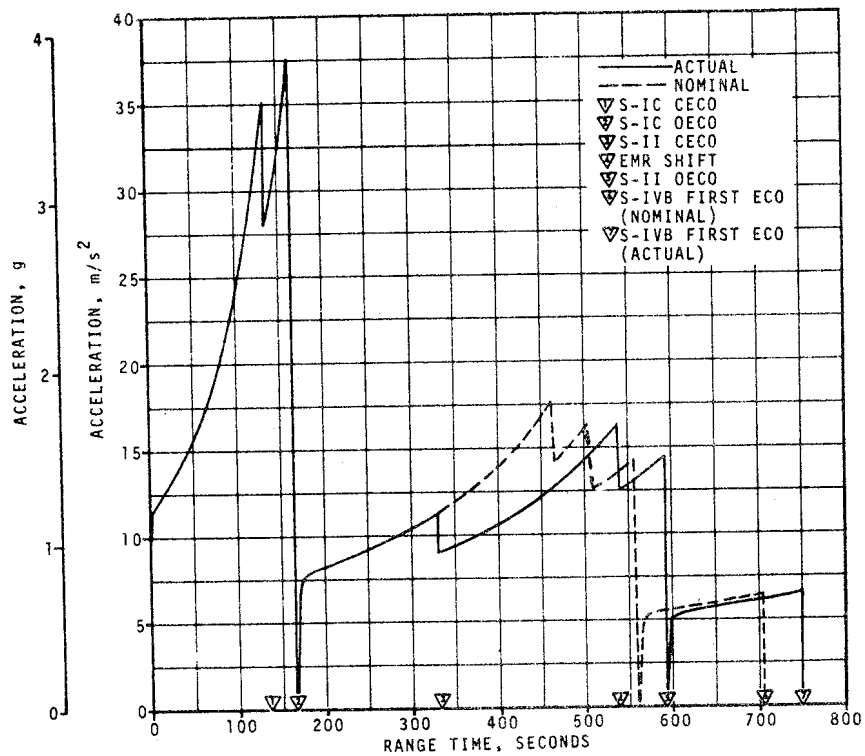


Figure 4-3. Ascent Trajectory Acceleration Comparison

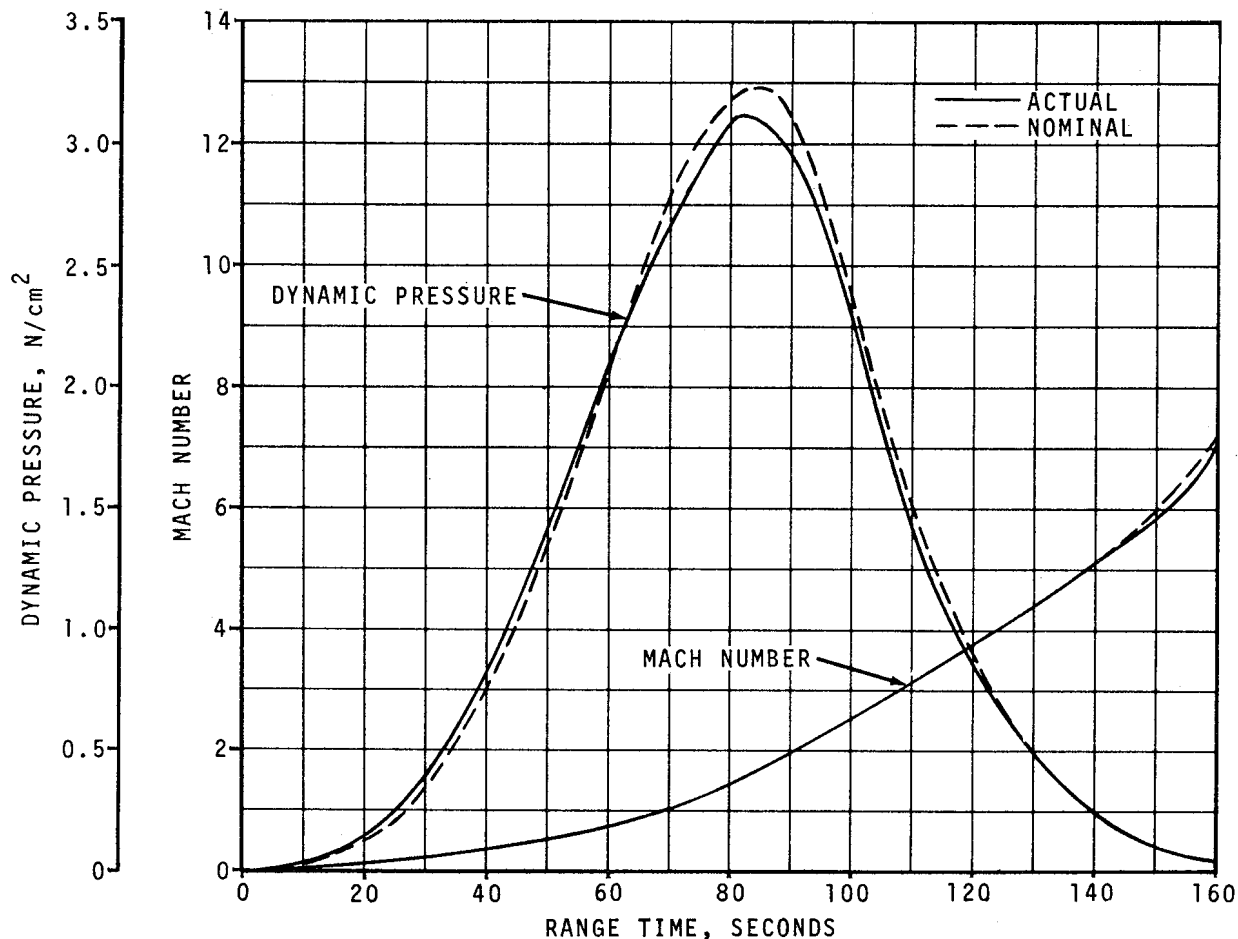


Figure 4-4. Dynamic Pressure and Mach Number Comparisons

Actual and nominal values of parameters at significant trajectory event times, cutoff events, and separation events are shown in Tables 4-1, 4-2, and 4-3, respectively.

The free-flight trajectories of the spent S-IC and S-II stages were simulated using initial conditions from the final postflight trajectory. The simulation was based upon the separation impulses for both stages and nominal tumbling drag coefficients. No tracking data were available for verification. Table 4-1 presents a comparison of free-flight parameters to nominal at apex for the S-IC and S-II stages. Table 4-4 presents a comparison of free-flight parameters to nominal at impact for the S-IC and S-II stages.

Table 4-1. Comparison of Significant Trajectory Events

EVENT	PARAMETER	ACTUAL	NOMINAL	ACT-NOM		
First Motion	Range Time, sec	0.3	0.3	0.0		
	Total Inertial Acceleration, m/s ² (ft/s ²) (g)	10.35 (33.96) (1.06)	10.41 (34.15) (1.06)	-0.06 (-0.19) (0.00)		
Mach 1	Range Time, sec	68.4	68.6	-0.2		
	Altitude, km (n mi)	8.1 (4.4)	7.9 (4.3)	0.2 (0.1)		
Maximum Dynamic Pressure	Range Time, sec	81.3	85.3	-4.0		
	Dynamic Pressure, N/cm ² (lb/ft ²)	3.12 (651.6)	3.23 (674.6)	-0.11 (-23.0)		
	Altitude, km (n mi)	12.5 (6.7)	13.6 (7.3)	-1.1 (-0.6)		
Maximum Total Inertial Acceleration:	S-IC	Range Time, sec	163.70	163.18	0.52	
		Acceleration, m/s ² (ft/s ²) (g)	37.60 (123.36) (3.83)	37.53 (123.13) (3.83)	0.07 (0.23) (0.00)	
	S-II	Range Time, sec	537.00	463.09	73.91	
		Acceleration, m/s ² (ft/s ²) (g)	16.25 (53.31) (1.66)	17.65 (57.91) (1.80)	-1.40 (-4.60) (-0.14)	
	S-IVB 1st Burn	Range Time, sec	750.00	705.84	44.16	
		Acceleration, m/s ² (ft/s ²) (g)	6.66 (21.85) (0.68)	6.53 (21.42) (0.67)	0.13 (0.43) (0.01)	
	S-IVB 2nd Burn	Range Time, sec	9,697.23	9,683.67	13.56	
		Acceleration, m/s ² (ft/s ²) (g)	14.03 (46.03) (1.43)	13.89 (43.57) (1.42)	0.14 (0.46) (0.01)	
	Maximum Earth-Fixed Velocity:	S-IC	Range Time, sec	164.10	164.51	-0.41
			Velocity, m/s (ft/s)	2,383.8 (7,820.9)	2,379.0 (7,805.1)	4.8 (15.8)
		S-II	Range Time, sec	593.50	559.02	34.48
			Velocity, m/s (ft/s)	6,492.7 (21,301.5)	6,558.5 (21,517.4)	-65.8 (-215.9)
S-IVB 1st Burn		Range Time, sec	750.50	715.76	34.74	
		Velocity, m/s (ft/s)	7,389.3 (24,243.1)	7,389.5 (24,243.8)	-0.2 (-0.7)	
S-IVB 2nd Burn		Range Time, sec	9,697.80	9,683.80	14.00	
		Velocity, m/s (ft/s)	10,433.6 (34,231.0)	10,429.8 (34,218.5)	3.8 (12.5)	
Apex:		S-IC Stage	Range Time, sec	271.7	270.3	1.4
			Altitude, km (n mi)	116.9 (63.1)	114.6 (61.9)	2.3 (1.2)
			Surface Range, km (n mi)	325.9 (176.0)	322.0 (173.9)	3.9 (2.1)
		S-II Stage	Range Time, sec	632.2	600.3	31.9
		Altitude, km (n mi)	190.7 (103.0)	189.4 (102.3)	1.3 (0.7)	
		Surface Range, km (n mi)	2,035.0 (1,098.8)	1,919.7 (1,036.6)	115.3 (62.2)	

NOTE: The Range Time used are times of occurrence at the vehicle, reference Figure 2-1.

Table 4-2. Comparison of Cutoff Events

PARAMETER	ACTUAL	NOMINAL	ACT-NOM	ACTUAL	NOMINAL	ACT-NOM
S-IC CECO (ENGINE SOLENOID)			S-IC DECO (ENGINE SOLENOID)			
Range Time, sec	135.18	135.27	-0.09	163.60	164.00	-0.40
Altitude, km (n mi)	43.5 (23.5)	42.6 (23.0)	0.9 (0.5)	67.4 (36.4)	66.5 (35.9)	0.9 (0.5)
Surface Range, km (n mi)	44.9 (24.2)	44.3 (23.9)	0.6 (0.3)	94.4 (51.0)	94.2 (50.9)	0.2 (0.1)
Space-Fixed Velocity, m/s (ft/s)	1,928.9 (6,328.4)	1,915.8 (6,285.4)	13.1 (43.0)	2,744.0 (9,002.6)	2,739.9 (8,989.2)	4.1 (13.4)
Flight Path Angle, deg	23.612	23.442	0.170	19.480	19.250	0.230
Heading Angle, deg	76.609	76.369	0.240	75.696	75.356	0.340
Crossrange, km (n mi)	0.5 (0.3)	0.1 (0.1)	0.4 (0.2)	1.0 (0.5)	0.3 (0.2)	0.7 (0.3)
Crossrange Velocity, m/s (ft/s)	11.1 (36.4)	3.0 (9.8)	8.1 (26.6)	23.4 (76.8)	8.0 (26.2)	15.4 (50.6)
S-II CECO (ENGINE SOLENOID)			S-II DECO (ENGINE SOLENOID)			
Range Time, sec	330.64	463.01	-132.37	592.64	558.11	34.53
Altitude, km (n mi)	159.6 (86.2)	179.4 (96.9)	-19.8 (-10.7)	189.1 (102.1)	187.6 (101.3)	1.5 (0.8)
Surface Range, km (n mi)	552.0 (298.1)	1,105.1 (596.7)	-553.1 (-298.6)	1,786.4 (964.6)	1,651.7 (891.8)	134.7 (72.8)
Space-Fixed Velocity, m/s (ft/s)	3,919.6 (12,859.6)	5,652.5 (18,544.9)	-1,732.9 (-5,685.3)	6,891.8 (22,610.9)	6,958.6 (22,830.1)	-66.8 (-219.2)
Flight Path Angle, deg	4.158	0.894	3.264	0.657	0.699	-0.042
Heading Angle, deg	76.956	79.576	-2.620	83.348	82.565	0.783
Crossrange, km (n mi)	6.4 (3.5)	13.7 (7.4)	-7.3 (-3.9)	32.0 (17.3)	27.1 (14.6)	4.9 (2.7)
Crossrange Velocity, m/s (ft/s)	44.7 (146.7)	109.0 (357.6)	-64.3 (-210.9)	183.2 (601.0)	176.8 (580.1)	6.4 (20.9)
S-IVB 1ST GUIDANCE CUTOFF SIGNAL			S-IVB 2ND GUIDANCE CUTOFF SIGNAL			
Range Time, sec	749.83	705.76	44.07	9,697.15	9,683.59	13.56
Altitude, km (n mi)	191.6 (103.5)	191.4 (103.3)	0.2 (0.2)	324.0 (174.9)	328.4 (177.3)	-4.4 (-2.4)
Surface Range, km (n mi)	2,840.2 (1,533.6)	2,646.8 (1,429.2)	193.4 (104.4)			
Space-Fixed Velocity, m/s (ft/s)	7,790.8 (25,560.4)	7,791.4 (25,562.3)	-0.6 (-1.9)	10,839.5 (35,562.7)	10,836.6 (35,553.1)	2.9 (9.6)
Flight Path Angle, deg	0.004	-0.001	0.005	7.182	7.224	-0.042
Heading Angle, deg	89.713	88.484	1.229	59.443	59.425	0.018
Crossrange, km (n mi)	69.3 (37.4)	60.2 (32.5)	9.1 (4.9)			
Crossrange Velocity, m/s (ft/s)	297.0 (974.4)	275.6 (904.2)	21.4 (70.2)			
Eccentricity				0.9758	0.9760	-0.0002
C_3^* , m^2/s^2 (ft^2/s^2)				-1,463,628 (-15,754,361)	-1,447,169 (-15,577,197)	-16,459 (-177,164)
Inclination, deg				31.818	31.834	-0.016
Descending Node, deg				122.996	123.030	-0.034
<p>NOTE: The Range Times used are times of occurrence at the vehicle, reference Figure 2-1.</p> <p>*C_3 is twice the specific energy of orbit</p> $C_3 = v^2 - \frac{2u}{R}$ <p>where v = Inertial Velocity u = Gravitational Constant R = Radius Vector From Center of Earth</p>						

Table 4-3. Comparison of Separation Events

PARAMETER	ACTUAL	NOMINAL	ACT-NOM
S-IC/S-II SEPARATION			
Range Time, sec	164.3	164.7	-0.4
Altitude, km (n mi)	68.0 (36.7)	67.2 (36.3)	0.8 (0.4)
Surface Range, km (n mi)	96.0 (51.8)	95.7 (51.7)	0.3 (0.1)
Space-Fixed Velocity, m/s (ft/s)	2,754.3 (9,036.4)	2,749.5 (9,020.7)	4.8 (15.7)
Flight Path Angle, deg	19.383	19.145	0.238
Heading Angle, deg	75.693	75.353	0.340
Crossrange, km (n mi)	1.0 (0.5)	0.3 (0.2)	0.7 (0.3)
Crossrange Velocity, m/s (ft/s)	23.6 (77.4)	8.2 (26.9)	15.4 (50.5)
Geodetic Latitude, deg N	28.864	28.869	-0.005
Longitude, deg E	-79.666	-79.670	0.004
S-II/S-IVB SEPARATION			
Range Time, sec	593.5	559.0	34.5
Altitude, km (n mi)	189.2 (102.2)	187.7 (101.3)	1.5 (0.9)
Surface Range, km (n mi)	1,791.8 (967.5)	1,657.5 (895.0)	134.3 (72.5)
Space-Fixed Velocity, m/s (ft/s)	6,895.9 (22,624.3)	6,961.6 (22,839.9)	-65.7 (-215.6)
Flight Path Angle, deg	0.650	0.689	-0.039
Heading Angle, deg	83.380	82.599	0.781
Crossrange, km (n mi)	32.2 (17.4)	27.3 (14.7)	4.9 (2.7)
Crossrange Velocity, m/s (ft/s)	183.7 (602.7)	177.3 (581.7)	6.4 (21.0)
Geodetic Latitude, deg N	32.087	31.940	0.147
Longitude, deg E	-62.380	-63.791	1.411
S-IVB/CSM SEPARATION			
Range Time, sec	11,198.9	11,160.0	38.9
Altitude, km (n mi)	6,997.9 (3,778.6)	6,866.8 (3,707.8)	131.1 (70.8)
Space-Fixed Velocity, m/s (ft/s)	7,628.9 (25,029.2)	7,667.7 (25,156.5)	-38.8 (-127.3)
Flight Path Angle, deg	45.030	44.741	0.289
Heading Angle, deg	72.315	71.988	0.327
Geodetic Latitude, deg N	26.952	26.764	0.188
Longitude, deg E	-129.677	-130.188	0.511
NOTE: The Range Times used are times of occurrence at the vehicle, reference Figure 2-1.			

Table 4-4. Stage Impact Location

PARAMETER	ACTUAL	NOMINAL	ACT-NOM
S-IC STAGE IMPACT			
Range Time, sec	546.9	544.3	2.6
Surface Range, km (n mi)	658.0 (355.3)	650.4 (351.2)	7.6 (4.1)
Crossrange, km (n mi)	12.1 (6.5)	7.3 (3.9)	4.8 (2.6)
Geodetic Latitude, deg N	30.177	30.197	-0.020
Longitude, deg E	-74.065	-74.153	0.088
S-II STAGE IMPACT			
Range Time, sec	1,258.1	1,241.4	16.7
Surface Range, km (n mi)	4,542.3 (2,452.6)	4,533.7 (2,448.0)	8.6 (4.6)
Crossrange, km (n mi)	150.1 (81.0)	149.1 (80.5)	1.0 (0.5)
Geodetic Latitude, deg N	31.320	31.316	0.004
Longitude, deg E	-33.289	-33.383	0.094

4.2.2 Parking Orbit Phase

Orbital tracking data for six passes was obtained from four C-Band stations and one S-Band station of the NASA Manned Space Flight Network.

The parking orbit trajectory was calculated by integrating corrected insertion conditions forward to 8950 seconds. The insertion conditions, as determined by the Orbital Correction Program, were obtained by a differential correction procedure which adjusted the estimated insertion conditions to fit the tracking data in accordance with the weights assigned to the data. The venting model, utilized to fit the tracking data, was derived from telemetered guidance velocity data from the ST-124M-3 guidance platform.

The actual and nominal parking orbit insertion parameters are presented in Table 4-5. The ground track from insertion to S-IVB/CSM separation is given in Figure 4-5.

Table 4-5. Parking Orbit Insertion Conditions

PARAMETER	ACTUAL	NOMINAL	ACT-NOM
Range Time, sec	759.83	715.76	44.07
Altitude, km (n mi)	191.6 (103.5)	191.4 (103.3)	0.2 (0.2)
Space-Fixed Velocity, m/s (ft/s)	7,792.5 (25,565.9)	7,793.0 (25,567.6)	-0.5 (-1.7)
Flight Path Angle, deg	0.005	0.000	0.005
Heading Angle, deg	90.148	88.918	1.230
Inclination, deg	32.525	32.539	-0.014
Descending Node, deg	123.084	123.125	-0.041
Eccentricity	0.0001	0.0000	0.0001
Apogee*, km (n mi)	185.7 (100.3)	185.2 (100.0)	0.5 (0.3)
Perigee*, km (n mi)	183.9 (99.3)	185.1 (99.9)	-1.2 (-0.6)
Period, min	88.19	88.19	0.00
Geodetic Latitude, deg N	32.694	32.692	0.002
Longitude, deg E	-50.490	-52.552	2.062

NOTE: The Range Times used are times of occurrence at the vehicle, reference Figure 2-1.

*Based on a spherical earth of radius 6,378.165 km (3,443.934 n mi).

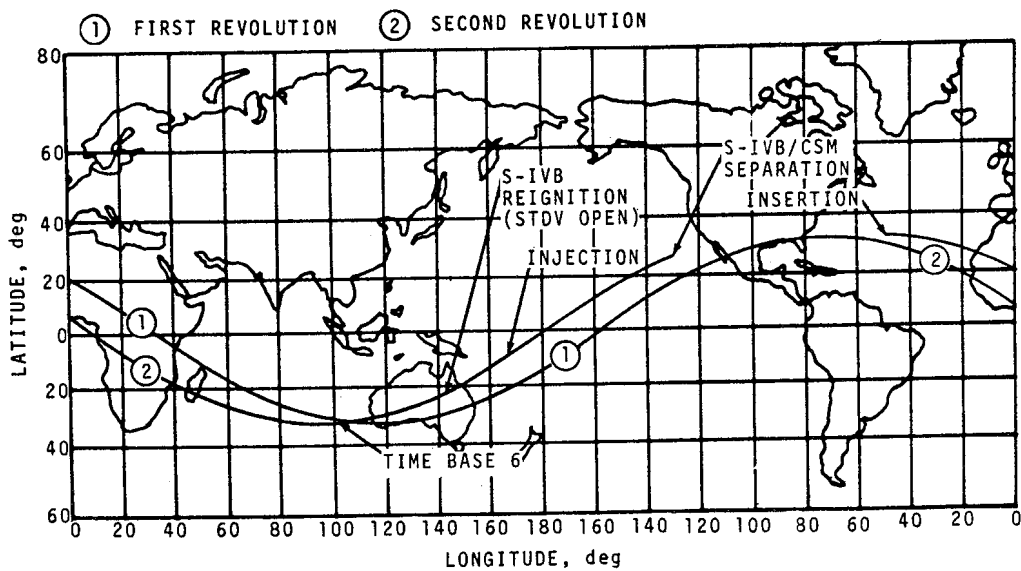


Figure 4-5. Ground Track

4.2.3 Injection Phase

The injection phase trajectory was generated by the integration of the telemetered guidance accelerometer data. These accelerometer data were initialized from a parking orbit state vector at 8950 seconds and were constrained to a state vector at TLI obtained from the post TLI trajectory. There were no tracking data available during S-IVB second burn.

Comparisons between the actual and nominal space-fixed velocity and flight path angle are shown in Figure 4-6. The actual and nominal total inertial acceleration comparisons are presented in Figure 4-7. The space-fixed velocity and flight path angle were greater than nominal with deviations more noticeable towards the end of the time period. The actual and nominal targeting parameters at S-IVB second guidance cutoff are presented in Table 4-2.

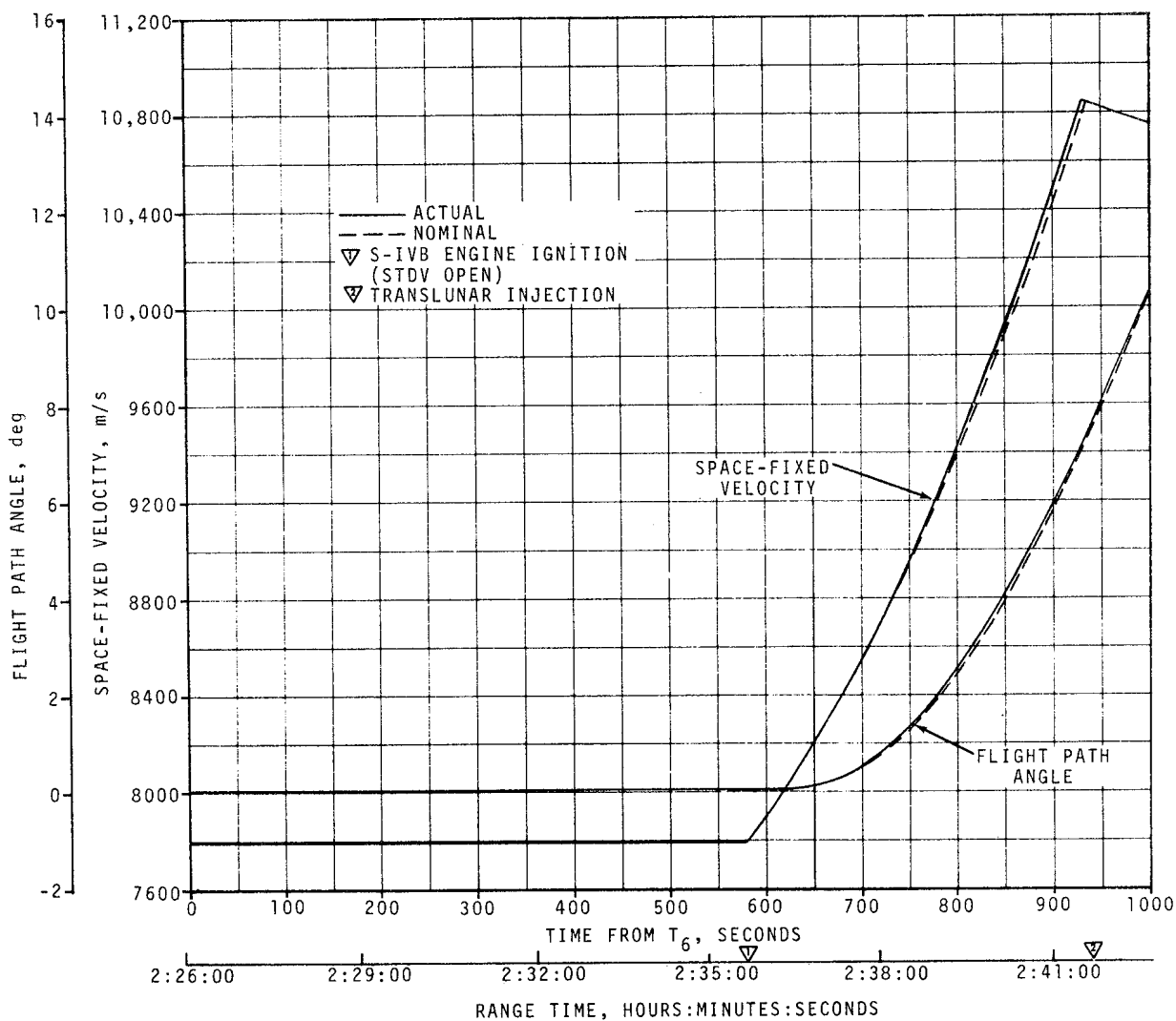


Figure 4-6. Injection Phase Space-Fixed Velocity and Flight Path Angle Comparisons

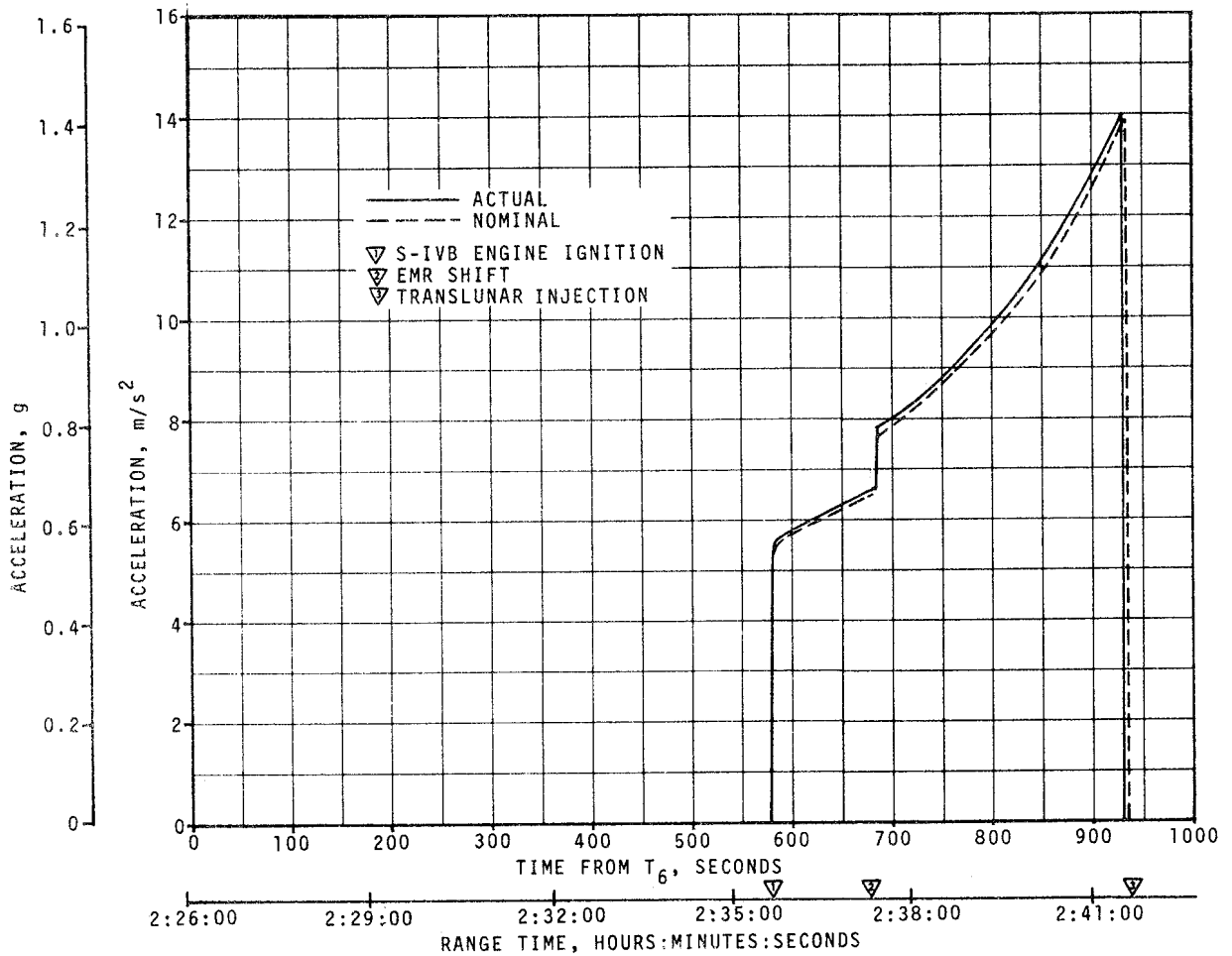


Figure 4-7. Injection Phase Acceleration Comparison

4.2.4 Post TLI Phase

The post TLI trajectory spans the interval from translunar injection to S-IVB/CSM separation. Tracking data from three C-Band stations and three S-Band stations were utilized in the reconstruction of this trajectory segment. The post TLI trajectory reconstruction utilizes the same methodology as outlined in paragraph 4.2.2. The actual and nominal translunar injection conditions are compared in Table 4-6. The S-IVB/CSM separation conditions are presented in Table 4-3.

Table 4-6. Translunar Injection Conditions

PARAMETER	ACTUAL	NOMINAL	ACT-NOM
Range Time, sec	9,707.15	9,693.59	13.56
Altitude, km (n mi)	337.9 (182.5)	342.4 (184.9)	-4.5 (-2.4)
Space-Fixed Velocity, m/s (ft/s)	10,832.1 (35,538.4)	10,828.4 (35,526.2)	3.7 (12.2)
Flight Path Angle, deg	7.635	7.676	-0.041
Heading Angle, deg	59.318	59.299	0.019
Inclination, deg	31.817	31.833	-0.016
Descending Node, deg	122.997	123.031	-0.034
Eccentricity	0.9772	0.9772	0.0000
C ₃ , m ² /s ² (ft ² /s ²)	-1,376,274 (-14,814,090)	-1,376,265 (-14,813,993)	-9 (-97)
NOTE: The Range Times used are times of occurrence at the vehicle, reference Figure 2-1			

SECTION 4A

LUNAR IMPACT

4A.1 SUMMARY

All aspects of the S-IVB/IU Lunar Impact objective were accomplished successfully except the precise determination of impact point. The final impact solution is expected to satisfy the mission objective. At 280,599.7 \pm 0.1 seconds (77:56:39.7) vehicle time the S-IVB/IU impacted the lunar surface at approximately 2.5 \pm 0.5 degrees south latitude and 27.9 \pm 0.1 degrees west longitude, which is approximately 65.5 \pm 7.8, -4.8 kilometers (35.4 \pm 4.2, -2.6 n mi) from the target of 3 degrees south latitude and 30 degrees west longitude. Impact velocity was 2579 m/s (8461 ft/s). The mission objectives were to maneuver the S-IVB/IU such that it would have at least a 50 percent probability of impacting the lunar surface within 350 kilometers (189 n mi) of the target, and to determine the actual impact point within 5 kilometers (2.7 n mi) and the time of impact within 1 second.

Preliminary results of the seismic experiment indicate that the S-IVB/IU impact signal was 20 to 30 times greater in amplitude and four times longer in duration than the Apollo 12 Lunar Module (LM) impact.

4A.2 TIME BASE 8 MANEUVERS

The Auxiliary Propulsion System (APS) evasive burn, Continuous Vent System (CVS) vent, LOX dump, and APS lunar impact burn occurred as planned and were close to nominal. Following CSM/LM ejection, the vehicle was maneuvered to an inertially fixed attitude as required for the evasive APS burn. After the evasive attitude was attained, Time Base 8 (T₈) was initiated 239.3 seconds later than nominal at 15,479.4 seconds (04:17:59.4) and the APS ullage engines burned for 80 seconds to provide the required spacecraft/launch vehicle separation velocity. At 16,060.0 seconds (04:27:40.0), the stage maneuvered to the CVS/LOX dump attitude. The initial lunar targeting velocity change was accomplished by means of a 300-second duration CVS vent and 48-second duration LOX dump. The S-IVB/IU was targeted to a lunar impact of 9.0 degrees south latitude and 72.3 degrees west longitude (selenographic coordinates); however, this impact point was not sufficiently close to the desired target. A maneuver consisting of an attitude change and an APS ullage engine burn to occur at 21,600 seconds (06:00:00), in order to improve the targeting, was

defined at approximately 18,000 seconds (05:00:00) at the Huntsville Operations Support Center (HOSC). The maneuver was based on a post-Translunar Injection (TLI) tracking vector sent from the Mission Control Center (MCC) and received at Marshall Space Flight Center (MSFC) prior to T_g as planned. The maneuver considered actual event times and velocity increments of the APS evasive burn, CVS vent and LOX dump. The velocity increments were obtained in real-time by telemetered accelerometer measurements. At 19,200 seconds (05:20:00), the maneuver command was transmitted to MCC, and at 20,887 seconds (05:48:07), the command was uplinked to the IU. The S-IVB/IU maneuvered -1 degree in pitch and -3 degrees in yaw. The resulting attitude was 182 degrees in pitch and -8 degrees in yaw, referenced to the local horizontal system. At this attitude and at approximately 21,600 seconds (06:00:00), the APS ullage engines burned for a duration of 217 seconds, as commanded.

At 27,900 seconds (07:45:00) a tracking vector, which included data subsequent to the 217-second APS burn, was sent from the MCC to MSFC as planned. This vector was integrated out to lunar distance and indicated that the stage would impact the moon within 200 kilometers (108 n mi) of the desired target. This vector indicated that no additional targeting maneuvers would be required to assure that the spent stage would have at least a 50 percent probability of impacting within a 350-kilometer (189-n mi) radius of the target.

Tracking vectors were received at regular intervals, and indicated that the S-IVB/IU would impact approximately 200 kilometers (108 n mi) southwest of the target site. At 70,150 seconds (19:29:10), a shift was observed in range rate tracking data and was interpreted as a velocity change due to a propulsive force acting on the spent stage. This velocity change is discussed in paragraph 10.4.4. Figure 4A-1 shows a decrease in range rate of approximately 2 to 3 m/s (7 to 10 ft/s) beginning at 70,150 seconds (19:29:10). The decrease in range rate lasted approximately 60 seconds. The projected impact location of all subsequent tracking vectors out to actual lunar impact were slightly east of the target. The velocity change altered the predicted lunar impact point approximately 5 degrees in latitude, 150 kilometers (81 n mi), closer to the target. Analysis of the projected impact points before and after the unscheduled velocity change indicates that a velocity change of approximately 2.5 m/s (8.2 ft/s) at an attitude of 181 degrees pitch and -33 degrees yaw would cause an identical perturbation to the translunar trajectory. It should be noted that this is a representative perturbation effect and that there exists a family of such perturbations that would result in the same impact conditions. However, if the velocity change had occurred in less favorable directions the stage would not have impacted within the prescribed limits.

Table 4A-1 shows the actual and nominal velocity increments along the S-IVB/IU longitudinal body axis. Figure 4A-2 shows the velocity change

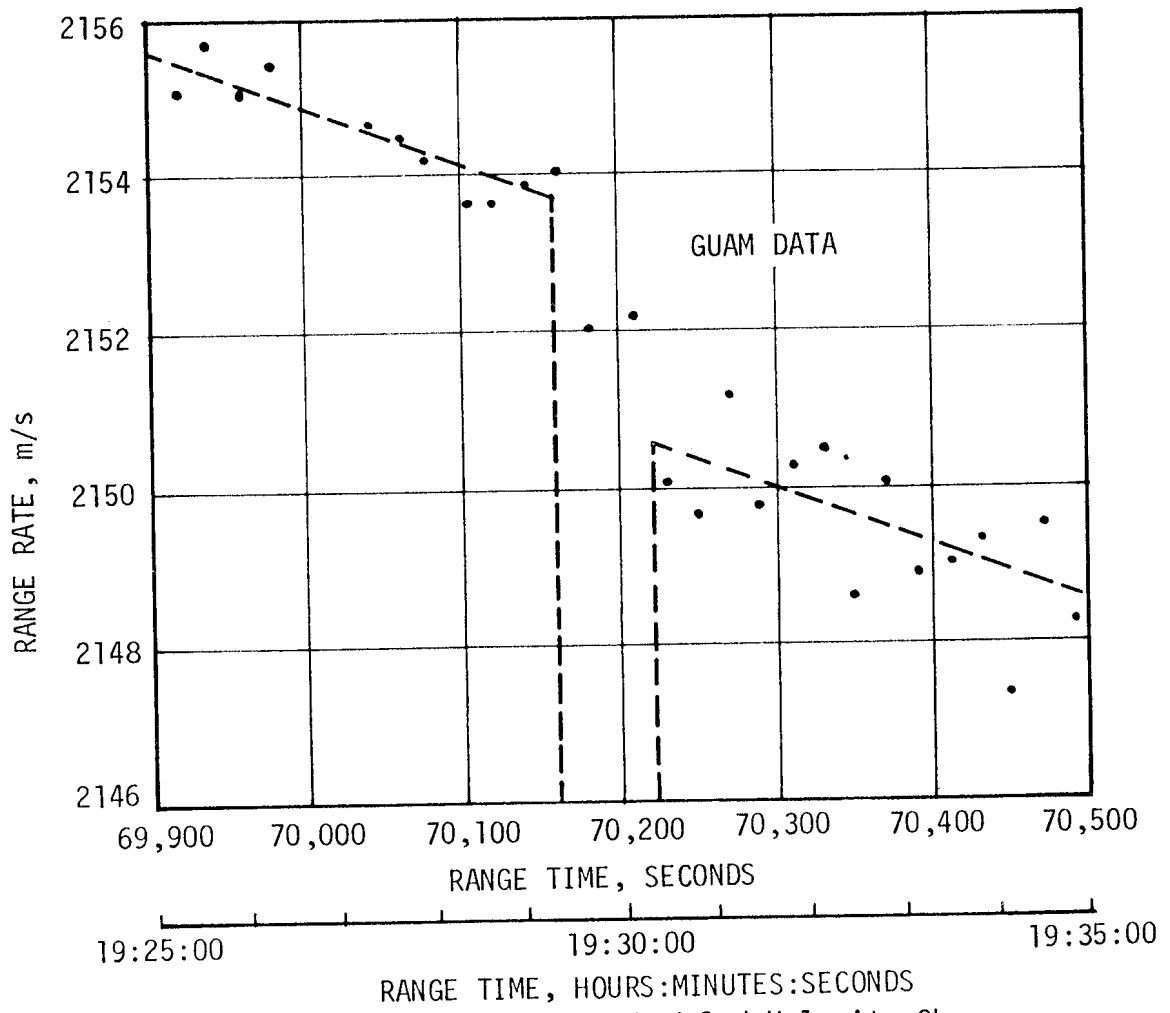
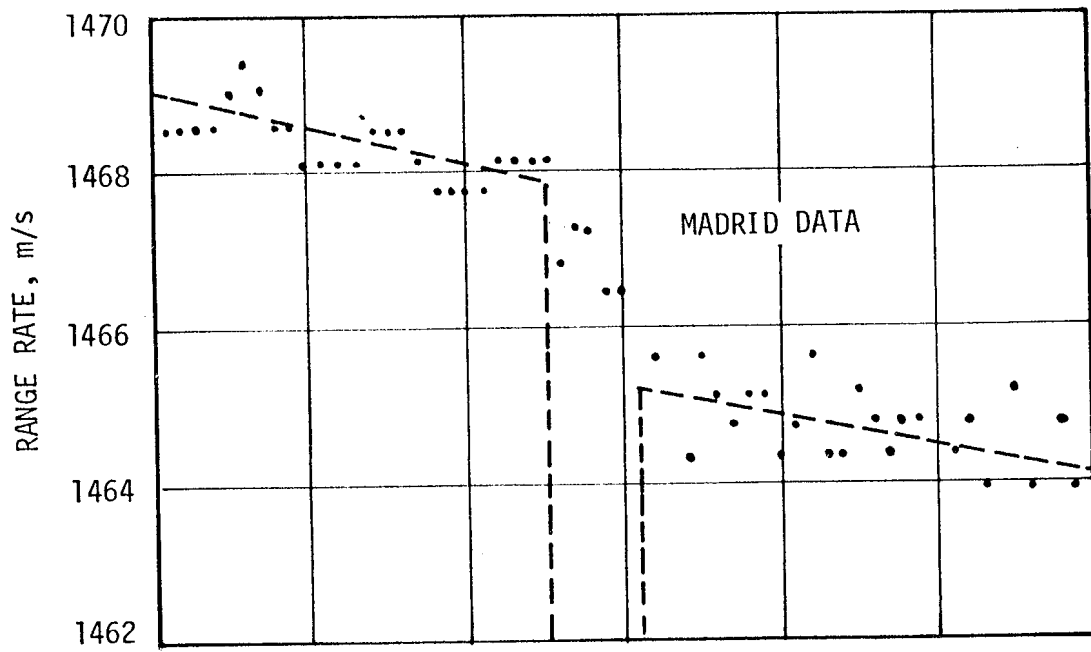


Figure 4A-1. S-IVB/IU Unscheduled Velocity Change

Table 4A-1. Comparison of Time Base 8 Velocity Increments

PARAMETER	ACTUAL	NOMINAL	ACT-NOM
APS Evasive Burn (80 seconds duration), m/s (ft/s)	2.98 (9.78)	2.90 (9.51)	0.08 (0.27)
CVS Vent (300 seconds duration), m/s (ft/s)	0.44 (1.44)	0.50 (1.64)	-0.06 (-0.20)
LOX Dump (48 seconds duration), m/s (ft/s)	8.73 (28.64)	8.30 (27.23)	0.43 (1.41)
APS Lunar Impact Burn (217 seconds duration), m/s (ft/s)	9.12 (29.92)	9.21* (30.22)	-0.09** (-0.30)

*Based on actual velocity increments from APS evasive burn, CVS, and LOX dump. Calculated in Real-Time.
 **Actual-Calculated.

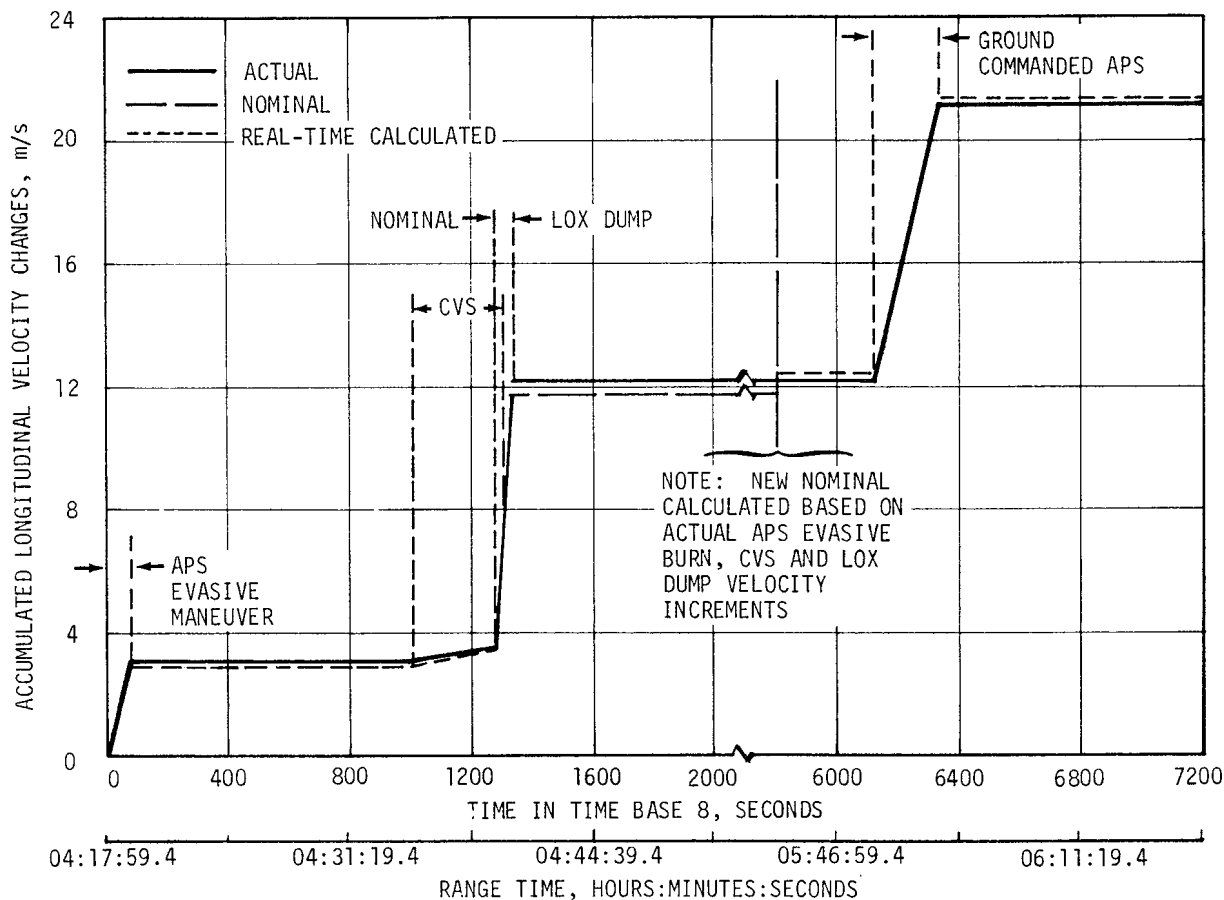


Figure 4A-2. Accumulated Longitudinal Velocity Change During Time Base 8

profile during T_8 . Table 4A-2 shows the actual and nominal attitudes at which the various events during T_8 were performed. The difference between the actual and nominal attitudes for the APS lunar impact burn is the magnitude of the commanded maneuver at 20,887 seconds (05:48:07).

4A.3 TRAJECTORY EVALUATION

Figure 4A-3 shows the radius and space-fixed velocity (earth centered) profiles from the APS lunar impact burn to lunar impact. Table 4A-3 shows the actual and nominal orbit parameters following the unscheduled velocity change. The orbit parameters are two-body calculations. The orbit parameters indicate a slightly lower energy orbit than nominal which is consistent with the actual impact location being further east than the target site. An increasing underspeed condition causes the impact point to move in a west to east direction.

4A.4 LUNAR IMPACT CONDITION

Figure 4A-4 shows various impact points relative to the target and seismometer locations. There are three significant comparisons to be made from this figure. First, comparison of the impact point of the TLI IU state vector (with actual velocity increments modeled through the APS lunar impact burn) with the projected impact site, prior to the unscheduled velocity change, shows the approximate projected error in the IU state vector at TLI. Second, comparison of the impact

Table 4A-2. Comparison of Attitude Time Line, Time Base 8

EVENT	ACTUAL		NOMINAL		ACT-NOM	
	PITCH	YAW	PITCH	YAW	PITCH	YAW
APS Evasive Burn, deg	176	40	176	40	0	0
CVS Vent, deg	183	-5	183	-5	0	0
LOX Dump, deg	183	-5	183	-5	0	0
APS Lunar Impact Burn, deg	182	-8	183	-5	-1	-3

NOTE: Attitudes referenced to Local Horizontal System.

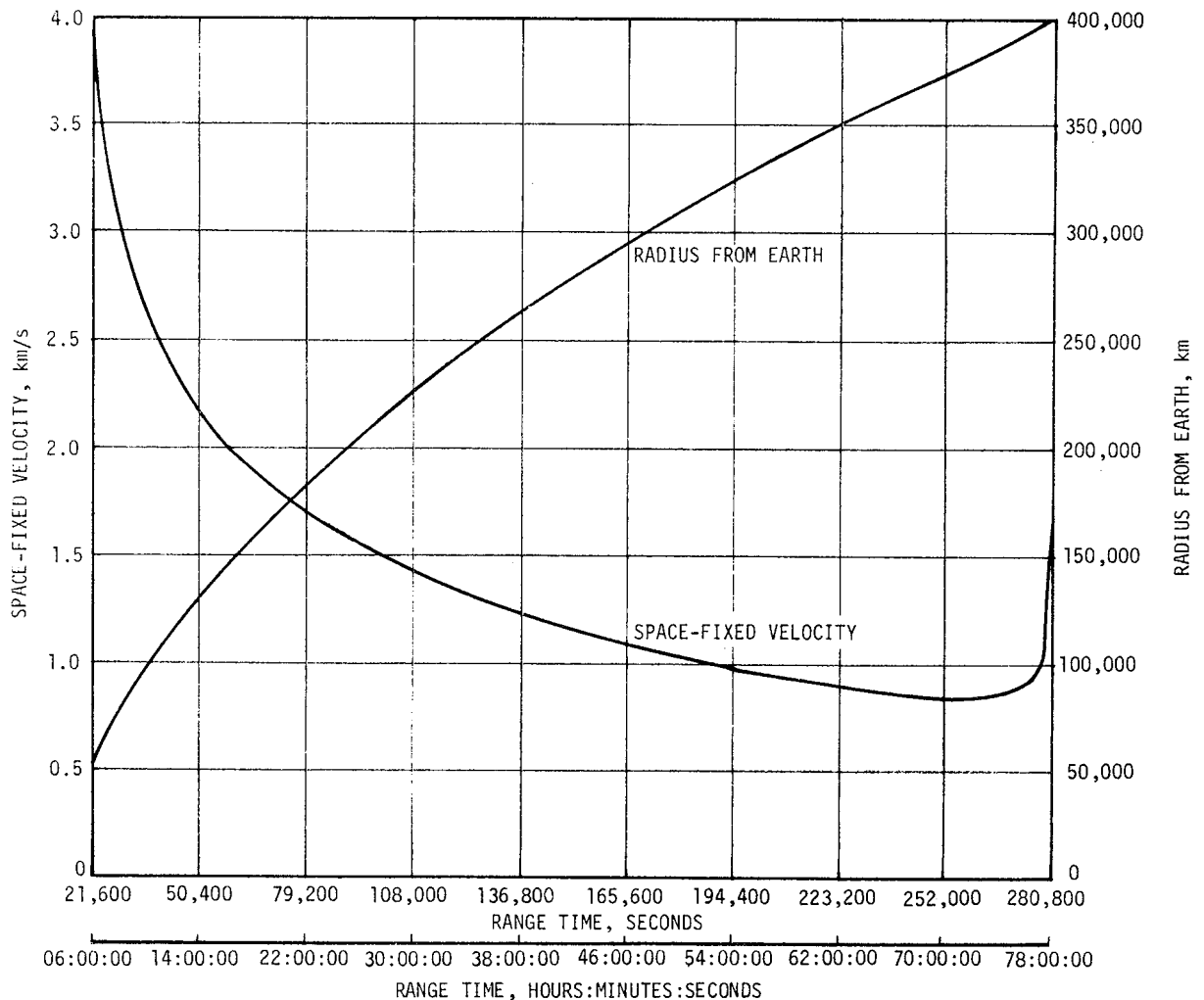


Figure 4A-3. Lunar Impact Trajectory Radius and Space-Fixed Velocity Profiles

point, prior to the unscheduled velocity change, with the target site shows the actual miss distance due to real-time targeting. Third, a comparison of the actual impact point with the target and seismometer locations illustrates actual miss distances. The miss distances with other impact parameters are shown in Table 4A-4. A summary of impact times recorded by the various tracking sites is shown in Table 4A-5. The average of the recorded times was used as the best available time of impact, and is considered accurate to within 0.1 second.

Preliminary results of the seismic experiment are that the overall characteristic of the seismic signal due to S-IVB/IU impact is similar to that of the Apollo 12 LM impact signal. The S-IVB/IU signal was 20 to 30 times greater in amplitude and four times longer in duration (approximately 4 hours versus 1 hour) than the Apollo 12 LM impact. A period of 30 seconds elapsed between time of impact and arrival of

Table 4A-3. Comparison of Orbit Parameters After the Unscheduled Delta V

PARAMETER	ACTUAL	NOMINAL	ACT-NOM
Semimajor Axis, km (n mi)	266,092 (143,678)	267,411 (144,390)	-1319 (-712)
Eccentricity	0.97585	0.97605	-0.00020
Inclination, deg*	31.8317	31.8498	-0.0181
C_3 , m^2/s^2 (ft^2/s^2)	-1,497,990 (-16,124,162)	-1,490,600 (-16,044,617)	-7390 (-79,545)
Right Ascension of Ascending Node, deg	170.1472	170.1475	-0.0003
Argument of Perigee, deg	249.655	248.623	1.032
Perigee Altitude, km (n mi)	47 (25)	25 (13)	22 (12)
Apogee Altitude, km (n mi)	519,381 (280,443)	522,040 (281,879)	-2659 (-1436)

*Referenced to earth's equatorial plane.

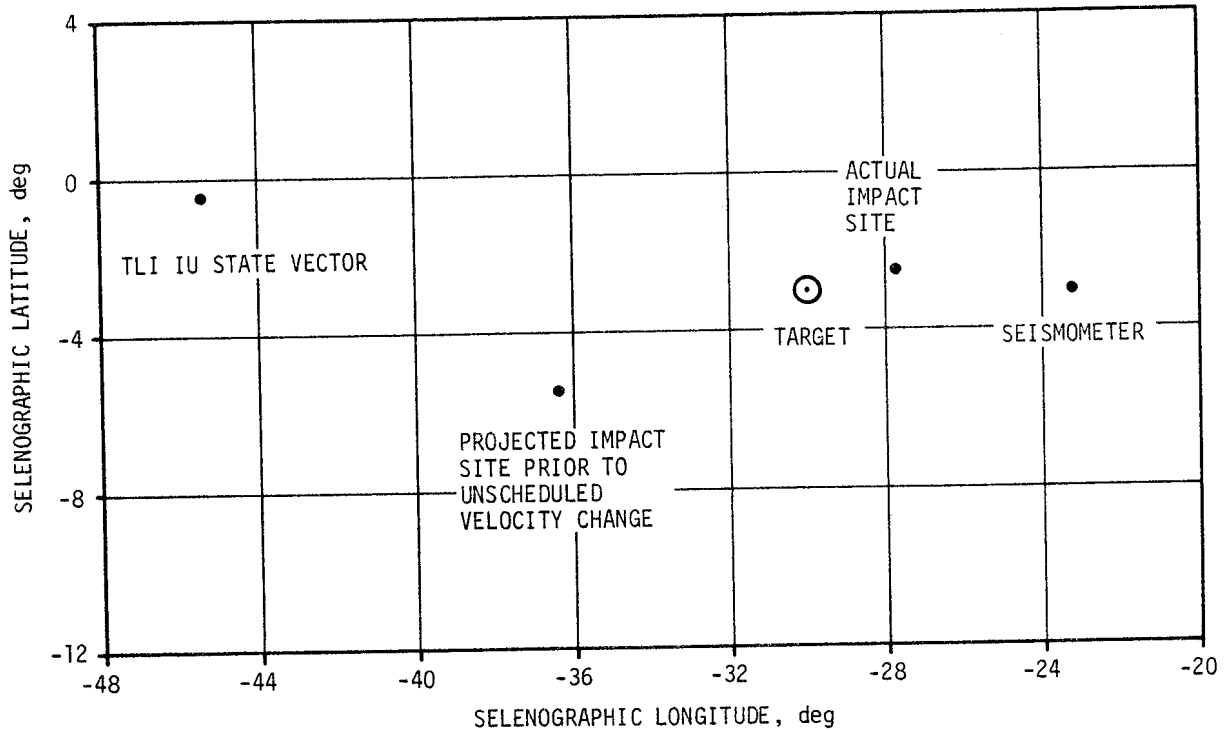


Figure 4A-4. Comparison of Projected Lunar Impact Points

Table 4A-4. S-IVB/IU Lunar Impact Parameters

PARAMETER AT IMPACT	ACTUAL	NOMINAL	ACT-NOM
Stage Mass, kg (lbm)	13,426* (29,599)*	13,395 (29,532)	31 (67)
Moon Centered Space-Fixed Velocity, m/s (ft/s)	2579 (8461)	2580 (8464)	-1 (-3)
Path Angle Measured from Local Vertical, deg	13.2	12.0	1.2
Heading Angle (North to West), deg	100.6	100.0	0.6
Tumble Rate, deg/s	12†	N.A.	N.A.
Selenographic West Longitude, deg	27.9 ±0.1	30.0	-2.1 ±0.1
Selenographic South Latitude, deg	2.5 ±0.5	3.0	-0.5 ±0.5
Impact Time, HR:MIN:SEC**	77:56:39.7	77:45:00	00:11:39.7
Distance to Target, km (n mi)	65.5 +7.8 -4.8 (35.4 +4.2) -2.6)	0 (0)	65.5 +7.8 -4.8 (35.4 +4.2) -2.6)
Distance to Seismometer, km (n mi)	139.1 +5.4 -3.8 (75.1 +2.9) -2.1)	0 (0)	139.1 +5.4 -3.8 (75.1 +2.9) -2.1)
*Stage dry weight - all residual propellants assumed dissipated. **Actual time (Signal delay time = 1.323 sec).			

the seismic wave at the seismometer. Peak intensity of the seismometer signal occurred approximately 450 seconds after impact. In addition to the seismic data, the Suprathermal Ion Detector Experiment (SIDE) recorded an increase in the ion count 22 seconds after impact.

A more accurate determination of the impact location and related analyses is continuing.

4A.5 TRACKING

Approximately 75 hours of S-IVB/IU tracking data, from TLI to lunar impact, were obtained. Prior to activating the LM communication system, both Goddard Space Flight Center (GSFC) and Manned Spacecraft Center (MSC)

Table 4A-5. Summary of Lunar Impact Times

TRACKING STATION	RECORDED IMPACT TIME, HR:MIN:SEC	
	GREENWICH MEAN TIME APRIL 15, 1970	RANGE TIME
Madrid	01:09:41.025	77:56:41.025
Ascension	01:09:41.04	77:56:41.04
GSFC (ETC 3)	01:09:41.01	77:56:41.01
Goldstone	01:09:41.02	77:56:41.02
Hawaii	01:09:41.015	77:56:41.015
MILA	01:09:41.026	77:56:41.026
Average	01:09:41.023	77:56:41.023

NOTE: Signal Delay Time = 1.323 sec
 Actual Impact Time = 77:56:39.7 ±0.1 sec

monitored and analyzed the data in real-time; however, after the CSM problem began, only GSFC continued to analyze real-time data and provide tracking vectors. Figure 4A-5 shows the data considered by GSFC in the orbit and impact location determinations. Table 4A-6 lists the tracking sites, their configuration sizes, and abbreviations used.

An increase in the spent stage tumble rate after the unscheduled velocity change caused the range rate data to be relatively noisy, which hindered an accurate determination of the actual impact point to date. There was a temporary tracking frequency conflict between the LM and IU which resulted in the loss of some tracking data. The frequency conflict was solved by driving the IU frequency off-center in order to differentiate between the LM and IU signals, as discussed in paragraph 15.6. The final solution of the actual impact coordinates are expected to be accurate to within 0.10 degree in latitude, and 0.05 degree in longitude which is within approximately 3.4 kilometers (1.8 n mi).

Table 4A-6. S-IVB/IU CCS Tracking Network

STATION	CONFIGURATION	ABBREVIATION
Madrid, Spain	Main Site - 85 ft dish Wing Site - 85 ft dish	MAD MADX
Honeysuckle Creek, Australia	Main Site - 85 ft dish Wing Site - 85 ft dish	HSK HSKX
Goldstone, California	Main Site - 85 ft dish Wing Site - 85 ft dish	GDS GDSX
Merritt Island, Florida	30 ft dish	MIL
Canary Island	30 ft dish	CYI
Ascension Island	30 ft dish	ACN
Carnarvon, Australia	30 ft dish	CRO
Guam Island	30 ft dish	GWM
Hawaii	30 ft dish	HAW
Guaymas, Mexico	30 ft dish	GYM
Corpus Christi, Texas	30 ft dish	TEX
Goddard Experimental Test Center	30 ft dish	ETC 3

SECTION 5

S-IC PROPULSION

5.1 SUMMARY

All S-IC propulsion systems performed satisfactorily and the propulsion performance level was very close to predicted. Stage site thrust (averaged from liftoff to Outboard Engine Cutoff [OECO]) was 0.26 percent higher than predicted. Total propellant consumption rate was 0.06 percent higher than predicted with the total consumed Mixture Ratio (MR) 0.24 percent higher than predicted. Specific impulse was 0.20 percent higher than predicted. Total propellant consumption from Holddown Arm (HDA) release to OECO was low by 0.06 percent.

Center Engine Cutoff (CECO) was initiated by the Instrument Unit (IU) at 135.18 seconds as planned. Outboard engine cutoff, initiated by LOX low level sensors, occurred at 163.60 seconds which was 0.40 second earlier than predicted. This is a small difference compared to the predicted 3-sigma limits of +5.58, -3.89 seconds. The LOX residual at OECO was 38,921 lbm compared to the predicted 39,403 lbm. The fuel residual at OECO was 27,573 lbm compared to the predicted 31,957 lbm.

There were three unplanned events that occurred during the S-IC countdown and boost, although they did not cause launch delay or problems during flight. These events were:

- a. LOX tank vent and relief valve temporarily stuck open during countdown.
- b. The planned 1-2-2 start sequence was not attained.
- c. Engine No. 2 LOX pump bearing jet pressure exhibited unexpected shifts and operated at a higher level than predicted.

S-IC hydraulic system performance was normal throughout the flight.

5.2 S-IC IGNITION TRANSIENT PERFORMANCE

The fuel pump inlet preignition pressure was 45.7 psia and within F-1 Engine Model Specification limits of 43.5 to 110 psia.

The LOX pump inlet preignition pressure and temperature were 82.5 psia and -285.1°F and were within the F-1 Engine Model Specification limits, as shown in Figure 5-1.

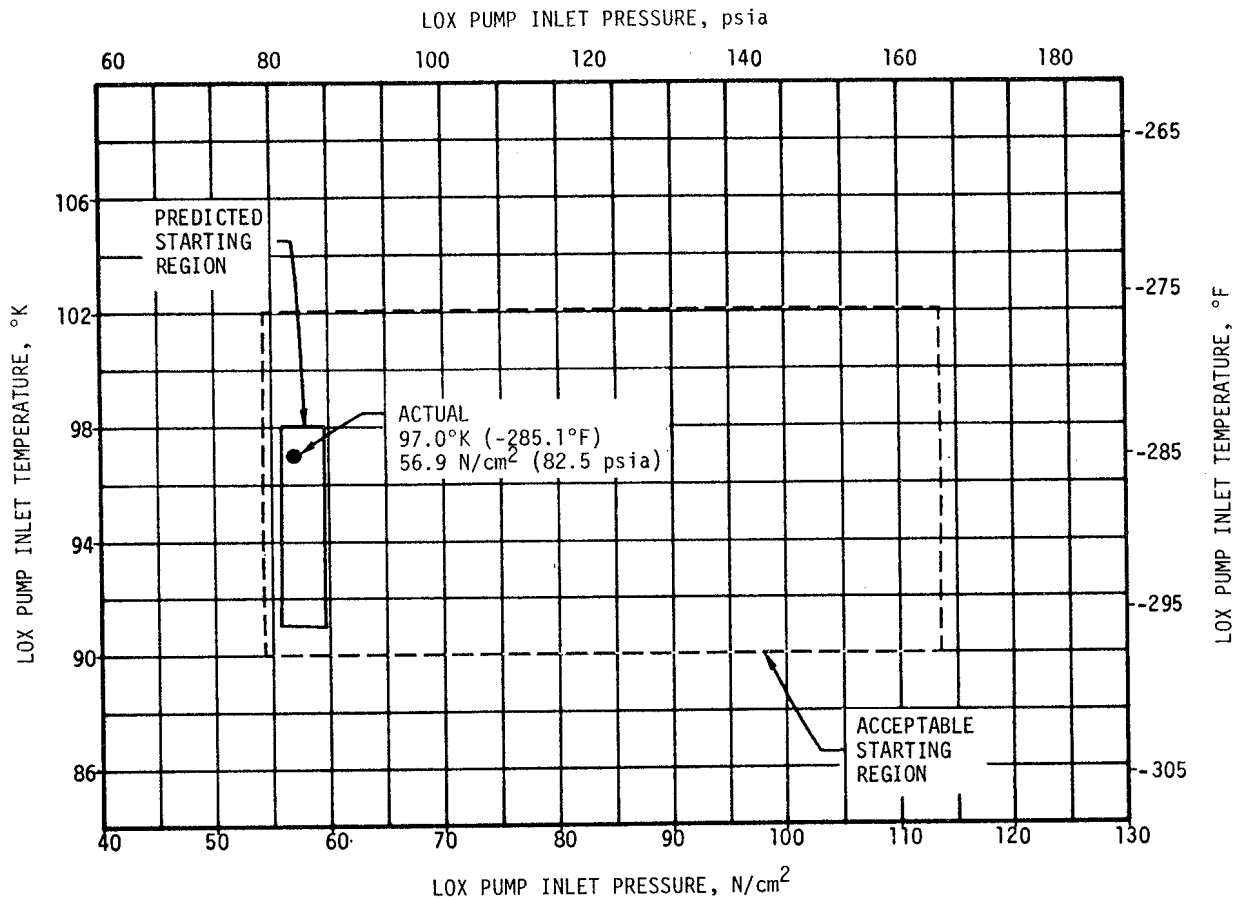


Figure 5-1. S-IC LOX Start Box Requirements

The planned 1-2-2 start was not attained since engines No. 2 and 4 combustion chamber pressures did not reach 100 psig within the desired 100-millisecond time period. See Figure 5-2. Engine No. 4 reached 100 psig chamber pressure 0.303 second slower than predicted and 0.317 second later than engine No. 2, resulting in a 1-2-1-1 start. Structurally, a 1-2-2 start is desired for minimizing the start and liftoff dynamics caused by thrust buildup of the engines. Each F-1 engine has distinctive starting characteristics requiring individually programmed start signals in order to minimize the dispersions in achieving the planned start sequence. Determination of start signal presettings is one objective of static firing the S-IC stage. Engine No. 4 was replaced after the stage static firing. Consequently, only single engine firing data for engine No. 4 was available for determining the start signal presetting. It is well known that presettings based only on single engine firings are inaccurate, therefore the AS-508 1-2-1-1 start was not unexpected. The 1-2-1-1 start caused no problems.

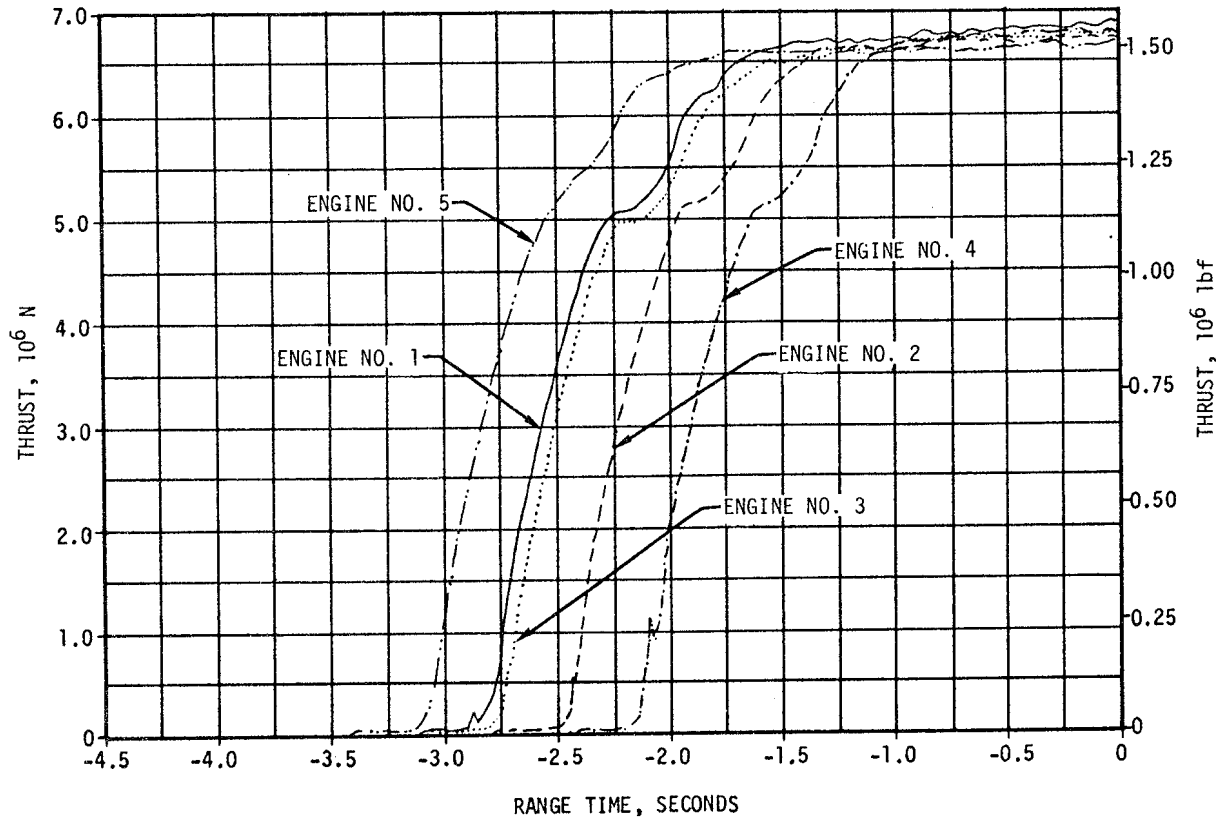


Figure 5-2. S-IC Engines Thrust Buildup

5.3 S-IC MAINSTAGE PERFORMANCE

S-IC stage propulsion performance was very close to the predicted level, as shown in Figure 5-3. The stage site thrust (averaged from range time zero to OECO) was 0.26 percent higher than predicted.

Total propellant consumption rate was 0.06 percent higher than predicted and the total consumed propellant MR was 0.24 percent higher than predicted. The specific impulse was 0.20 percent higher than predicted. Total propellant consumption from HDA release to OECO was low by 0.06 percent.

For comparison of F-1 engine flight performance with predicted performance, the flight performance has been analytically reduced to standard conditions and compared to the predicted performance which is based on ground firings and also reduced to standard conditions. These values are shown in Table 5-1 at the 35 to 38-second time slice. Individual engine deviations from predicted thrust ranged from 0.199 percent lower (engine No. 2) to 0.397 percent higher (engine No. 3). Individual engine deviations from specific impulse ranged from 0.038 percent lower (engines No. 2, 4, and 5) to 0.038 percent higher (engines No. 1 and 3).

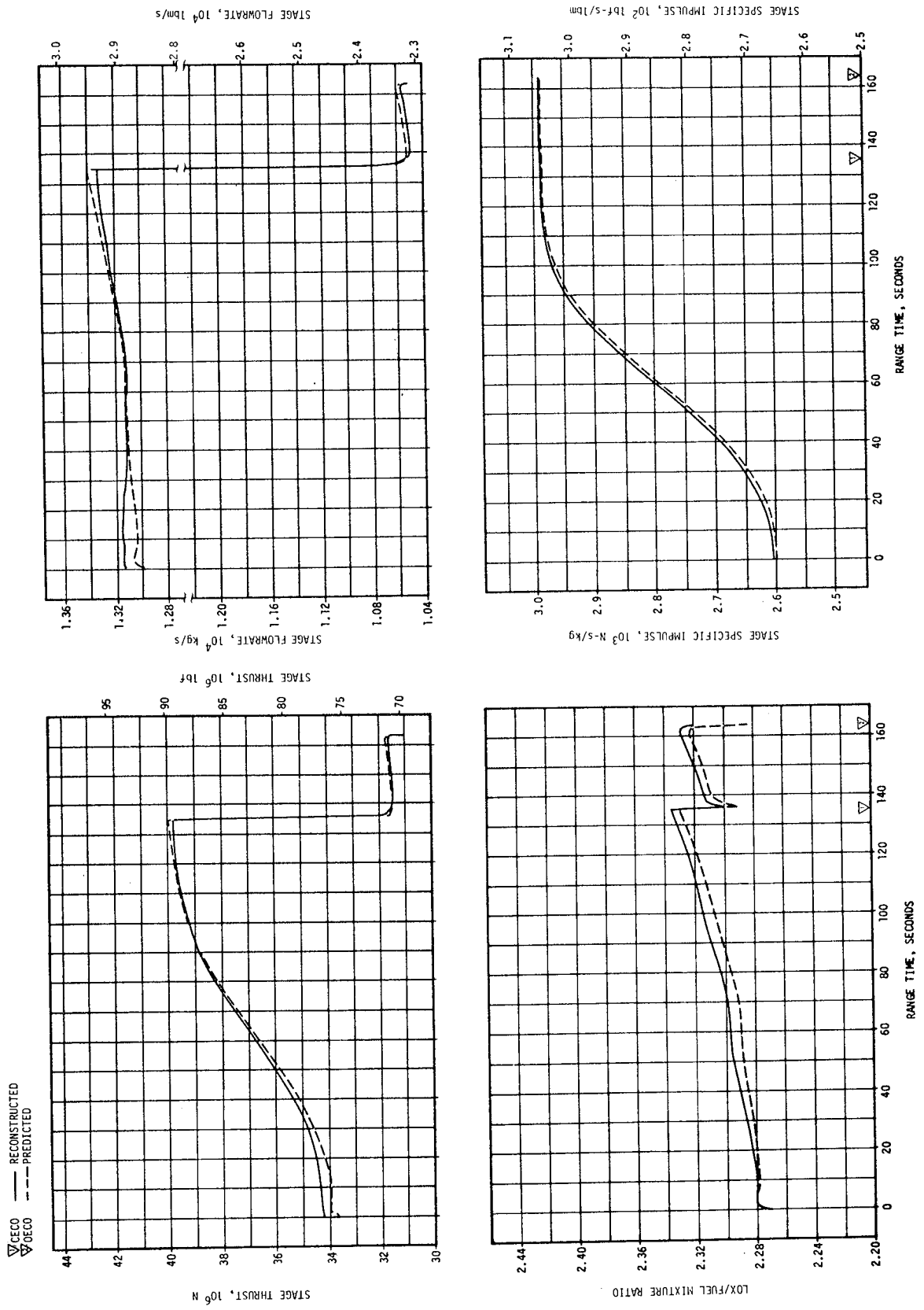


Figure 5-3. S-IC Stage Propulsion Performance

Table 5-1. S-IC Individual Engine Performance

PARAMETER	ENGINE	PREDICTED	RECONSTRUCTION ANALYSIS	DEVIATION PERCENT	AVERAGE DEVIATION PERCENT
Thrust, 10 ³ lbf	1	1514	1520	0.396	0.053
	2	1504	1501	-0.199	
	3	1510	1516	0.397	
	4	1516	1513	-0.198	
	5	1512	1510	-0.132	
Specific Impulse, lbf-s/lbm	1	264.5	264.6	0.038	-0.008
	2	264.9	264.8	-0.038	
	3	264.8	264.9	0.038	
	4	266.0	265.9	-0.038	
	5	264.7	264.6	-0.038	
Total Flowrate lbm/s	1	5724	5746	0.384	0.052
	2	5680	5670	-0.176	
	3	5702	5722	0.351	
	4	5698	5689	-0.158	
	5	5713	5705	-0.140	
Mixture Ratio LOX/Fuel	1	2.272	2.268	-0.176	-0.088
	2	2.256	2.255	-0.044	
	3	2.260	2.257	-0.133	
	4	2.261	2.260	-0.044	
	5	2.242	2.241	-0.045	
NOTE: Performance levels were reduced to standard sea level and pump inlet conditions. Data was taken from the 35 to 38-second time slice.					

Engine No. 2 (S/N F2058) LOX pump bearing jet pressure stabilized initially at 468 psia, approximately 88 psi higher than that demonstrated during acceptance and stage static tests. At 10 seconds, the jet pressure sharply increased 48 psi to a level of 516 psia and remained stable at that level until 88 seconds, at which time it sharply decayed 78 psi and remained stable at a pressure of approximately 438 psia until OECO. At no time did the pressure exceed the ground test redline value of 555 psia, see Figure 5-4.

The F-1 turbopump has three shaft bearings. Each bearing is cooled during operation by fuel which is routed from the fuel pump discharge volute, through the bearing coolant valve which filters the fuel and reduces fuel pressure to the desired level and then through three jets, for each bearing, which direct the fuel onto the bearing surfaces.

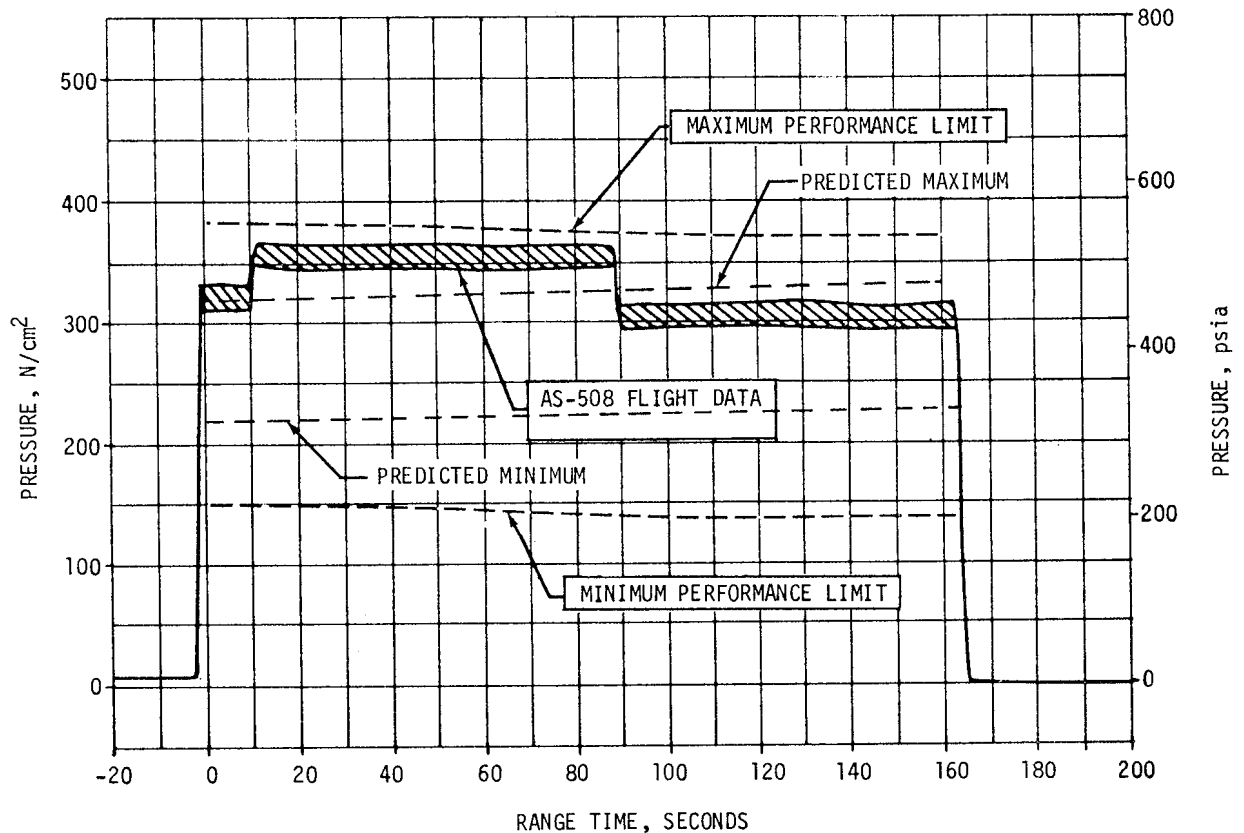


Figure 5-4. F-1 LOX Pump Bearing Jet Pressure, Engine No. 2

The bearing jet pressure changes, experienced by engine No. 2, were probably due to contaminant restrictions within the bearing jets. It is postulated that one of the nine jets was restricted prior to attaining the stabilized operating level, which would account for the initial level being higher than expected. At 10 seconds another jet could have become restricted, resulting in the pressure increase. At 88 seconds the initial restriction could have become dislodged resulting in a pressure decrease.

Similar turbopump bearing jet pressure changes have been experienced during single engine testing without any accompanying turbopump problems. Several turbopumps which experienced a pressure increase were disassembled prior to subsequent testing and disclosed no hardware damage; however, machining particle contamination of the jet assembly was found. Consequently, an improved manufacturing cleaning procedure was instituted. No similar jet pressure increases have occurred since incorporation of this cleaning procedure. The only remaining flight engines not incorporating the improved cleaning procedure are engine S/N F2059 installed in stage S-IC-11, and engine S/N F2061 installed in stage S-IC-9. Engines S/N F2059 and S/N F2061 acceptance and stage test data indicated normal turbopump bearing jet pressure characteristics.

The turbopump bearing coolant system incorporates redundancy by having three jets for each bearing. Furthermore, machine particle contamination, as previously noted, is usually associated with the number two bearing which receives additional coolant fluid from the number one bearing drainage. The occurrence of a bearing jet pressure discrepancy during flight, similar to that experienced by engine S/N F2058 during the AS-508 flight, is not considered detrimental to F-1 engine turbopump reliability.

5.4 S-IC ENGINE SHUTDOWN TRANSIENT PERFORMANCE

Center engine cutoff, initiated by a signal from the IU, was at 135.18 seconds as planned. Outboard engine cutoff, initiated by LOX low level sensors, occurred at 163.60 seconds which was 0.40 second earlier than predicted. This is a small difference compared to the predicted 3-sigma limits of +5.58, -3.89 seconds.

Thrust decay of the F-1 engines was normal.

5.5 S-IC STAGE PROPELLANT MANAGEMENT

Outboard engine cutoff was initiated by the LOX low level sensors as planned, and resulted in residual propellants being very close to the predicted values. The residual LOX at OECO was 38,921 lbm compared to the predicted value of 39,403 lbm. The fuel residual at OECO was 27,573 lbm compared to the predicted value of 31,957 lbm. A summary of the propellants remaining at major event times is presented in Table 5-2.

Table 5-2. S-IC Stage Propellant Mass History

EVENT	PREDICTED, LBM		LEVEL SENSOR DATA, LBM		RECONSTRUCTED, LBM	
	LOX	FUEL	LOX	FUEL	LOX	FUEL
Ignition Command	3,306,503	1,434,963	-	1,431,365	3,304,734	1,431,384
Holddown Arm Release	3,240,439	1,416,385	3,233,269	1,412,475	3,236,952	1,412,322
CECO	509,112	234,432	496,929	226,836	502,675	226,924
OECO	39,403	31,957	42,808	27,681	38,921	27,573
Separation	34,633	29,582	-	-	33,854	25,098
Zero Thrust	34,144	29,007	-	-	33,457	24,453

NOTE: Predicted and reconstructed values do not include pressurization gas so they will compare with level sensor data.

5.6 S-IC PRESSURIZATION SYSTEMS

5.6.1 S-IC Fuel Pressurization System

The fuel tank pressurization system performed satisfactorily. The low flow prepressurization system was commanded on at -97 seconds. High flow pressurization, accomplished by the onboard pressurization system, performed as expected. Helium flow control valve No. 1 was commanded on at -2.7 seconds and was supplemented by the high flow prepressurization system until umbilical disconnect.

Fuel tank ullage pressure was within the predicted limits throughout flight, as shown in Figure 5-5. Helium flow control valves No. 2, 3, and 4 were commanded open during flight by the switch selector, within acceptable limits. Helium bottle pressure was 3000 psia at -2.8 seconds and decayed to 520 psia at OECO. Total helium flowrate and heat exchanger performance were as expected.

Fuel pump inlet pressure was maintained above the required minimum Net Positive Suction Pressure (NPSP) during flight.

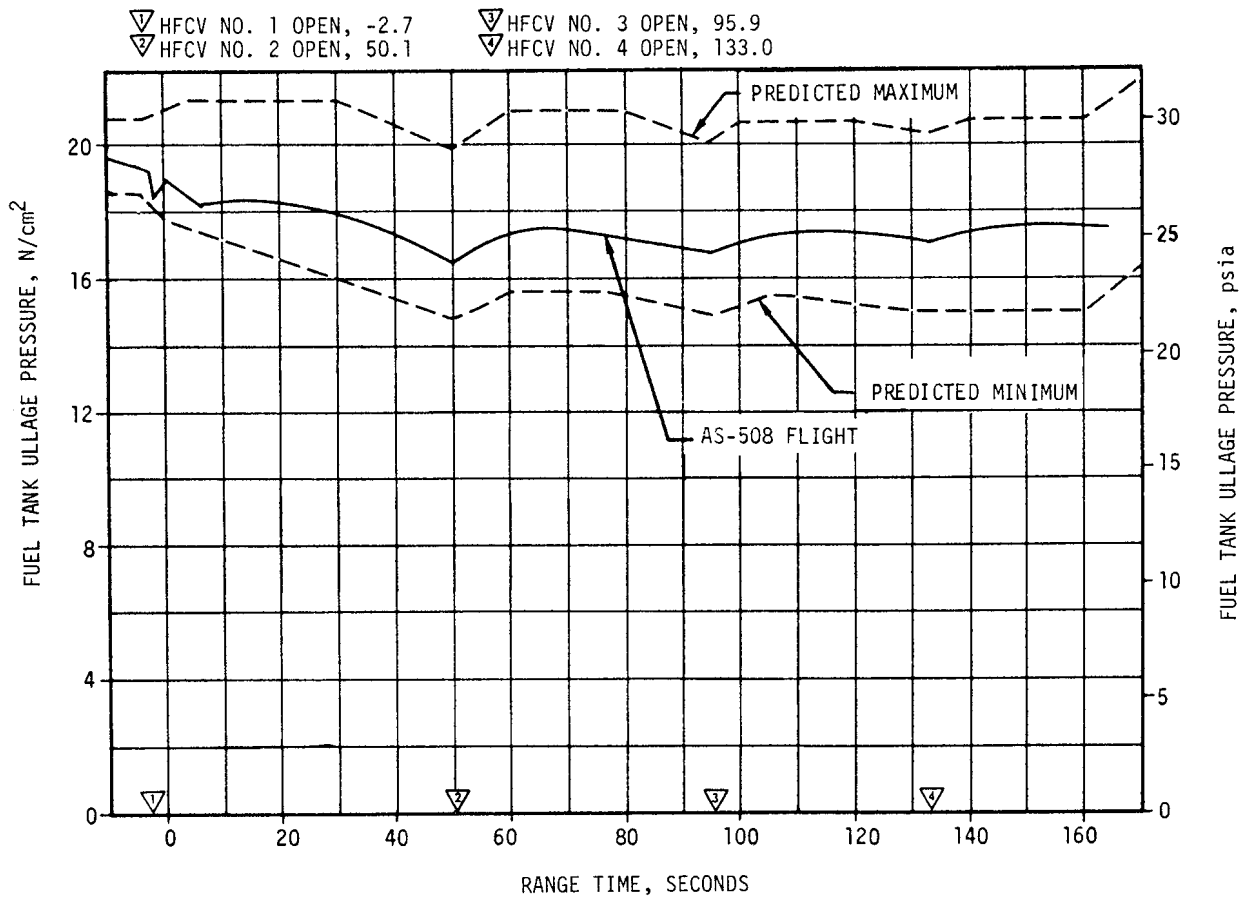


Figure 5-5. S-IC Stage Fuel Ullage Pressure

5.6.2 S-IC LOX Pressurization System

The LOX pressurization system performed satisfactorily and all performance requirements were met. The ground prepressurization system maintained ullage pressure within acceptable limits until launch commit. The onboard pressurization system subsequently maintained ullage pressure within the GOX Flow Control Valve (GFCV) band during flight. The prepressurization system was initiated at -72 seconds. Ullage pressure increased to the prepressurization switch band and flow was terminated at -57 seconds. The low flow system was cycled on two additional times at -37 and -11 seconds. At -4.7 seconds the high flow system was commanded on and maintained ullage pressure within acceptable limits until launch commit.

The LOX tank ullage pressure during flight, as shown in Figure 5-6, was maintained within the required limits throughout flight by the GFCV. The maximum GOX flowrate to the tank, at CECO, was 55.6 lbm/s. The heat exchangers performed as expected.

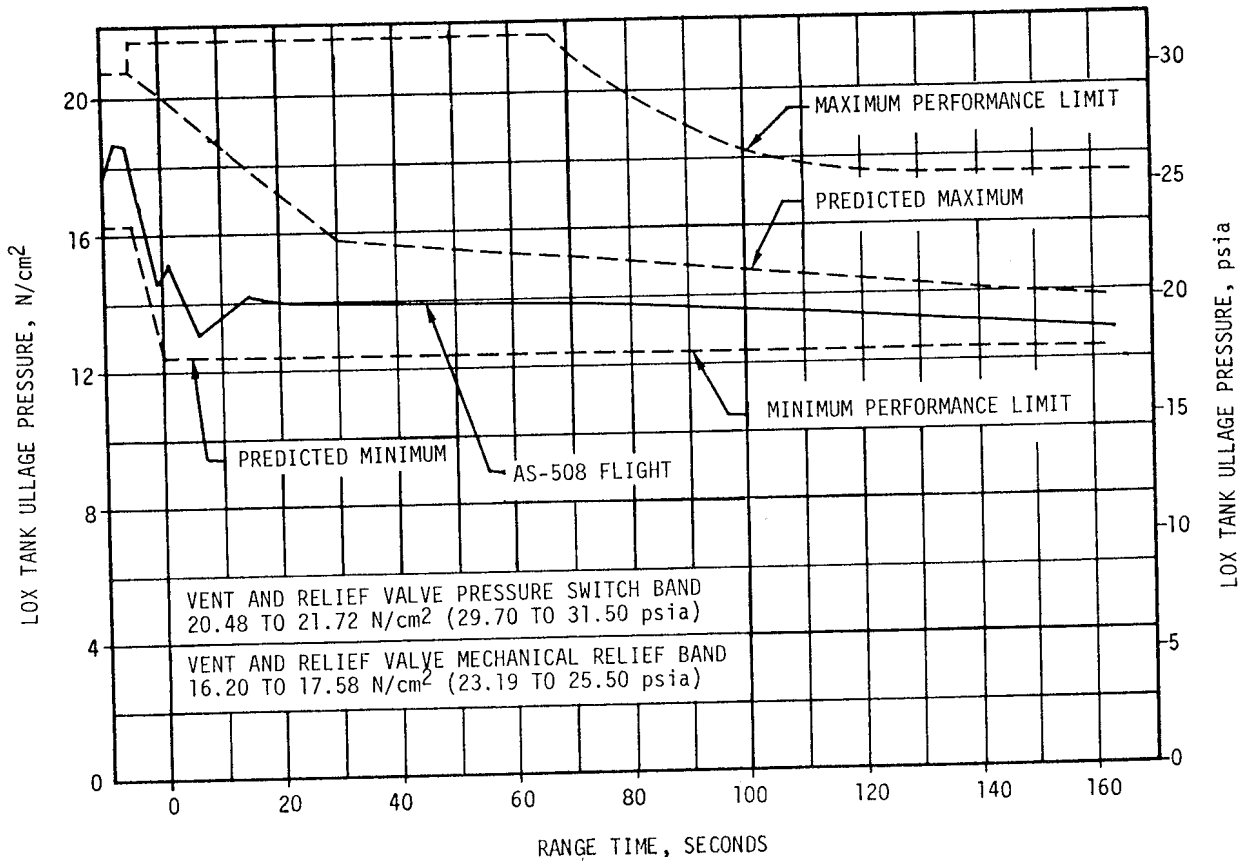


Figure 5-6. S-IC Stage LOX Tank Ullage Pressure

During the prelaunch activities the LOX tank vent and relief valve stuck in the open position for about 41 minutes beginning at -2 hours and 5 minutes. The valve closed at -1 hour and 24 minutes and no further problem occurred during the remainder of the countdown or during flight. See paragraph 3.4.2 for additional details.

LOX pump inlet pressure was maintained above the required minimum NPSP during flight.

5.7 S-IC PNEUMATIC CONTROL PRESSURE SYSTEM

The control pressure system functioned satisfactorily throughout S-IC flight.

Sphere pressure was 2997 psia at liftoff and remained steady until CECO when it decreased to 2845 psia. The decrease was due to actuation of the center engine prevalues. There was a further decrease to 2445 psia after OECO. The engine prevalues were closed after engine cutoff as required.

5.8 S-IC PURGE SYSTEMS

Performance of the S-IC purge systems was satisfactory during flight.

The turbopump LOX seal purge storage sphere pressure was within the limits of 2700 to 3300 psia until ignition, and 3300 to 1000 psia from liftoff to OECO.

5.9 S-IC POGO SUPPRESSION SYSTEM

The POGO suppression system performed satisfactorily during S-IC flight.

Outboard LOX prevalue temperature measurements indicated that the prevalue cavities were filled with helium prior to liftoff as planned. The measurements in the outboard prevalues went cold momentarily at liftoff, indicating LOX sloshed on the probes. They remained warm throughout flight, indicating helium in the prevalues. At cutoff, the increased pressure forced LOX into the prevalues once more. The two measurements in the center engine prevalue indicated cold, which meant LOX was in this valve as planned.

5.10 S-IC HYDRAULIC SYSTEM

The performance of the S-IC hydraulic system was satisfactory. All servoactuator supply pressures were within required limits. The engine control system return pressures were within predicted limits, and the hydraulic control system valves operated as planned.

SECTION 6

S-II PROPULSION

6.1 SUMMARY

Engine No. 5 cut off earlier than planned because of high amplitude oscillations in the propulsion/structural system; otherwise, the S-II propulsion system performance was satisfactory. The S-II Engine Start Command (ESC), as sensed at the engines, occurred at 165.0 seconds. Center Engine Cutoff (CECO) occurred at 330.65 seconds or 132.36 seconds earlier than planned. Outboard Engine Cutoff (OECO) occurred at 592.64 seconds or 34.53 seconds later than predicted.

Total stage thrust at the standard time slice (62 seconds after S-II ESC) was 0.19 percent below predicted. Total propellant flowrate, including pressurization flow, was 0.25 percent below predicted and stage specific impulse was 0.09 percent above predicted at the standard time slice. Stage propellant mixture ratio was 0.18 percent below predicted. Engine thrust buildup and cutoff transients were normal.

Low amplitude oscillations were observed on all engines during S-II boost prior to CECO. Net engine performance levels of outboard engines were not affected.

The propellant management system performance was satisfactory, except for sporadic wet indications of the overflow point sensors prior to launch. The system used open-loop control of the engine Propellant Utilization (PU) valves, similar to the AS-507 flight. The Instrument Unit (IU) command to shift Engine Mixture Ratio (EMR) from high to low was initiated upon attainment of a preprogrammed stage velocity increase as sensed by the Launch Vehicle Digital Computer (LVDC). Due mainly to early CECO the guidance sensed EMR shift occurred 32.2 seconds later than predicted.

S-II OECO, initiated by the LOX engine cutoff sensors, was achieved following a planned 1.5-second time delay. Residual propellant in the tanks at OECO signal was 6057 lbm, compared to the prediction of 6026 lbm.

The performance of the LOX and LH₂ tank pressurization systems was within predicted limits. Ullage pressure in both tanks was more than adequate to meet established engine inlet propellant requirements throughout mainstage. As commanded by the IU, step pressurization occurred at 263.6 seconds for the LOX tank and 463.6 seconds for the LH₂ tank.

The engine servicing, recirculation, helium injection and valve actuation systems all performed satisfactorily.

S-II hydraulic system performance was normal throughout the flight.

6.2 S-II CHILLDOWN AND BUILDUP TRANSIENT PERFORMANCE

The engine servicing operations required to condition the engines prior to engine start were satisfactorily accomplished. Thrust chamber temperatures were within predicted limits at both prelaunch and engine start. Thrust chamber chilldown requirements are -200°F maximum at prelaunch commit and -150°F maximum at engine start. Thrust chamber temperatures ranged between -296 and -274°F at prelaunch commit and between -240 and -212°F at engine start. Thrust chamber temperature warmup rates during S-IC boost agreed closely with those experienced on previous flights.

Both temperature and pressure conditions of the J-2 engine start tanks were within the required prelaunch and engine start boxes as shown in Figure 6-1.

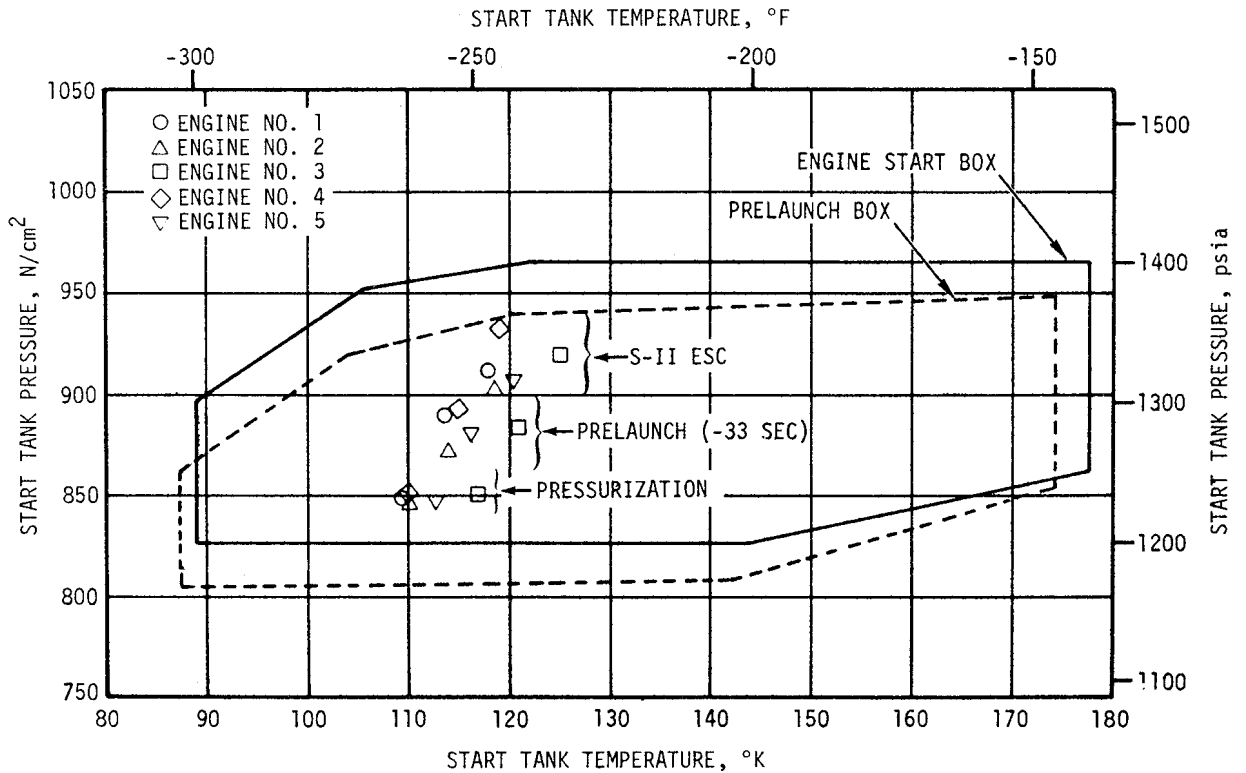


Figure 6-1. S-II Engine Start Tank Performance

Start tank temperatures at the conclusion of chilldown were approximately 18°F colder than on AS-507. This performance resulted from operating the A7-71 Heat Exchanger Unit, with all ullage vents open continuously, from the initiation of start tank chilldown at -22 minutes. The start tank system performance was entirely satisfactory.

Prelaunch and S-IC boost start tank temperature and pressure heat-up rates were normal and within the spread reported for AS-507. No indications of start tank relief valve operation were noted.

All engine helium tank pressures were within the prelaunch and engine start limits of 2800 to 3450 psia. Engine helium tank pressures ranged between 3190 and 3075 psia prior to launch (at -19 seconds) and between 3300 and 3175 psia at S-II ESC.

The LOX and LH₂ recirculation systems used to chill the feed ducts, turbo-pumps, and other engine components performed satisfactorily during prelaunch and S-IC boost. Engine pump inlet temperatures and pressures at engine start were well within the requirements as shown in Figure 6-2. The LOX pump discharge temperatures at S-II ESC were approximately 16.5°F subcooled, well below the 3°F subcooling requirement.

Prepressurization of the propellant tanks was accomplished satisfactorily. Ullage pressures at S-II ESC were 39.3 psia for LOX and 28.0 psia for LH₂.

S-II ESC was received at 165.0 seconds and the Start Tank Discharge Valve (STDV) solenoid activation signal occurred 1.0 second later. The engine thrust buildup was satisfactory and within the required thrust buildup envelope. All engines reached their mainstage levels (pressure switch pickup) within 2.8 seconds after S-II ESC.

6.3 S-II MAINSTAGE PERFORMANCE

The propulsion reconstruction analysis showed that stage performance, during mainstage operation, was satisfactory except that engine No. 5 was shut down prematurely because of high amplitude, low frequency oscillations in propulsion and structural systems. These oscillations occurred in the frequency range of 14 to 16 hertz. Thrust chamber pressure oscillations reached an amplitude of approximately ±236 psi. High amplitude oscillations in the LOX feed system activated the thrust OK pressure switches and in turn initiated engine cutoff. Indications are that the oscillations caused no engine damage. See paragraph 8.2.3 for more detail.

A comparison of predicted and reconstructed performance of thrust, specific impulse, total flowrate, and mixture ratio versus time is shown in Figure 6-3. Stage performance during the high EMR portion of flight (prior to CECO) was very close to predicted. At the time slice of ESC +62 seconds, total stage thrust was 1,160,765 lbf which is 2184 lbf (0.19 percent) below the preflight prediction. Total propellant flowrate,

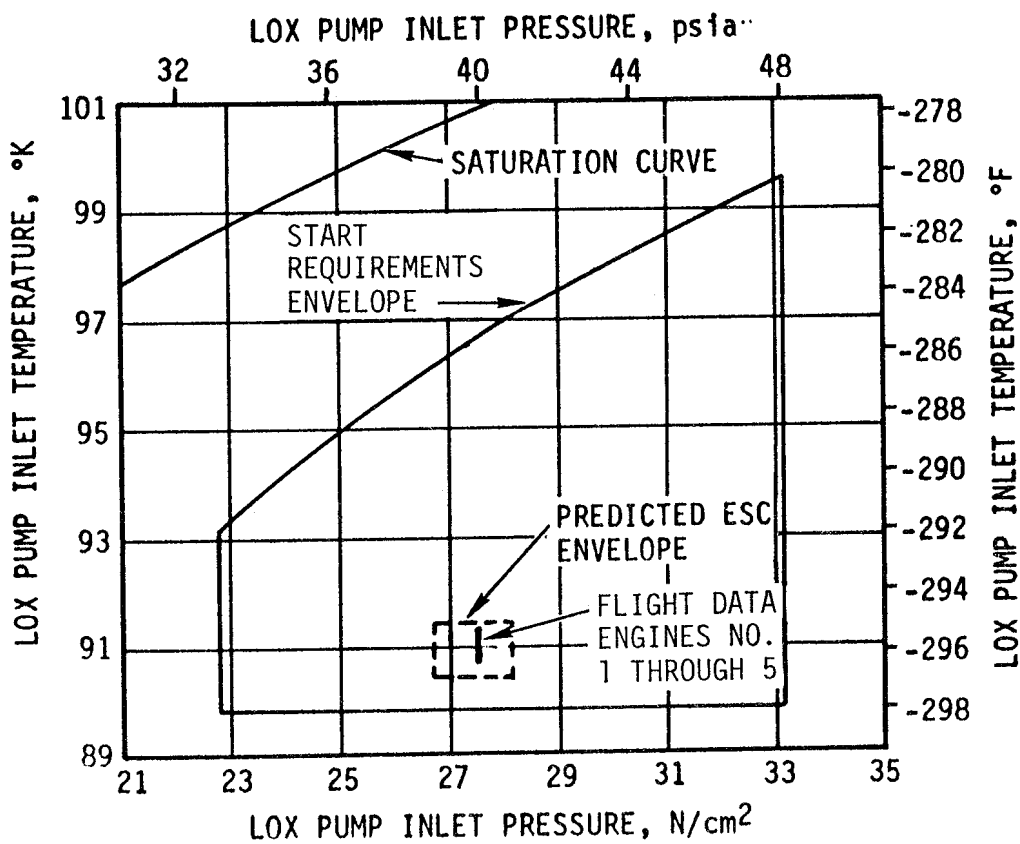
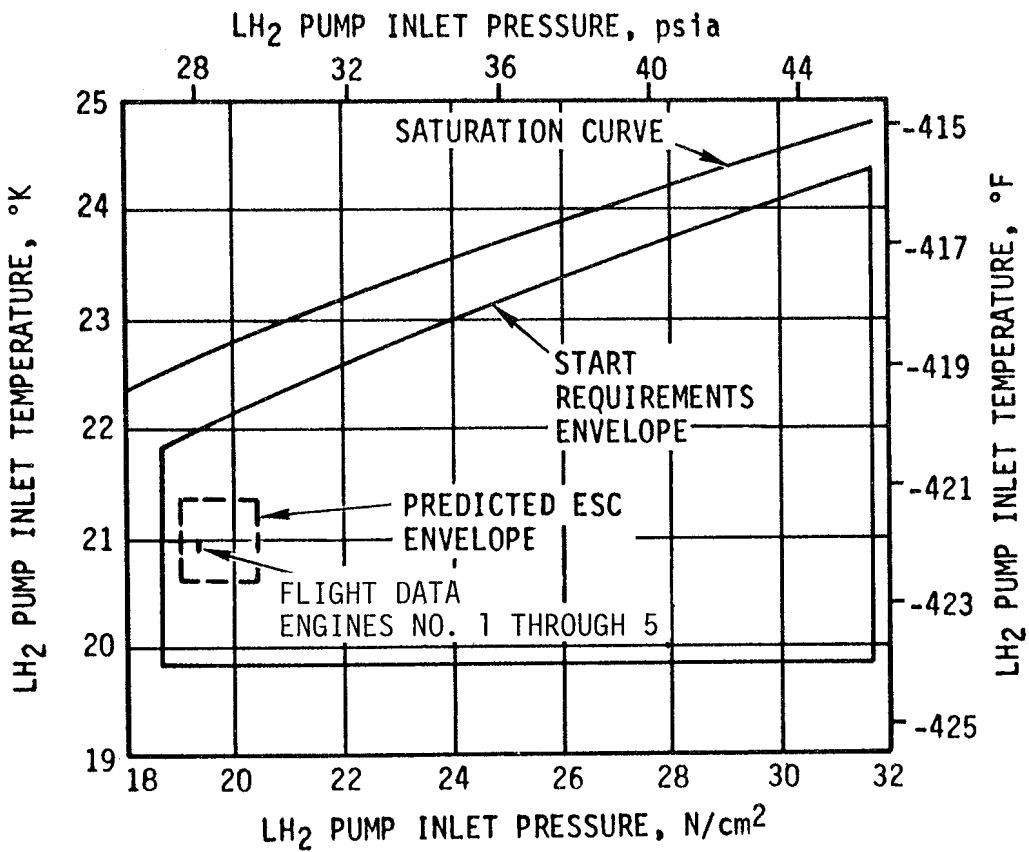


Figure 6-2. S-II Engine Pump Inlet Start Requirements

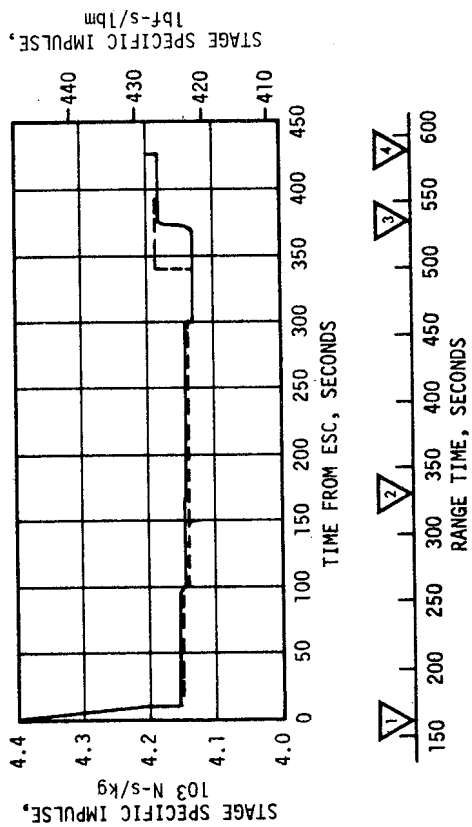
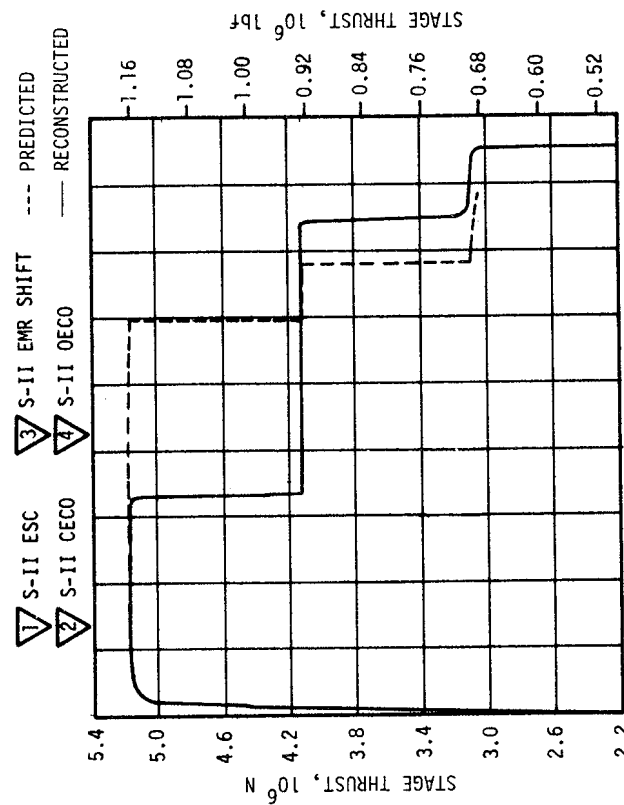
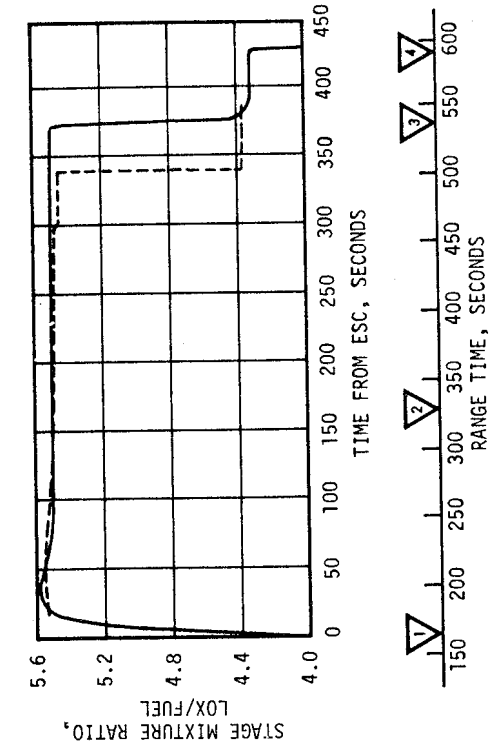
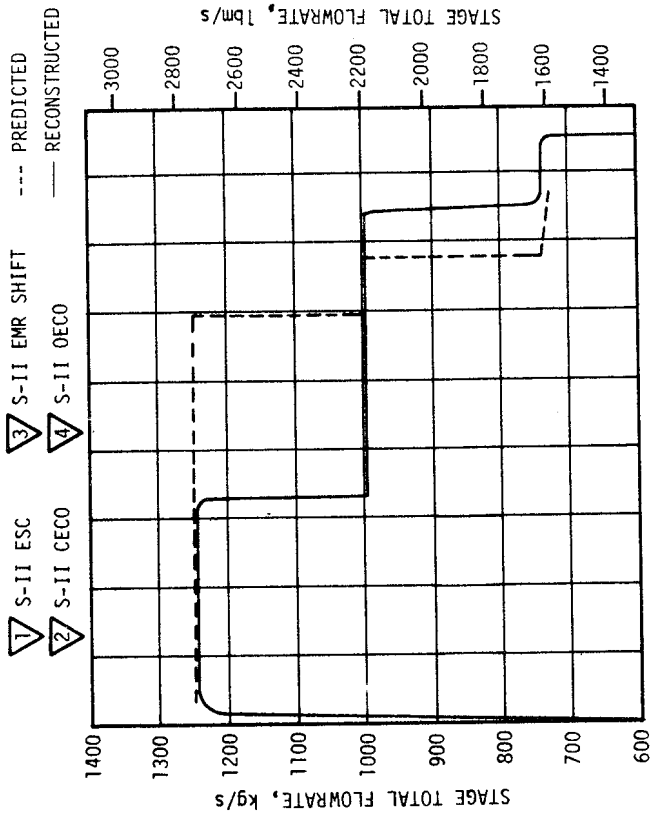


Figure 6-3. S-II Steady State Operation

including pressurization flow, was 2740.6 lbm/s; 0.25 percent below predicted. Stage specific impulse, including the effect of pressurization gas flowrate, was 423.5 lbf-s/lbm; 0.09 percent above predicted. Stage propellant MR was 0.18 percent below predicted.

At ESC +165.6 seconds, 132.4 seconds earlier than planned, the center engine was shut down by thrust OK pressure switch dropout. This action reduced total stage thrust by 233,917 lbf to a level of 924,762 lbf. The EMR shift from high to low occurred 372.5 seconds after ESC; 33.7 seconds later than predicted. The change of EMR resulted in further stage thrust reduction and at ESC +421.6 seconds the total vehicle thrust was 689,491 lbf; thus, a decrease in thrust of 235,271 lbf was indicated between high and low EMR operation. S-II burn duration was 427.64 seconds, which was 34.93 seconds longer than predicted, due primarily to early CECO.

Individual J-2 engine data, excluding the effects of pressurization flowrate, are presented in Table 6-1 for the ESC +62-second time slice. Good correlation between predicted and reconstructed flight performance is indicated by the small deviations.

The performance levels shown in Table 6-1 have not been adjusted to standard J-2 altitude conditions and do not include the effects of pressurization flow. Considering data that have been adjusted to standard conditions, very little difference from the results shown in Table 6-1 has been observed. The adjusted data show all engine thrust levels to be within 0.81 percent of those achieved during stage acceptance test.

Typical minor engine performance shifts were observed during analysis of stage flight data. Available flight instrumentation does not permit a detailed investigation of the cause for each performance shift. However, the more familiar ones can be recognized by their characteristic effects on basic flight parameters (see Table 6-2).

6.4 S-II SHUTDOWN TRANSIENT PERFORMANCE

S-II OECO was initiated by the stage LOX depletion cutoff system. The LOX depletion cutoff system again included a 1.5-second delay timer. As in previous flights (AS-504 and subs), this resulted in engine thrust decay (observed as a drop in thrust chamber pressure) prior to receipt of the cutoff signal. However, due to early CECO, the precutoff decay was greatly reduced as compared with AS-504 without CECO. Only engine No. 1 exhibited a significant thrust chamber pressure decay, decreasing 110 psi in the final 0.4 second before cutoff. All other outboard engine thrust chamber pressure decays were approximately 42 psi.

At S-II OECO signal (592.64 seconds), total stage thrust was down to 635,725 lbf. Stage thrust dropped to 3 percent of this level within 0.94 second. The stage cutoff impulse through the 3 percent thrust level was estimated to be 193,024 lbf-s.

Table 6-1. S-II Engine Performance

PARAMETER	ENGINE NUMBER	PREDICTED	RECONSTRUCTED	PERCENT INDIVIDUAL DEVIATION	PERCENT AVERAGE DEVIATION
Thrust, lbf	1	234,462	233,602	- 0.37	- 0.19
	2	232,817	232,956	0.06	
	3	234,034	233,060	- 0.42	
	4	230,056	230,216	0.07	
	5	231,580	230,933	- 0.28	
Specific Impulse, lbf-s/lbm	1	425.2	425.5	0.07	0.15
	2	424.9	425.9	0.24	
	3	424.6	425.0	0.09	
	4	423.5	424.1	0.14	
	5	424.5	425.4	0.21	
Engine Flowrate, lbm/s	1	551.4	549.0	- 0.44	- 0.34
	2	547.9	546.9	- 0.18	
	3	551.2	548.3	- 0.53	
	4	543.2	542.8	- 0.07	
	5	545.6	542.9	- 0.49	
Engine Mixture Ratio, LOX/Fuel	1	5.54	5.54	0.00	- 0.22
	2	5.64	5.64	0.00	
	3	5.58	5.55	- 0.54	
	4	5.56	5.57	0.18	
	5	5.53	5.49	- 0.72	

NOTE: Values do not include pressurization flow.

Table 6-2. S-II Engine Performance Shifts

ENGINE NO.	PERFORMANCE SHIFT (MAGNITUDE AND TIME OF OCCURRENCE)	REMARKS
1	-2300 lbf in-run thrust shift at 255 seconds (ESC +90 seconds)	Shift in Gas Generator (GG) oxidizer system resistance.
4	+1500 lbf in-run thrust shift at 215 seconds (ESC +50 seconds)	Shift in GG oxidizer system resistance
5	-1600 lbf run-to-run shift in thrust from engine acceptance	Shift in GG oxidizer system resistance
All Outboard Engines	In-run low frequency thrust oscillations at ESC +164 seconds	During center engine high amplitude oscillations. (See paragraph 8.2.3 for more detail.)

NOTE: None of the shifts are considered to be unusual in either magnitude or cause.

6.5 S-II STAGE PROPELLANT MANAGEMENT

The propellant management system performed satisfactorily during the propellant loading operation and during flight, except as noted below. The S-II stage employed an open-loop system utilizing fixed, open-loop commands from the IU rather than feedback signals from the tank mass sensing probes. Open-loop PU is also planned for all subsequent vehicles.

The launch facility Propellant Tanking Control System (PTCS) and the propellant management system properly controlled S-II loading and replenishment. However, during the prelaunch countdown, both LOX and LH₂ overflow point sensors sporadically indicated wet. An investigation of this problem is now in progress.

The open-loop PU system responded as expected during flight and no instabilities were noted. Open-loop PU system operation commenced when "High EMR select" was commanded at ESC +5.5 seconds, as planned. The PU valves then moved to the high EMR position, providing an average EMR of 5.50. The IU command to shift EMR from high to low was initiated at ESC +369.7 seconds (32.2 seconds later than predicted) upon attainment of a preprogrammed velocity increase as sensed by the LVDC. These deviations are attributed to the early CECO and to a smaller degree engine performance variations from predicted, and larger than predicted propellant loading of the upper stages. The IU command caused the PU valves to be driven to the low EMR position, providing an average EMR of 4.35 which was 0.02 less than predicted.

OECO was initiated by the LOX tank propellant depletion system (with a 1.5-second ECO time delay) 34.5 seconds later than predicted due to the previously mentioned deviations. The open-loop PU error at OECO was approximately +38 lbm LH₂ versus a 3-sigma tolerance of ± 2500 lbm LH₂. Based on corrected PU system data, propellant residuals (mass in tanks and sump) at OECO were 1797 lbm LOX and 4260 lbm LH₂.

Table 6-3 presents a comparison of propellant masses as measured by the PU probes and engine flowmeters. The best estimate propellant mass is based on integration of flowmeter data utilizing the propellant residuals as determined from PU system data corrected for nominal tank mismatch at OECO. Best estimates of propellant mass loaded correlate with the post-launch trajectory simulation within the accuracy of the measurements utilized. These mass values were 0.07 percent more than predicted for LOX and 0.13 percent more than predicted for LH₂.

6.6 S-II PRESSURIZATION SYSTEM

6.6.1 S-II Fuel Pressurization System

LH₂ tank ullage pressure, actual and predicted, is presented in Figure 6-4 for autosequence, S-IC boost, and S-II boost. The LH₂ vent valves were closed at -96.2 seconds and the ullage volume pressurized to 35.3 psia

Table 6-3. S-II Propellant Mass History

EVENT	PREDICTED, LBM		PU SYSTEM ANALYSIS, LBM		ENGINE FLOWMETER INTEGRATION (BEST ESTIMATE), LBM	
	LOX	LH ₂	LOX	LH ₂	LOX	LH ₂
Ground Ignition	834,558	159,500	834,004	159,778	835,116	159,700
S-II ESC	834,558	159,486	832,068	158,905	835,116	159,700
S-II PU Valve Step	77,929	21,513	78,725	20,921	76,270	21,367
S-II OECO	1801	4225	1800	4263	1797	4260
S-II Residual After Thrust Decay	1555	4117	Data not usable	Data not usable	1643	4187

NOTE: Table is based on mass in tanks and sump only. Propellant trapped external to tanks and LOX sump is not included.

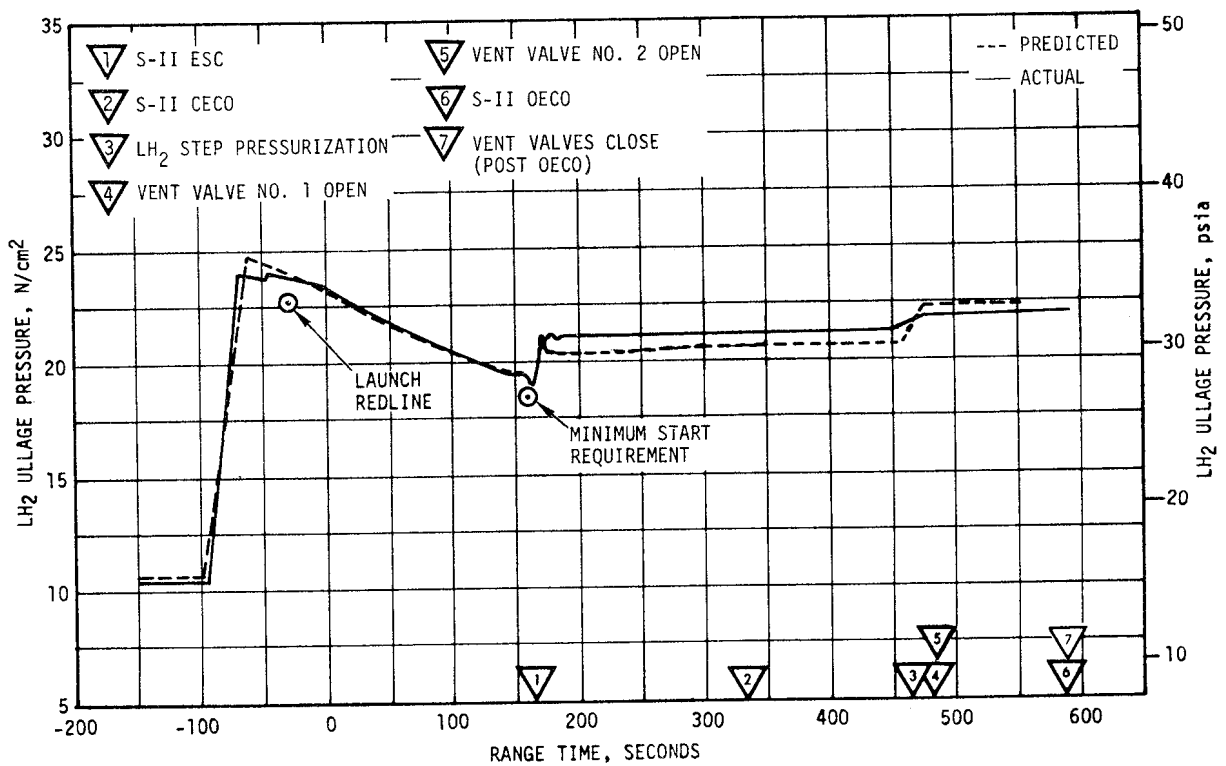


Figure 6-4. S-II Fuel Tank Ullage Pressure

in approximately 22.5 seconds. One make-up cycle was required at -41.1 seconds. The LH₂ tank vent valves opened during S-IC boost, limiting tank pressure; however, no main poppet operation was indicated. Differential pressure across the vent valve was kept below the low-mode upper limit of 29.5 psi. Ullage pressure at engine start was 28 psia exceeding the minimum engine start requirement of 27 psia. The LH₂ tank vent valves were switched to the high vent mode immediately prior to S-II engine start.

LH₂ tank ullage pressure remained slightly above its predicted value during S-II mainstage operation prior to step pressurization. The indicated ullage pressure was comparable to the pressure in this interval during S-II-8 static firing.

The LH₂ tank regulator was commanded open at 463.6 seconds and ullage pressure increased to 31.6 psia. The vent valves started to vent at 467.7 seconds and continued to vent throughout the remainder of the S-II burn. Ullage pressure remained within the high mode vent range of 30.5 to 33.0 psia.

Figure 6-5 shows LH₂ total inlet pressure, temperature and Net Positive Suction Pressure (NPSP) for the J-2 engines. The parameters were close to predicted values. The NPSP exceeded the minimum requirement throughout the S-II burn phase.

6.6.2 S-II LOX Pressurization System

LOX tank ullage pressure, actual and predicted, is presented in Figure 6-6 for autosequence, S-IC boost, and S-II burn. After a 2 minute cold helium chilldown flow through the LOX tank, the vent valves were closed at -185.3 seconds and the LOX tank was prepressurized to the pressure switch setting of 38.3 psia in approximately 32.5 seconds. At approximately -78 seconds, the pressure increased to 39 psia because of the LH₂ tank prepressurization. LOX ullage pressure was 39.3 psia at engine start.

After the ullage pressure recovered from the initial drop at engine start, the pressure was controlled within the LOX pressure regulator range of 36 to 38.5 psia until step pressurization. Step pressurization increased the ullage pressure to 38.2 psia. This was slightly lower than predicted as discussed in paragraph 8.2.3. In addition the LOX tank ullage pressure experienced a slump of 0.4 psi just after step pressurization. Review of S-II-8 static firing ullage pressure data also shows a slight slump of about 0.15 psi after step pressurization. This pressure slump was the result of the interaction of colder heat exchanger outlet temperature, smaller ullage volume and a slight variation in regulator response compared to previous flights.

1 S-II ESC

3 LH₂ STEP PRESSURIZATION

2 S-II CECO

4 S-II OECO

----- PREDICTED

———— ACTUAL

— · — · — · MINIMUM NPSP REQUIREMENT

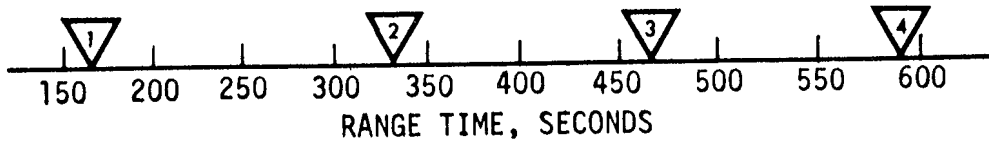
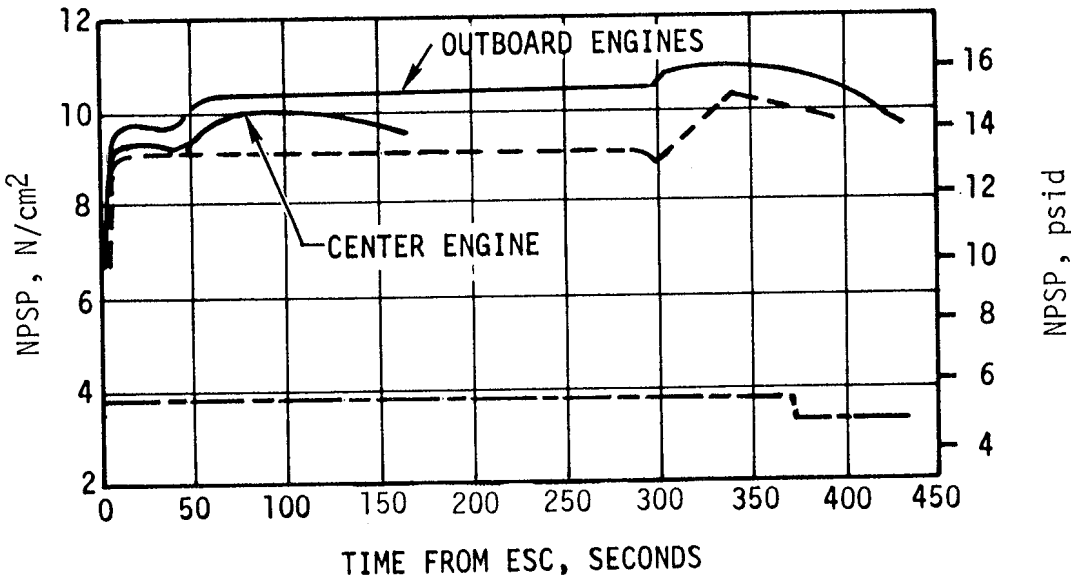
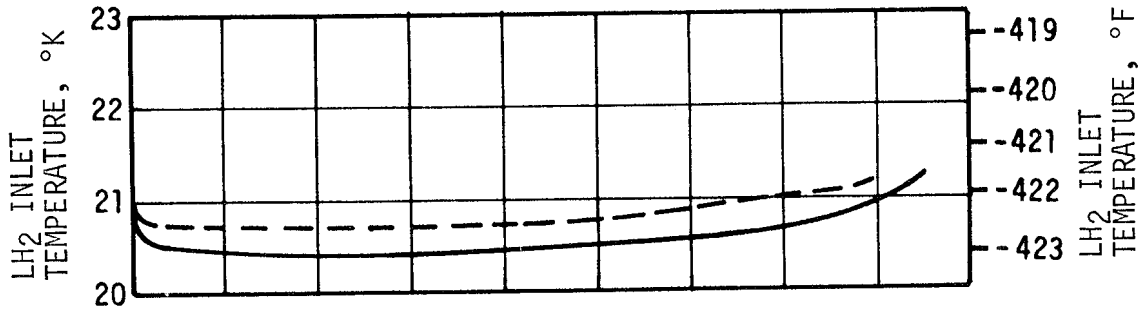
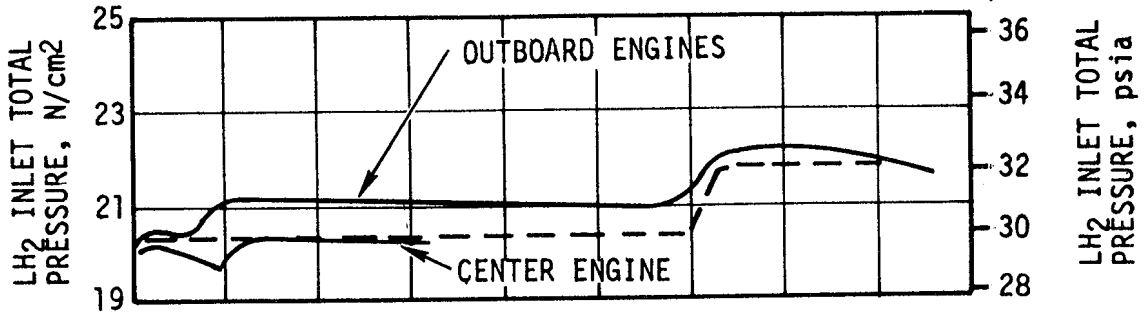


Figure 6-5. S-II Fuel Pump Inlet Conditions

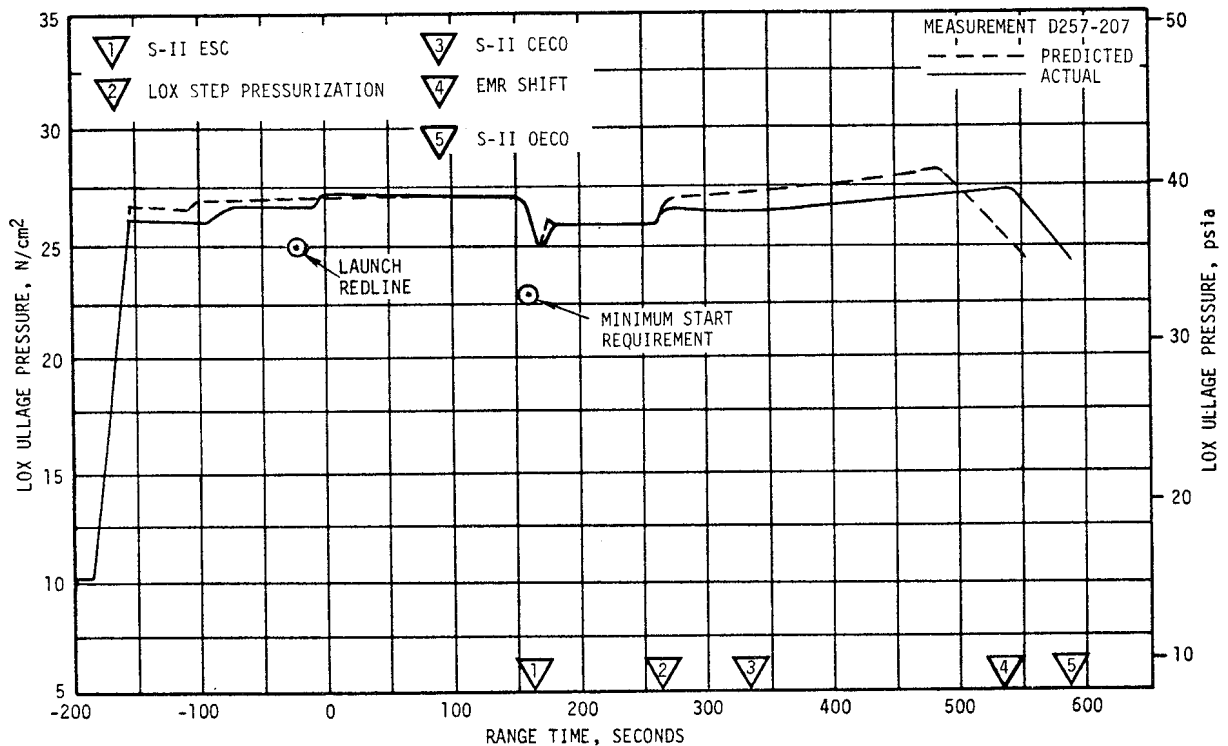


Figure 6-6. S-II LOX Tank Ullage Pressure

The ullage pressure recovered from the initial slump more slowly than it had during the S-II-8 static firing. The slow recovery of the ullage pressure is a result of early CECO. The heat transfer area within the LOX tank remains relatively constant after CECO but with only four engines supplying pressurant, instead of five, a slower ullage pressure buildup occurred.

The ullage pressure reached a maximum of 39.7 psia at EMR shift. As a result of EMR shift, the pressure began to decrease and had reached 35.5 psia at OECO. No LOX tank venting was observed. LOX pump total inlet pressure, temperature and NPSP are presented in Figure 6-7.

6.7 S-II PNEUMATIC CONTROL PRESSURE SYSTEM

The pneumatic control system functioned satisfactorily throughout the S-IC and S-II boost periods. Bottle pressure was 3030 psia at -30 seconds and due to normal valve activities during S-II burn, pressure decayed to approximately 2620 psia after S-II OECO.

Regulator outlet pressure during flight remained at a constant 715 psia, except for the expected momentary pressure drops when the recirculation or prevalues were actuated closed just after engine start, at CECO and OECO.

- 1 S-II ESC
- 2 LOX STEP PRESSURIZATION
- 3 S-II CECO
- 4 EMR SHIFT
- 5 S-II OEEO
- PREDICTED
- ACTUAL
- - - MINIMUM NPSP REQUIREMENT

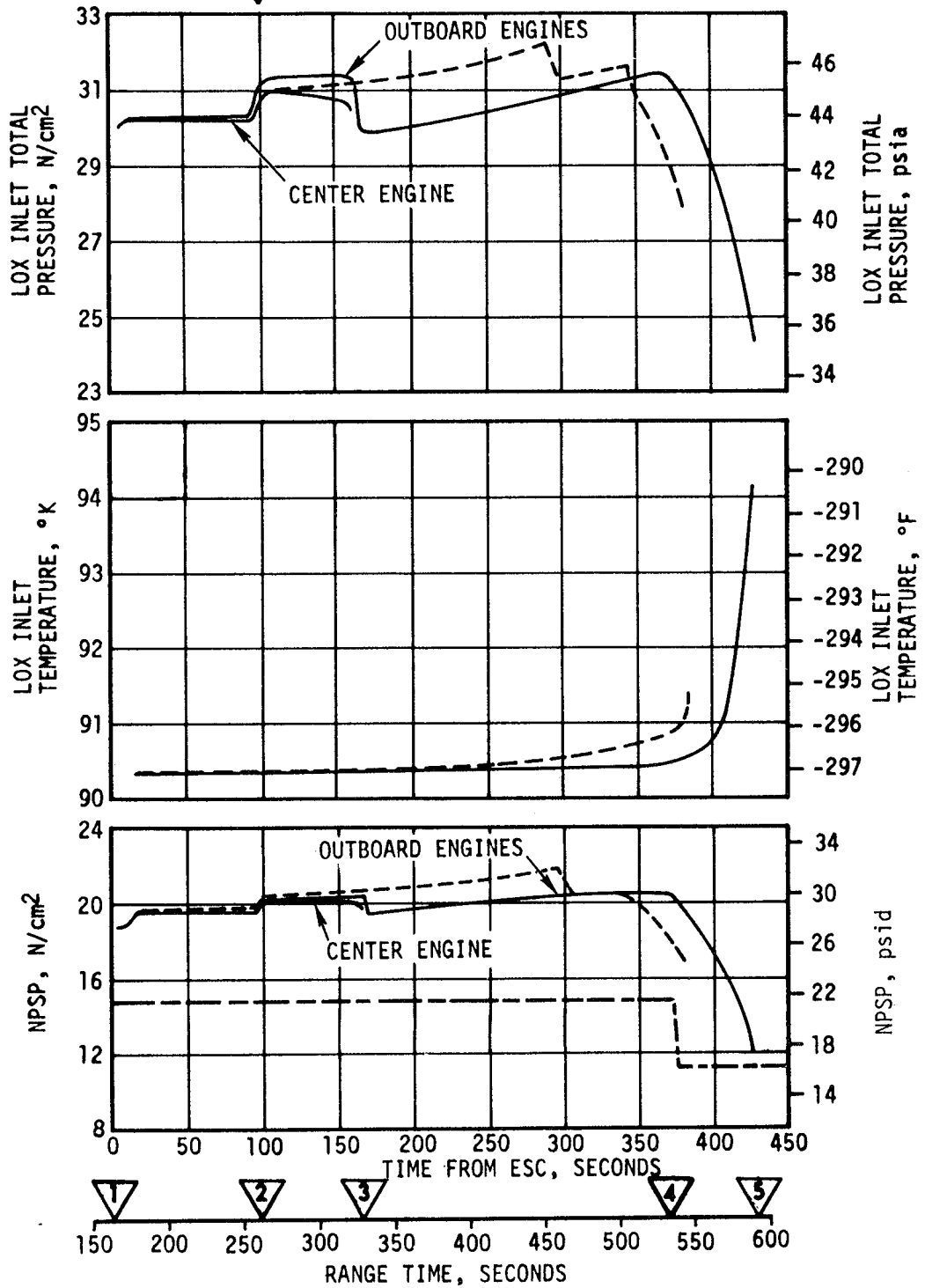


Figure 6-7. S-II LOX Pump Inlet Conditions

6.8 S-II HELIUM INJECTION SYSTEM

The performance of the helium injection system was satisfactory. Requirements were met and parameters were in agreement with predicted values. The supply bottle was pressurized to 3050 psia prior to liftoff and by ESC the pressure was 700 psia. Helium injection system average total flowrate during supply bottle blowdown (-30 to 163 seconds) was 72.5 SCFM.

6.9 S-II HYDRAULIC SYSTEM

S-II hydraulic system performance was normal throughout the flight. System supply and return pressures, reservoir volumes, and system fluid temperatures were within predicted ranges. Reservoir fluid temperatures were close to the predicted rate of increase. All servoactuators responded to commands with good precision.

Except for CECO-induced transients, forces acting on the actuators were well below a predicted maximum of 19,000 lbf. The maximum force in tension was 8450 lbf acting on the pitch actuator of engine No. 1. The maximum force in compression was 7150 lbf action on the pitch actuator of engine No. 2. All measurements showed the effects of the center engine oscillations and the resulting CECO. The greatest effect was noted on actuator differential pressure measurements where oscillating loads up to 20,800 lbf (0 to peak) were indicated. These loads were induced by the structural accelerations. There was no evidence of contribution to the oscillations in the actuator command data.

SECTION 7

S-IVB PROPULSION

7.1 SUMMARY

The J-2 engine operated satisfactorily throughout the operational phase of first and second burn and had normal shutdowns. S-IVB first burntime was 152.9 seconds which was 9.3 seconds longer than predicted, primarily due to the performance of lower stages. The J-2 engine thrust performance, during first burn, differed by 0.29 percent from the predicted (Start Tank Discharge Valve [STDV] open +130 seconds) as determined from standard altitude reconstruction analysis. Specific impulse was near that predicted. The S-IVB stage first burn Engine Cutoff (ECO) was initiated by the Launch Vehicle Digital Computer (LVDC) at 749.83 seconds.

The Continuous Vent System (CVS) adequately regulated LH₂ tank ullage pressure at an average level of 19.3 psia during earth orbit, and the Oxygen/Hydrogen (O₂/H₂) burner satisfactorily achieved LH₂ and LOX tank repressurization for restart. Engine restart conditions were within specified limits. The restart with the Propellant Utilization (PU) valve fully open was successful.

S-IVB second burntime was 350.8 seconds which was 4.9 seconds less than predicted. The engine performance during second burn, as determined from the standard altitude reconstruction analysis, differed from the predicted (STDV +130 seconds) by -0.24 percent for thrust and 0.09 percent for specific impulse. Second burn ECO was initiated by the LVDC at 9697.17 seconds.

Subsequent to second burn, the stage propellant tanks and helium spheres were safed satisfactorily. Sufficient impulse was derived from LOX dump, LH₂ CVS operation and Auxiliary Propulsion System (APS) ullage burn to achieve a successful lunar impact. An additional velocity change of 7 to 10 ft/s was accumulated during the unanticipated APS firings at 70,150 seconds (19:29:10).

The S-IVB hydraulic system performance was satisfactory during its complete mission.

7.2 S-IVB CHILLDOWN AND BUILDUP TRANSIENT PERFORMANCE FOR FIRST BURN

The propellant recirculation systems performed satisfactorily, meeting start and run box requirements for fuel and LOX as shown in Figure 7-1. The thrust chamber temperature at launch was well below the maximum allowable redline limit of -130°F . At S-IVB first burn Engine Start Command (ESC), the temperature was -151°F , which was within the requirement of $-189.6 \pm 110^{\circ}\text{F}$.

The chilldown and loading of the engine Gaseous Hydrogen (GH_2) start tank and pneumatic control sphere prior to liftoff was satisfactory. At first burn ESC the start tank conditions were within the required region of 1325 ± 75 psia and $-170 \pm 30^{\circ}\text{F}$ for start. The discharge was completed and the refill initiated at first burn ESC +3.8 seconds. The refill was satisfactory and in good agreement with the acceptance test.

The engine control bottle pressure and temperature at liftoff were 2964 psia and -173°F . LH_2 and LOX systems chilldown, which was continuous from before liftoff until just prior to first ESC, was satisfactory. At first ESC, the LOX pump inlet temperature was -295.5°F and the LH_2 pump inlet temperature was -421.8°F .

The first burn start transient was satisfactory. The thrust buildup was within the limits set by the engine manufacturer. This buildup was similar to the thrust buildups observed on AS-506 and AS-507. The PU valve was in the null position prior to first start, but, as expected, shifted 0.6 degree during start. The total impulse from STDV open to STDV open +2.5 seconds was 189,441 lbf-s for first start.

First burn fuel lead followed the predicted pattern and resulted in satisfactory conditions as indicated by the thrust chamber temperatures and the associated fuel injector temperatures.

7.3 S-IVB MAINSTAGE PERFORMANCE FOR FIRST BURN

The propulsion reconstruction analysis showed that the stage performance during mainstage operation was satisfactory. A comparison of predicted and actual performance of thrust, specific impulse, total flowrate, and Engine Mixture Ratio (EMR) versus time is shown in Figure 7-2. Table 7-1 shows the specific impulse, flowrates and EMR deviations from the predicted at the STDV +130 second time slice.

The performance of the J-2 engine helium control system was satisfactory during mainstage operation. The engine control bottle was connected to the stage ambient repressurization bottles and therefore, there was little pressure decay. Helium usage was approximately 0.32 lbm during first burn.

The PU valve position shifted 0.6 degree during first burn and 0.5 degree during second burn. These shifts are approximately the same as those observed on previous flights.

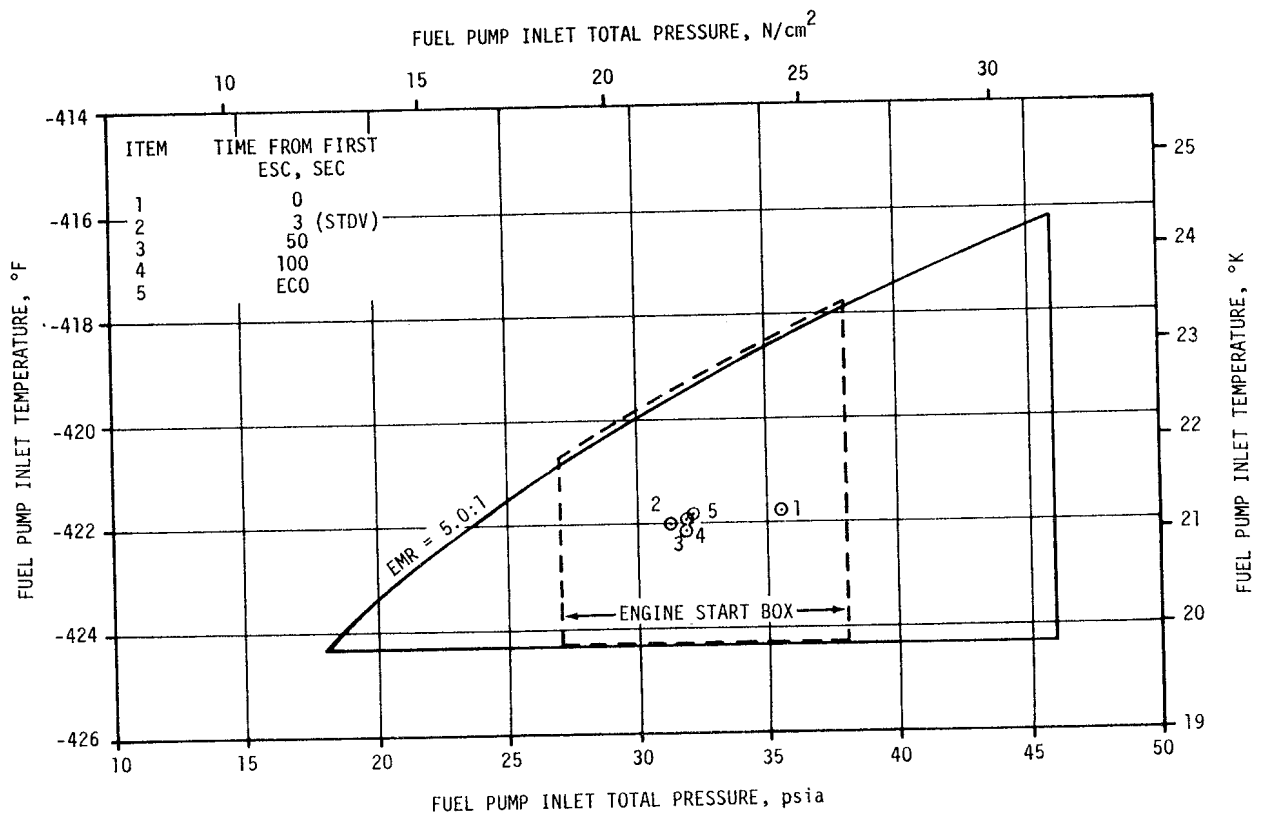
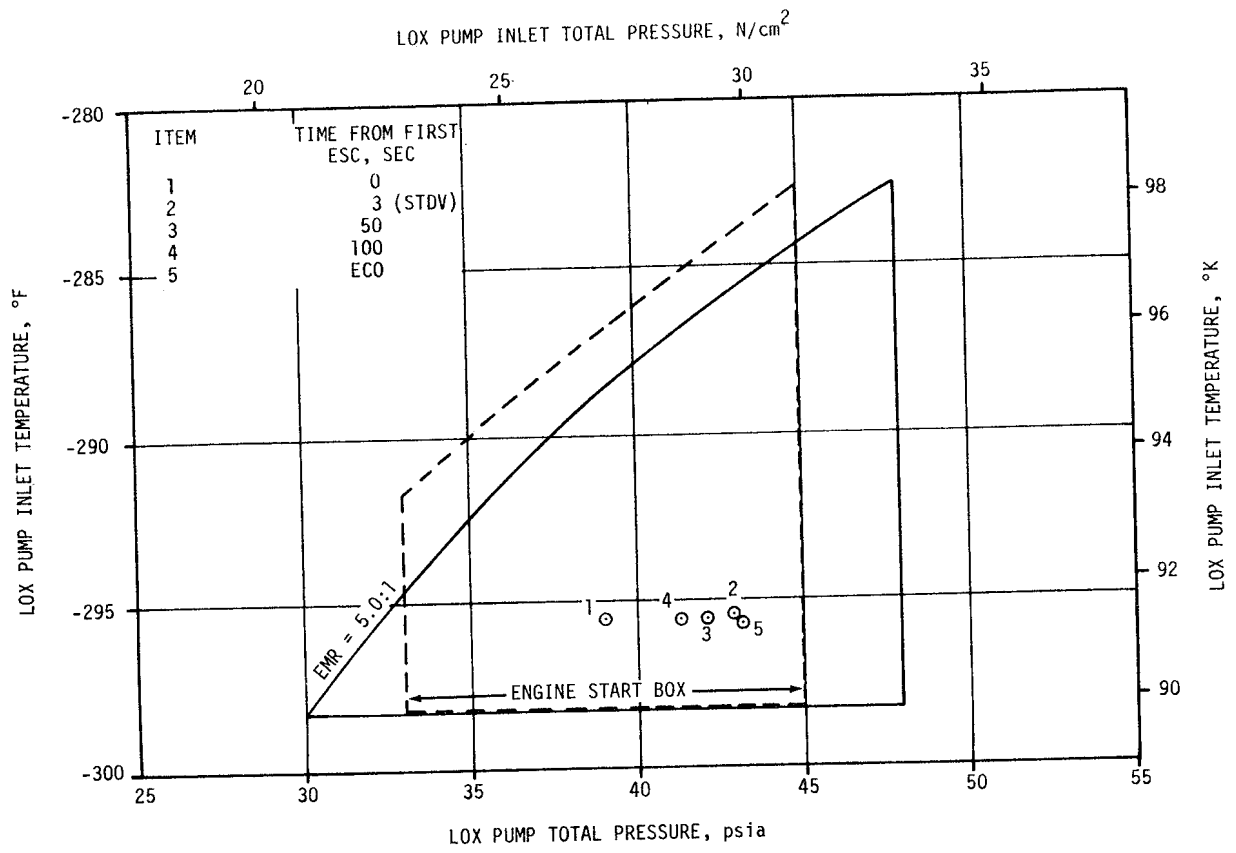


Figure 7-1. S-IVB Start Box and Run Requirements - First Burn

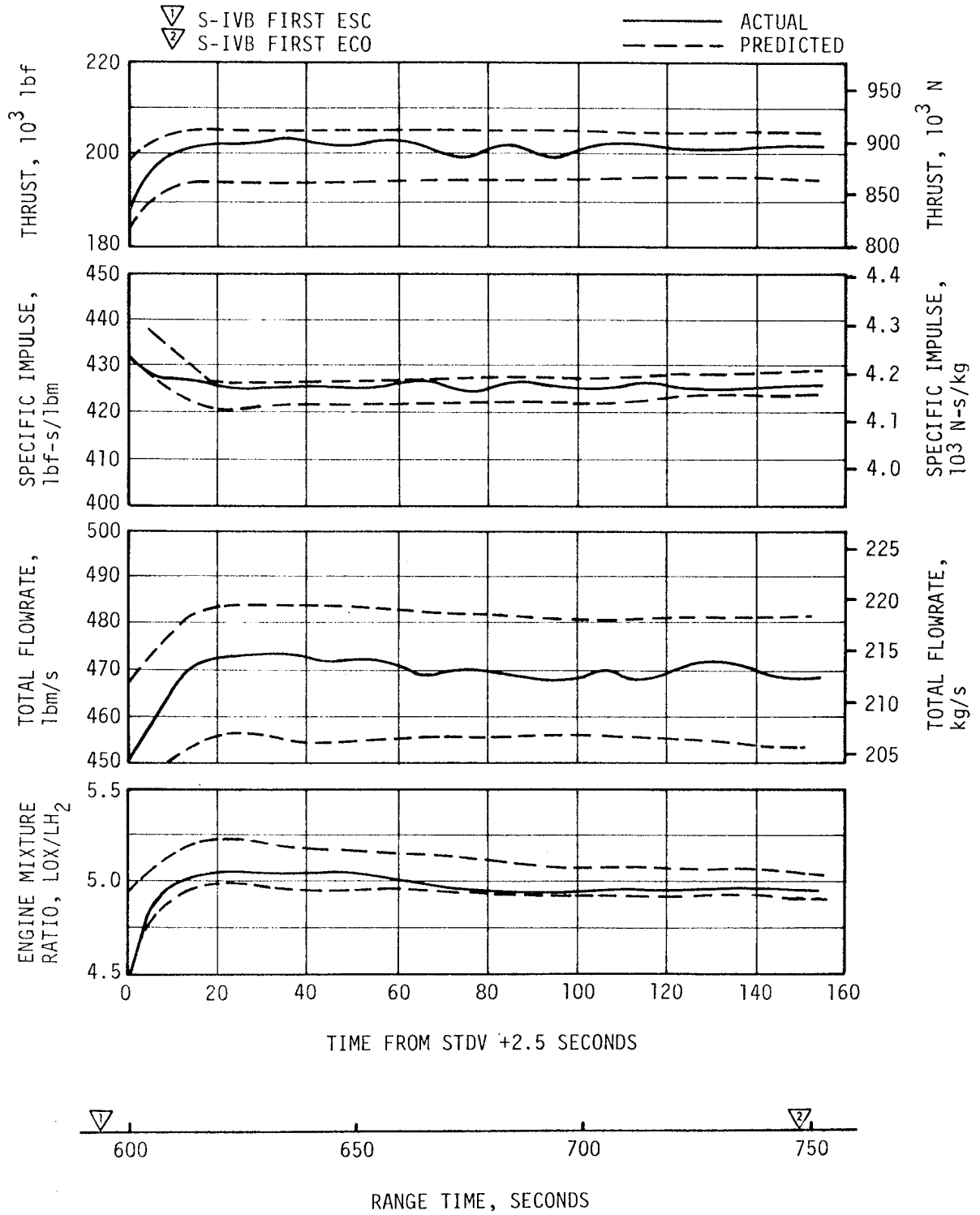


Figure 7-2. S-IVB Steady State Performance - First Burn

Table 7-1. S-IVB Steady State Performance - First Burn
(STDV +130 Second Time Slice at Standard Altitude Conditions)

PARAMETER	PREDICTED	RECONSTRUCTION	FLIGHT DEVIATION	PERCENT DEVIATION FROM PREDICTED
Thrust, lbf	199,003	199,577	574	0.288
Specific Impulse, lbf-s/lbm	426.8	427.2	0.4	0.094
LOX Flowrate, lbm/s	387.65	388.07	0.42	0.108
Fuel Flowrate, lbm/s	78.58	79.05	0.47	0.598
Engine Mixture Ratio, LOX/Fuel	4.933	4.909	-0.024	-0.486

7.4 S-IVB SHUTDOWN TRANSIENT PERFORMANCE FOR FIRST BURN

S-IVB first ECO was initiated at 749.83 seconds by a guidance velocity cutoff command which resulted in a burntime of 152.9 seconds. This was 9.3 seconds longer than predicted due to the performance of lower stages.

The ECO transient was satisfactory. The total cutoff impulse to zero percent of rated thrust was 44,319 lbf-s which was 3700 lbf-s less than predicted. Cutoff occurred with the PU valve in the null position.

7.5 S-IVB PARKING ORBIT COAST PHASE CONDITIONING

The LH₂ CVS performed satisfactorily, maintaining the fuel tank ullage pressure at an average level of 19.3 psia. This was well within the 18 to 21 psia band of the new inflight specification.

The continuous vent regulator was activated at 809.0 seconds and was terminated at 8810.3 seconds. The CVS performance is shown in Figure 7-3. The thrust between 1000 and 1500 seconds was below predicted but is within allowable performance limits.

Calculations based on estimated temperatures indicate that the mass vented during parking orbit was 1880 lbm and that the boiloff mass was 2010 lbm.

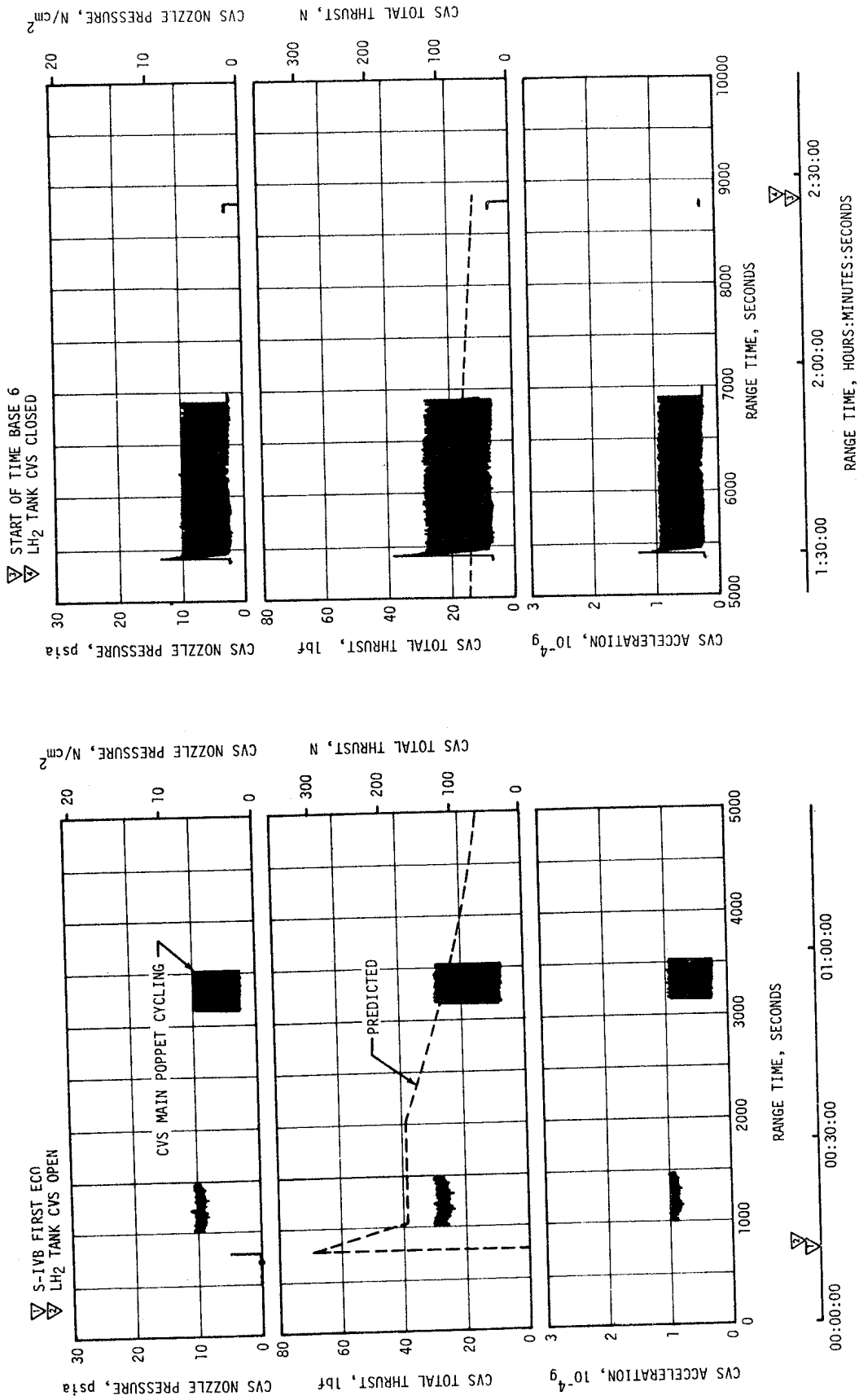


Figure 7-3. S-IVB CVS Performance - Coast Phase

7.6 S-IVB CHILLDOWN AND RESTART FOR SECOND BURN

Repressurization of the LOX and LH₂ tanks was satisfactorily accomplished by the O₂/H₂ burner. Helium heater "ON" command was initiated at 8810.1 seconds. The LH₂ repressurization control valves were opened at helium heater "ON" +6.1 seconds and the fuel tank was repressurized from 19.5 to 30.4 psia in 190.7 seconds. There were 25.8 lbm of cold helium used to repressurize the LH₂ tank. The LOX repressurization control valves were opened at O₂/H₂ burner "ON" +6.3 seconds and the LOX tank was repressurized from 38.5 to 40.0 psia in 65.2 seconds. There were 1.7 lbm of helium used to repressurize the LOX tank. LH₂ and LOX ullage pressures are shown in Figure 7-4. The burner continued to operate for a total of 454.8 seconds providing nominal propellant settling forces. The performance of the AS-508 O₂/H₂ burner was satisfactory as shown in Figure 7-5.

The S-IVB LOX recirculation system satisfactorily provided conditioned oxidizer to the J-2 engine for restart. The LOX and fuel pump inlet conditions are plotted in the start and run boxes in Figure 7-6. At second ESC, the LOX and fuel pump inlet temperatures were -295.0°F and -418.6°F, respectively. Fuel recirculation temperature at ESC was slightly out of the start box. This condition has occurred on previous flights and a change to the second ESC requirement is under consideration. Fuel recirculation system performance was adequate and conditions at the pump inlet were satisfactory at second STDV open. Second burn fuel lead generally followed the predicted pattern and resulted in satisfactory conditions as indicated by thrust chamber temperature and the associated fuel injector temperature. The S-IVB-508 stage was the first stage to have a start tank helium recharge capability using the LOX ambient repressurization system (bottle No. 2). Since the start system performance was nominal during coast and restart, no helium recharge was required. The start tank performed satisfactorily during second burn blowdown and recharge sequence. The engine start tank was recharged properly and maintained sufficient pressure during coast. The engine control sphere first burn gas usage was as predicted; the ambient helium spheres recharged the control sphere to a nominal level for restart.

The second burn start transient was satisfactory. The thrust buildup was within the limits set by the engine manufacturer and was similar to the thrust buildup on AS-506 and AS-507. The PU valve was in the proper full open (4.5 EMR) position prior to the second start. The total impulse from STDV open to STDV open +2.5 seconds was 174,932 lbf-s.

The helium control system performed satisfactorily during second burn mainstage. There was little pressure decay during the burn due to the connection to the stage repressurization system. Approximately 1.09 lbm of helium was consumed during second burn.

7.7 S-IVB MAINSTAGE PERFORMANCE FOR SECOND BURN

The propulsion reconstruction analysis showed that the stage performance during mainstage operation was satisfactory. A comparison of predicted and actual performance of thrust, specific impulse, total flowrate, and EMR

- 1 O₂/H₂ BURNER ON
- 2 LH₂ AND LOX CRYOGENIC REPRESS VALVES OPEN
- 3 TERMINATION OF LOX TANK REPRESS
- 4 TERMINATION OF LH₂ TANK REPRESS
- 5 O₂/H₂ BURNER OFF

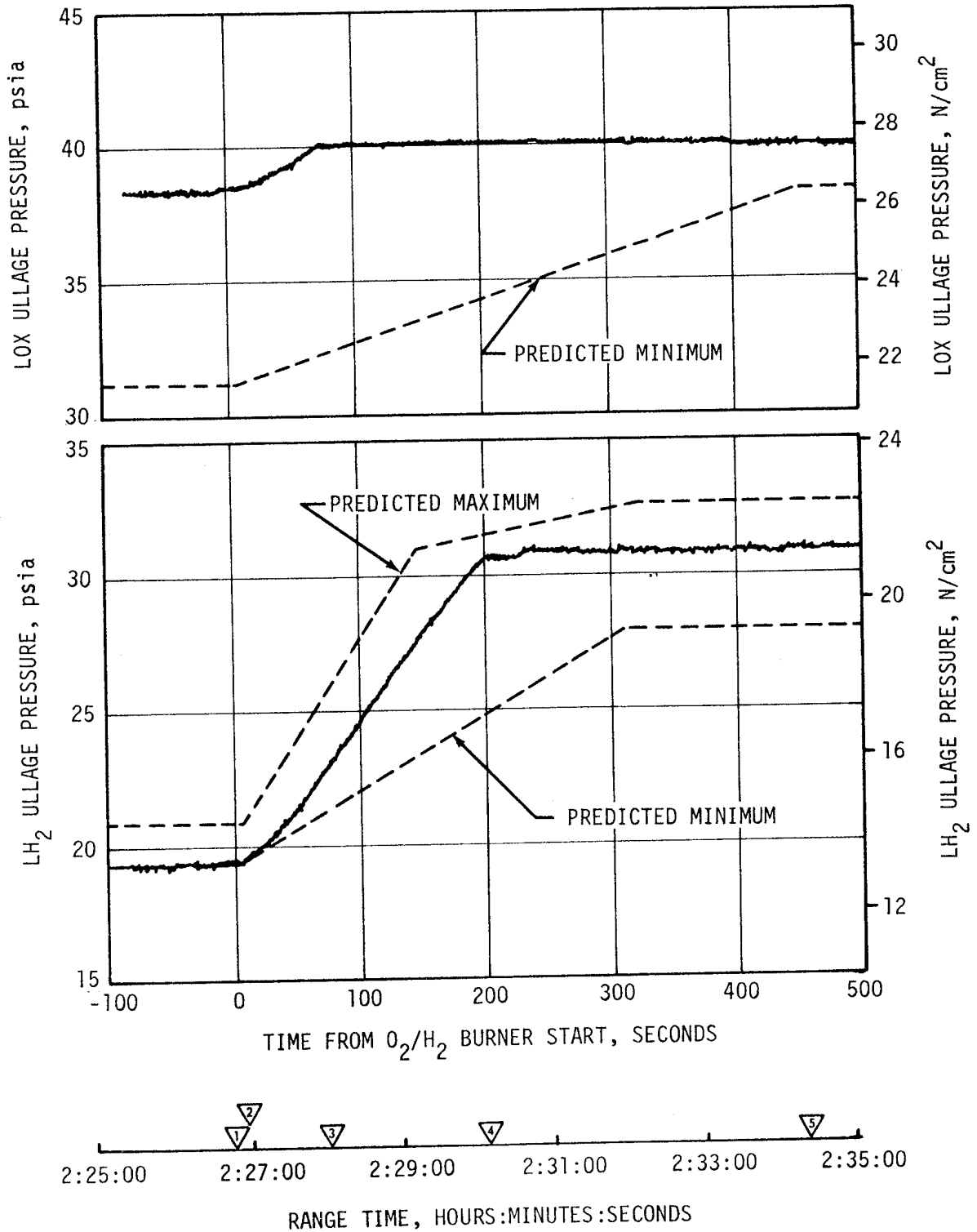


Figure 7-4. S-IVB Ullage Conditions During Repressurization Using O₂/H₂ Burner

- ▽1 HELIUM HEATER ON
- ▽2 LH₂ AND LOX CRYOGENIC REPRESS VALVES OPEN
- ▽3 TERMINATION OF LOX TANK REPRESS
- ▽4 TERMINATION OF LH₂ TANK REPRESS
- ▽5 HELIUM HEATER OFF

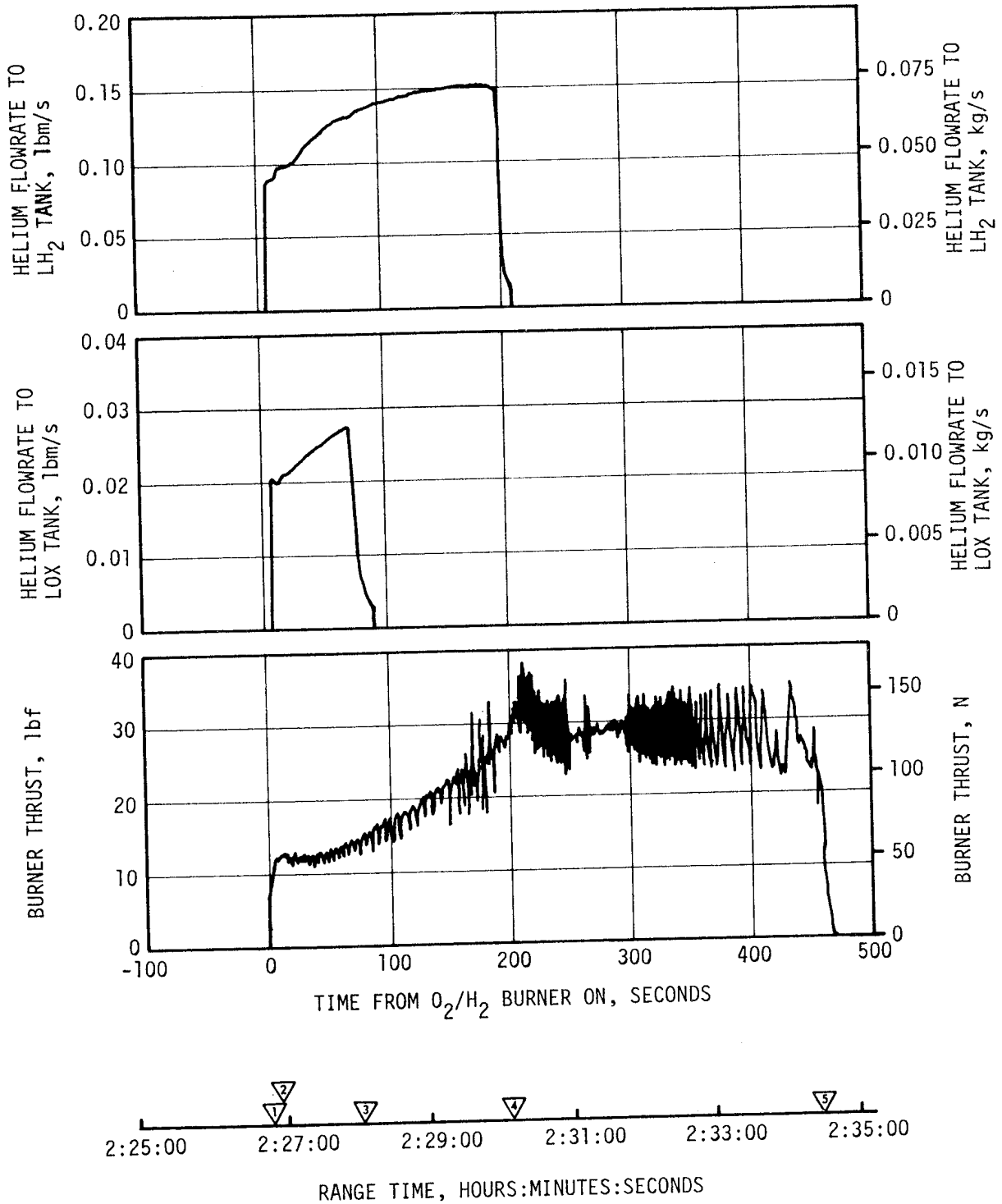


Figure 7-5. S-IVB O₂/H₂ Burner Thrust and Pressurant Flowrates

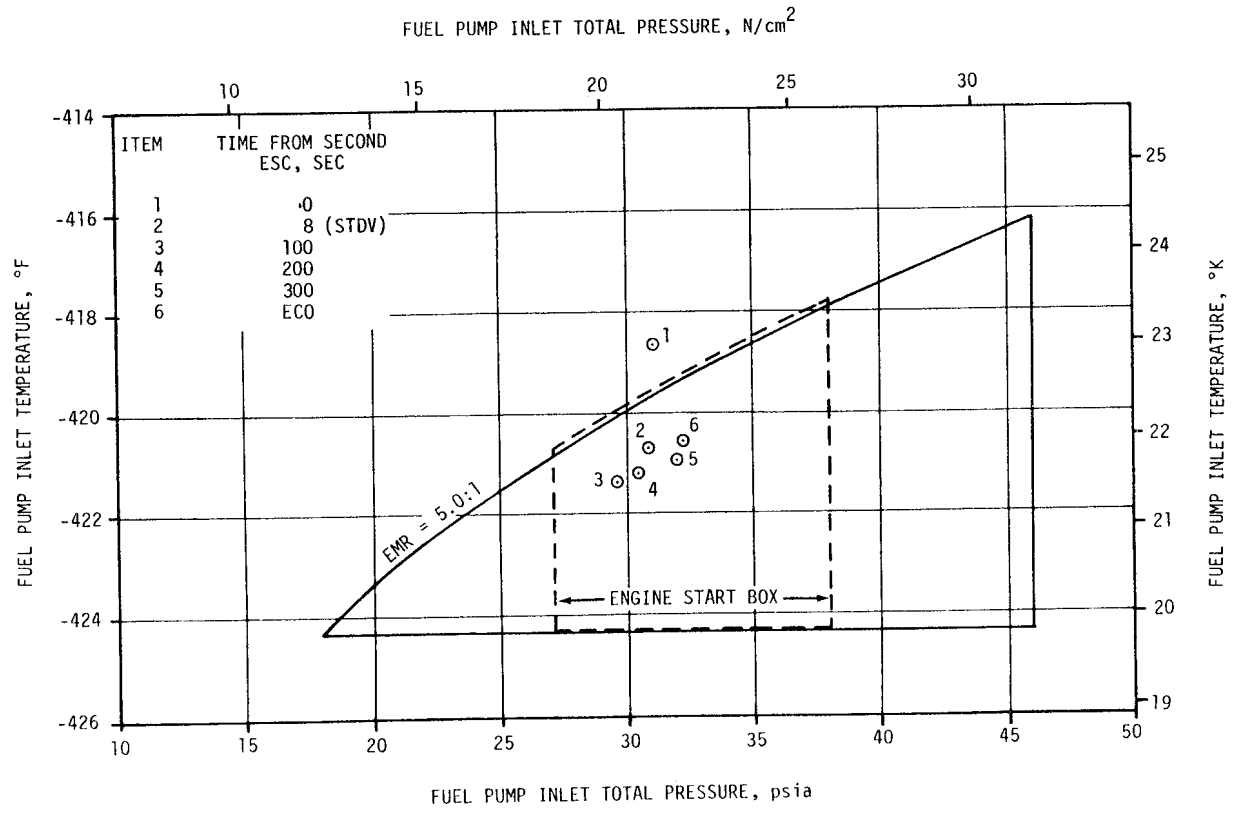
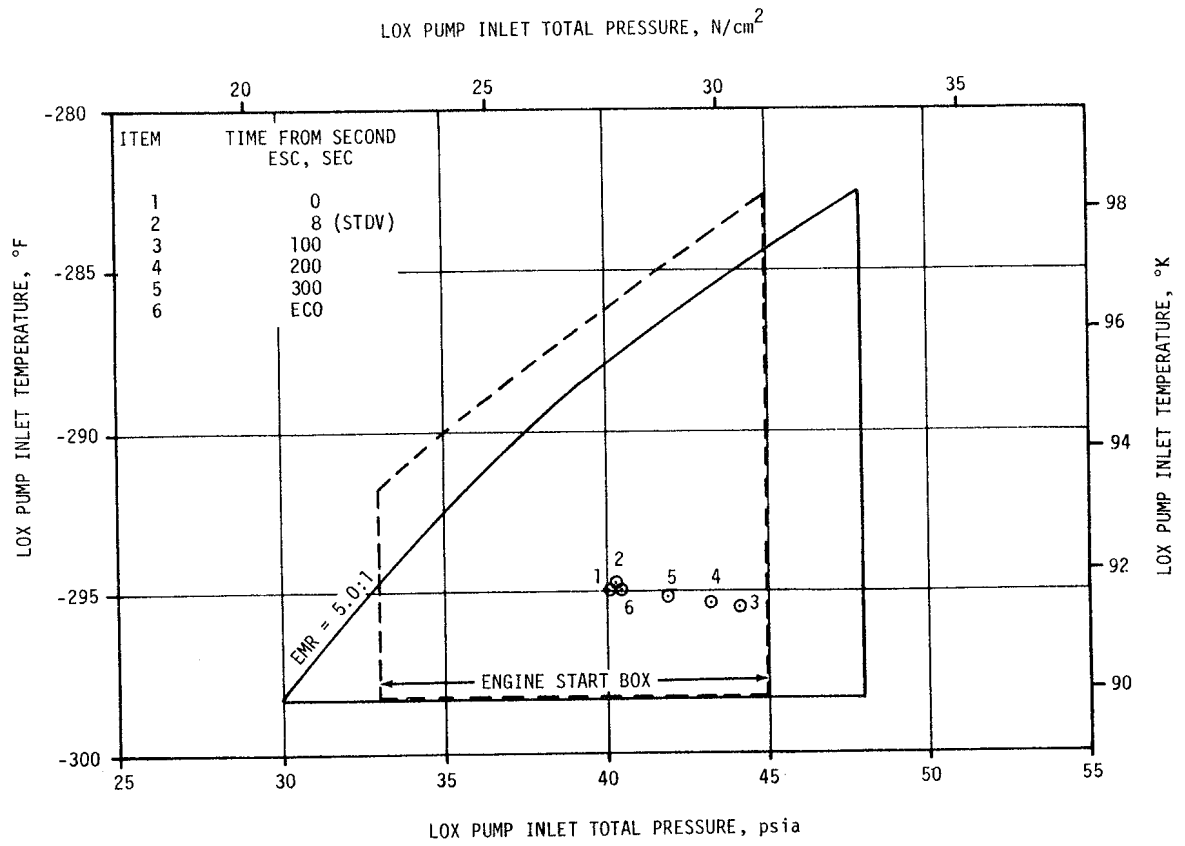


Figure 7-6. S-IVB Start Box and Run Requirements - Second Burn

versus time is shown in Figure 7-7. Table 7-2 shows the specific impulse, flowrates and EMR deviations from the predicted at the STDV +130 second time slice.

7.8 S-IVB SHUTDOWN TRANSIENT PERFORMANCE FOR SECOND BURN

S-IVB second ECO was initiated at 9697.17 seconds by a guidance velocity cutoff command for a burntime of 350.8 seconds. This burntime was 4.9 seconds less than that predicted.

The ECO transient was satisfactory. The total cutoff impulse to zero thrust was 46,235 lbf-s, which was 2224 lbf-s less than predicted. Cutoff occurred with the PU valve in the null position.

7.9 S-IVB STAGE PROPELLANT MANAGEMENT

The PU system was operated in the open-loop mode, which means the LOX flowrate is not controlled, to insure simultaneous depletion of propellants. The PU system successfully accomplished the requirements associated with propellant loading.

A comparison of propellant mass values at critical flight events, as determined by various analyses, is presented in Table 7-3. The best estimate full load propellant masses were 0.19 percent greater for LOX and 0.36 percent greater for LH₂ than the predicted values. This deviation was well within the required loading accuracy.

Extrapolation of propellant level sensor data to depletion, using the propellant flowrates, indicated that a LOX depletion would have occurred approximately 9.26 seconds after second burn velocity cutoff.

Table 7-2. S-IVB Steady State Performance - Second Burn
(STDV +130 Second Time Slice at Standard Altitude Conditions)

PARAMETER	PREDICTED	RECONSTRUCTION	FLIGHT DEVIATION	PERCENT DEVIATION FROM PREDICTED
Thrust, lbf	199,003	198,536	-467	-0.235
Specific Impulse, lbf-s/lbm	426.8	427.2	0.4	0.094
LOX Flowrate, lbm/s	387.65	386.54	-1.11	-0.286
Fuel Flowrate, lbm/s	78.58	78.24	-0.34	-0.433
Engine Mixture Ratio, LOX/Fuel	4.933	4.940	0.007	0.142

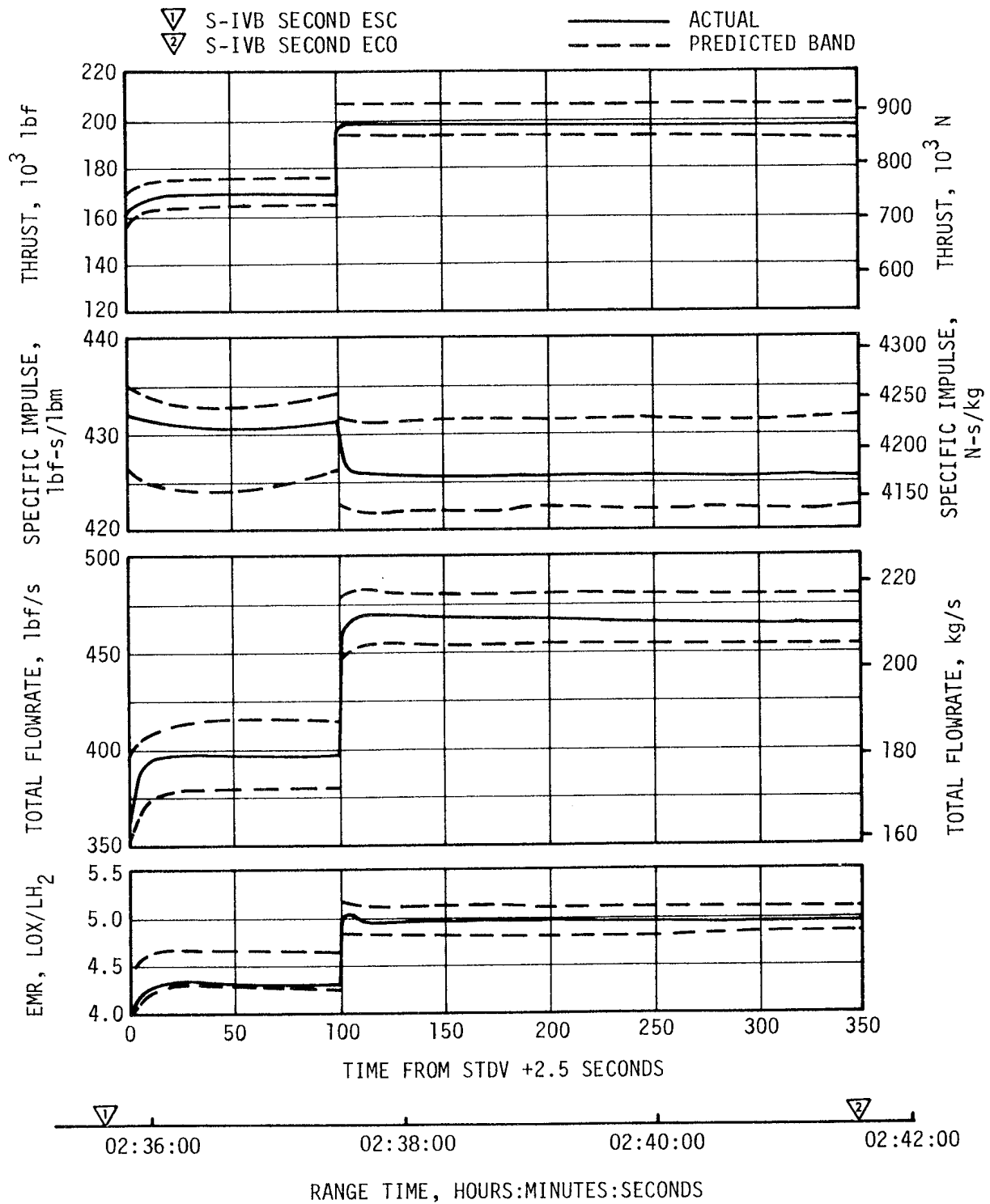


Figure 7-7. S-IVB Steady State Performance - Second Burn

Table 7-3. S-IVB Stage Propellant Mass History

EVENT	UNITS	PREDICTED*		PU INDICATED (CORRECTED)		PU VOLUMETRIC		FLOW INTEGRAL		BEST ESTIMATE**	
		LOX	LH2	LOX	LH2	LOX	LH2	LOX	LH2	LOX	LH2
S-IC Liftoff	1bm	191,532	43,500	191,588	43,585	191,615	43,892	192,123	43,418	191,890	43,657
First S-IVB ESC	1bm	191,526	43,500	191,588	43,585	191,615	43,892	192,123	43,418	191,890	43,657
First S-IVB ECO	1bm	131,552	31,398	132,641	31,420	132,826	31,590	132,799	31,336	132,738	31,445
Second S-IVB ESC	1bm	131,317	28,857	132,413	29,386	132,598	29,506	132,564	29,290	132,525	29,397
Second S-IVB ECO	1bm	1233	1451	4381	2280	4336	2252	4102	1977	4102	1977

* The predicted mass values have been adjusted for the actual burn times according to the predicted flowrates.
 ** The Best Estimate masses shown do not include mass below the main engine valves, as presented in Section 16.

During first burn the PU valve was positioned at null for start and remained there, as programmed, for the duration of the burn. The PU valve was commanded to the 4.5 EMR position 119.9 seconds prior to second ESC, and remained there for 230.5 seconds. At second ESC +110.6 seconds the valve was commanded to the null position (approximately 5.0 EMR) and remained there throughout the remainder of the flight. The actual times were within 28 milliseconds of predicted.

7.10 S-IVB PRESSURIZATION SYSTEMS

7.10.1 S-IVB Fuel Pressurization System

The LH₂ pressurization system met all of its operational requirements. The LH₂ pressurization system indicated acceptable performance during prepressurization, boost, first burn, coast phase, and second burn.

The LH₂ tank prepressurization command was received at -96.7 seconds and the tank pressurized signal was received 12.5 seconds later. Following the termination of prepressurization, the ullage pressure reached relief conditions, approximately 31.9 psia, and remained at that level until liftoff, as shown in Figure 7-8. A small ullage collapse occurred during the first 90 seconds of boost. The ullage pressure returned to the relief level by 130 seconds due to self pressurization.

During first burn, the average pressurization flowrate was approximately 0.66 lbm/s providing a total flow of 98.7 lbm. All during the burn the ullage pressure was at the relief level, as predicted.

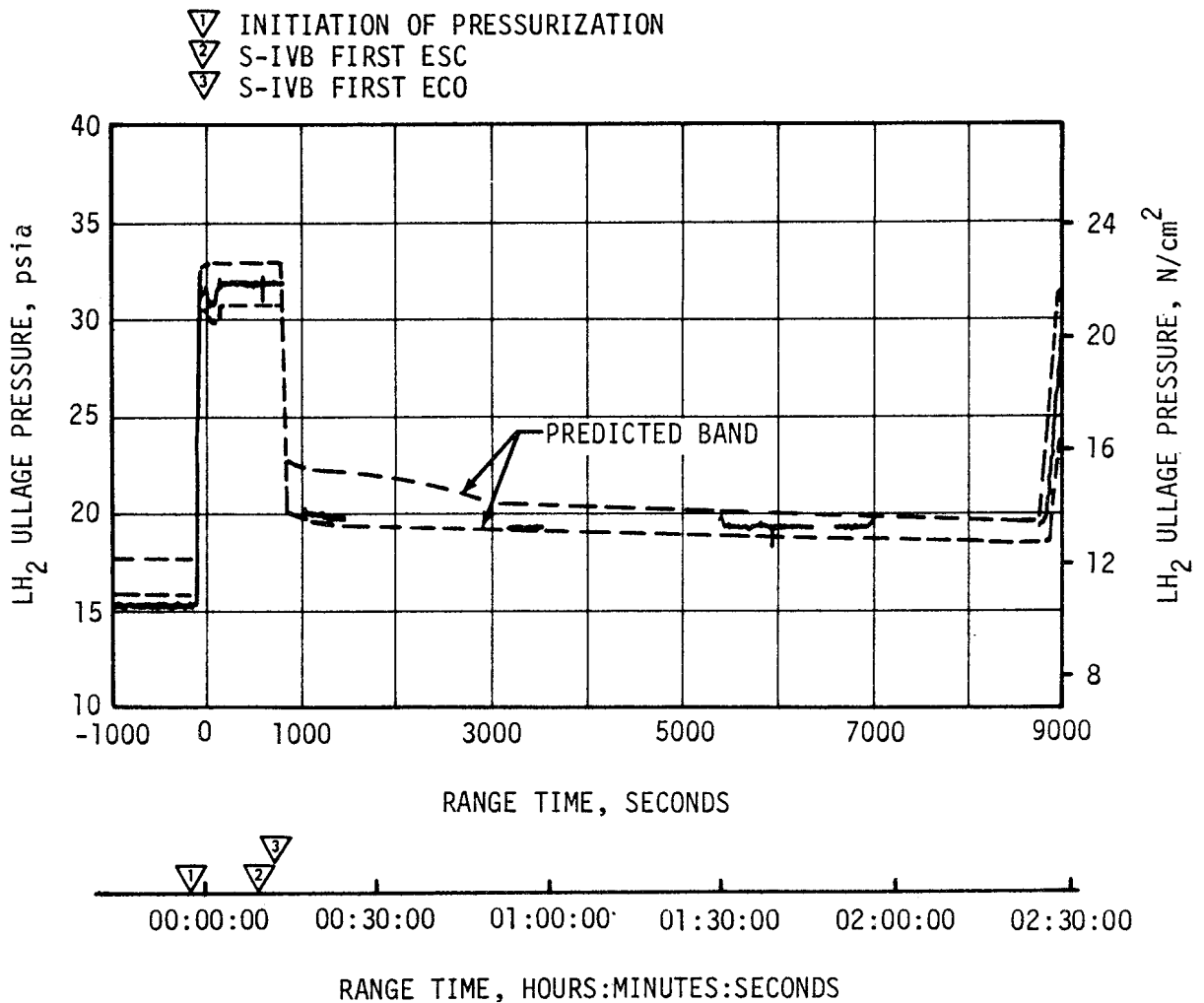


Figure 7-8. S-IVB LH₂ Ullage Pressure - First Burn and Parking Orbit

The LH₂ tank was satisfactorily repressurized for restart by the O₂/H₂ burner. The LH₂ ullage pressure was 31.0 psia at second burn ESC, as shown in Figure 7-9. The average second burn pressurization flowrate was 0.64 lbm/s until step pressurization when it increased to 1.27 lbm/s. This provided a total flow of 273.3 lbm during second burn. Significant venting during second burn occurred at second ESC +280 seconds when step pressurization was initiated. This behavior was as predicted.

The LH₂ pump inlet Net Positive Suction Pressure (NPSP) was calculated from the pump interface temperature and total pressure. These values indicated that the NPSP at first burn ESC was 16.2 psi. At the minimum point, the NPSP was 7.2 psi above the required value. Throughout the burn, the NPSP had satisfactory agreement with the predicted values. The NPSP at second burn ESC was 1.1 psi which was 3.4 psi below the required value. The NPSP requirement was met by second STDV open. Figures 7-10 and 7-11 summarize the fuel pump inlet conditions for first and second burns.

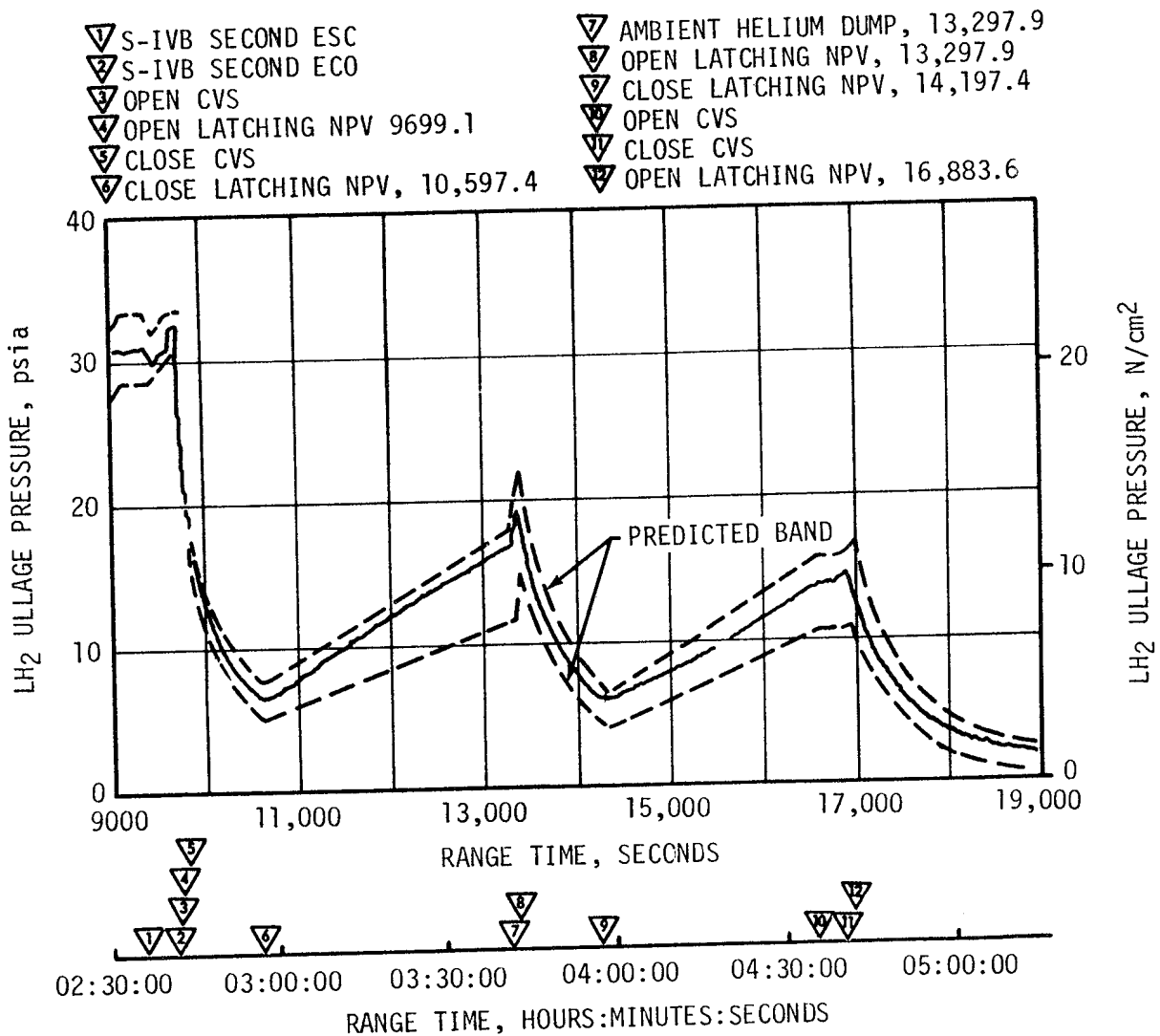


Figure 7-9. S-IVB LH2 Ullage Pressure - Second Burn and Translunar Coast

7.10.2 S-IVB LOX Pressurization System

LOX tank prepressurization was initiated at -167 seconds and increased the LOX tank ullage pressure from ambient to 40.8 psi within 20 seconds, as shown in Figure 7-12. Four makeup cycles were required to maintain the LOX tank ullage pressure before the ullage temperature stabilized. At -96 seconds the LOX tank ullage pressure increased from 39.9 to 42.5 psia due to fuel tank prepressurization. The pressure then gradually decreased to 42.1 psia at liftoff.

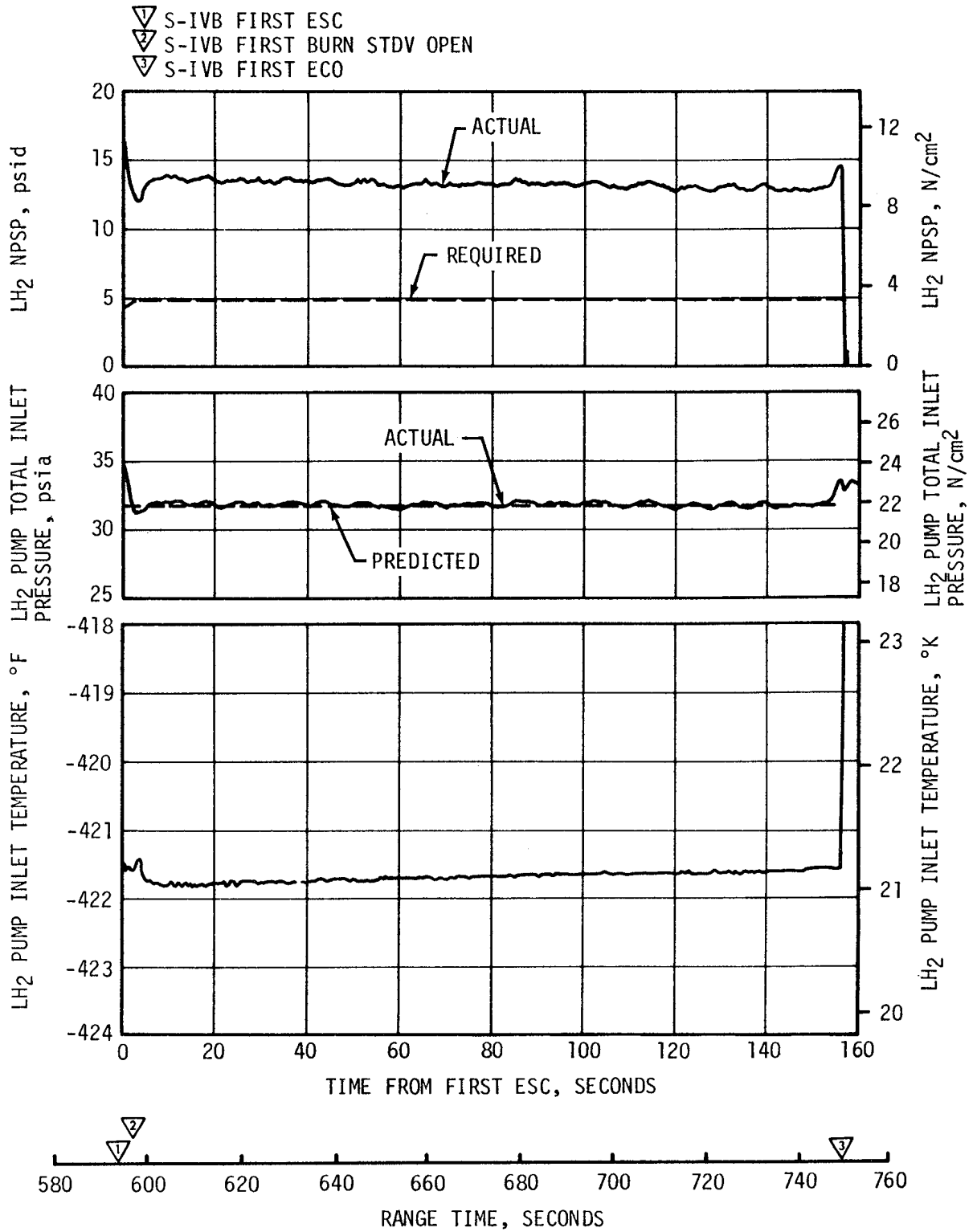


Figure 7-10. S-IVB Fuel Pump Inlet Conditions - First Burn

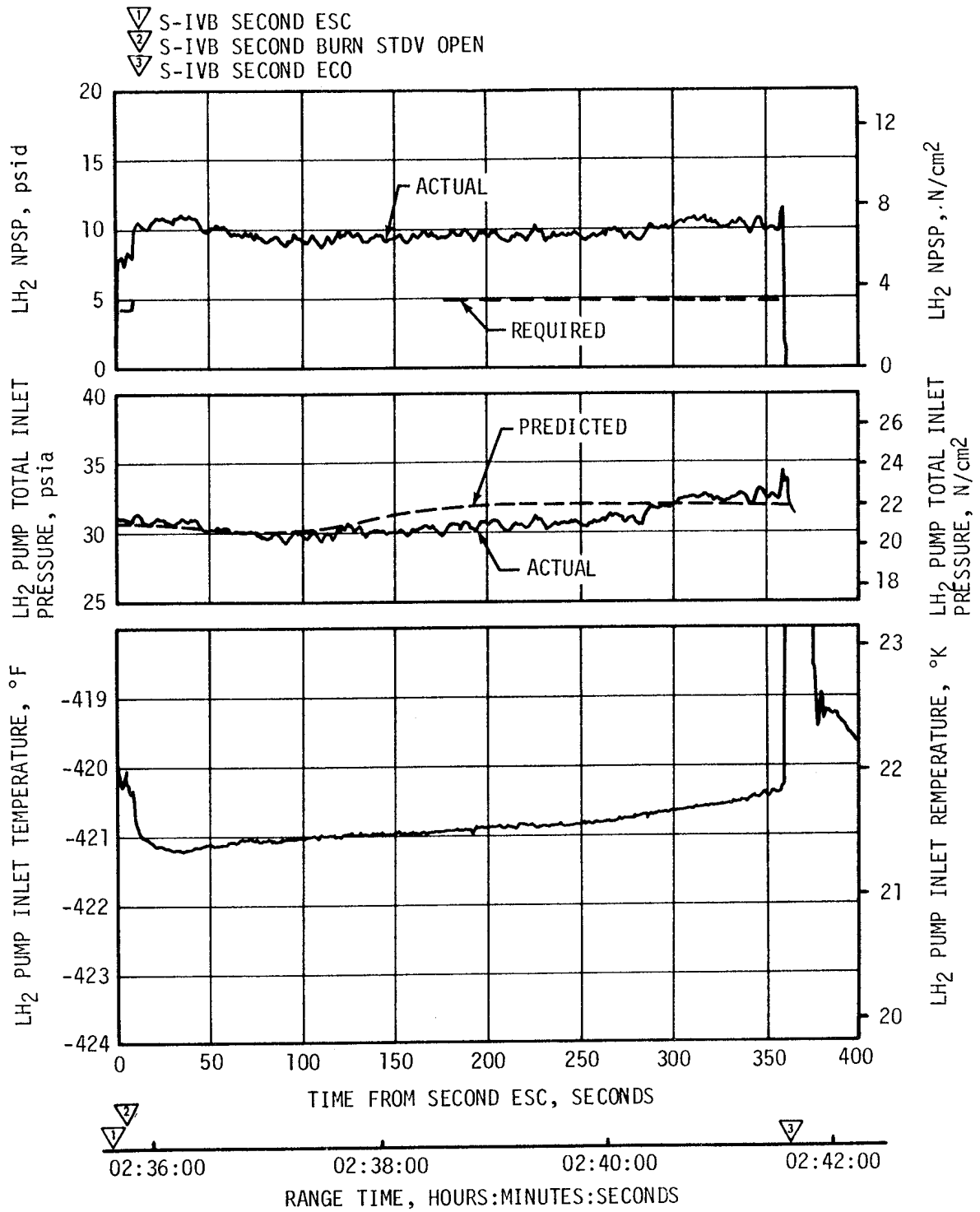


Figure 7-11. S-IVB Fuel Pump Inlet Conditions - Second Burn

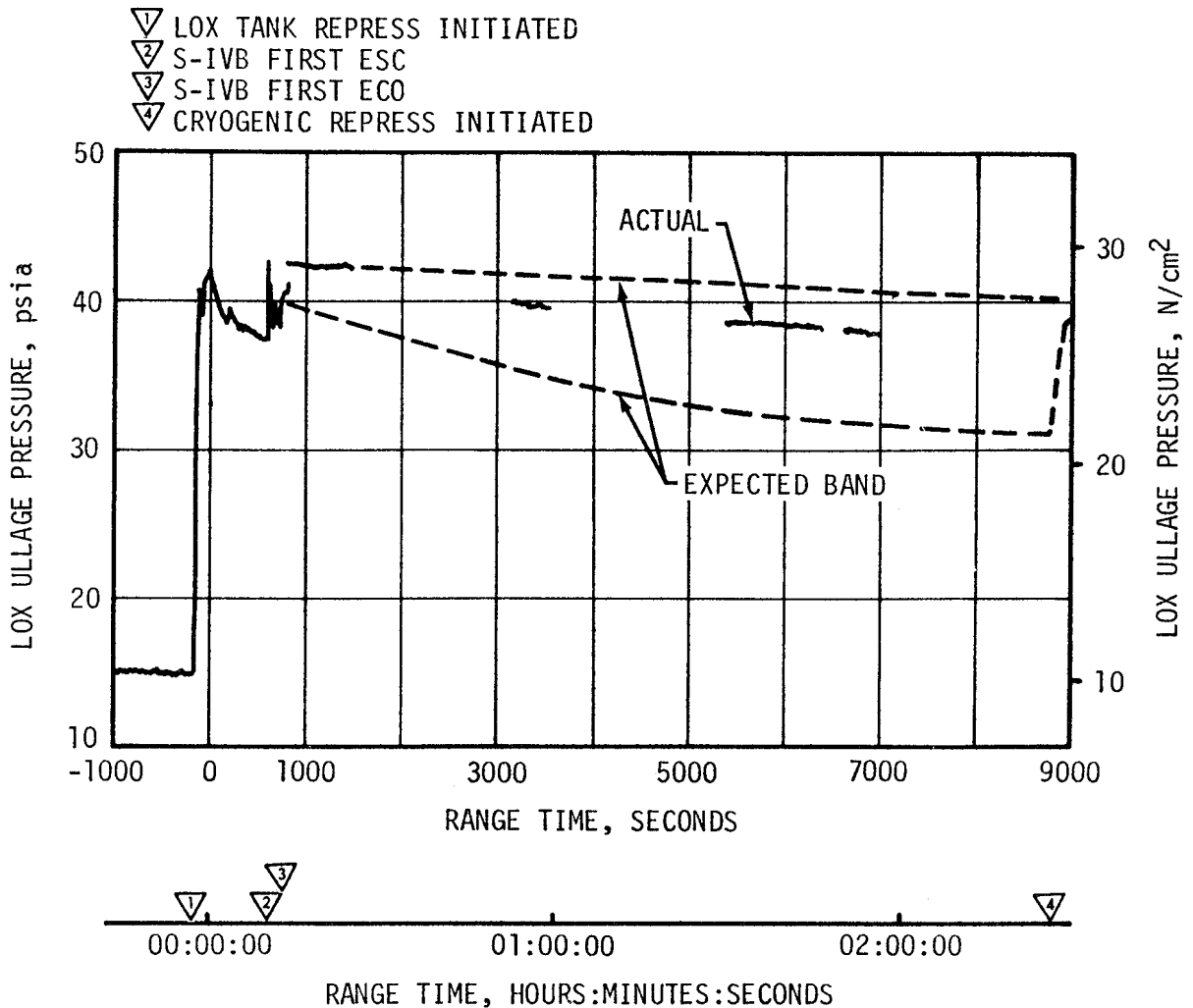


Figure 7-12. S-IVB LOX Tank Ullage Pressure - First Burn and Parking Orbit

During boost there was a normal rate of ullage pressure decay caused by an acceleration effect and ullage collapse. No makeup cycles occurred because of an inhibit until after Time Base 4 (T_4). LOX tank ullage pressure was 37.1 psia just prior to ESC and was increasing at ESC due to a makeup cycle.

During first burn, three over-control cycles were initiated, exactly matching the predicted three cycles. The LOX tank pressurization flowrate variation was 0.25 to 0.33 lbm/s during under-control system operation. This variation is normal and is caused by temperature effects. Heat exchanger performance during first burn was satisfactory.

During orbital coast the LOX tank ullage pressure experienced a decay similar to, though less than, that experienced on the AS-506 and AS-507 flights. This decay was within the predicted band, and was not a problem.

Repressurization of the LOX tank prior to second burn was required and was satisfactorily accomplished by the burner. The tank ullage pressure was 40.0 psia at second ESC and satisfied the engine start requirements, as shown in Figure 7-13.

Pressurization system performance during second burn was satisfactory and had the same characteristics noted during first burn. There were no over-control cycles, as compared to a prediction of from zero to one. Flowrate varied between 0.33 and 0.39 lbm/s. Heat exchanger performance was satisfactory.

The LOX NPSP calculated at the interface was 25.6 psi at first burn ESC. The NPSP decreased after start and reached a minimum value of 23.9 psi at 1 second after ESC. This was 11.1 psi above the required NPSP at that time.

The LOX pump static interface pressure during first burn followed the cyclic trends of the LOX tank ullage pressure. The NPSP calculated at the engine interface was 22.9 psi at second burn ESC. At all times during second burn, NPSP was above the required level. Figures 7-14 and 7-15 summarize the LOX pump conditions for the first burn and second burn. The run requirements for first and second burn were satisfactorily met.

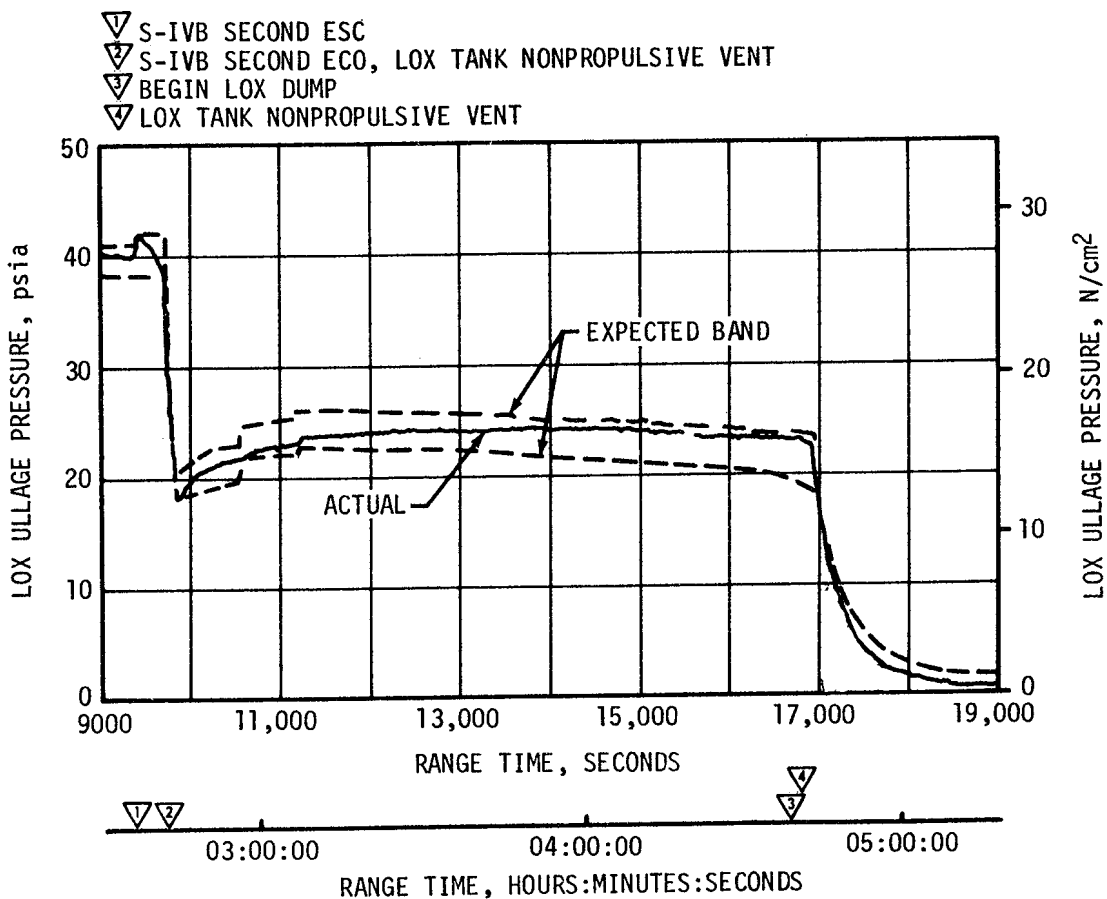


Figure 7-13. S-IVB LOX Tank Ullage Pressure - Second Burn and Translunar Coast

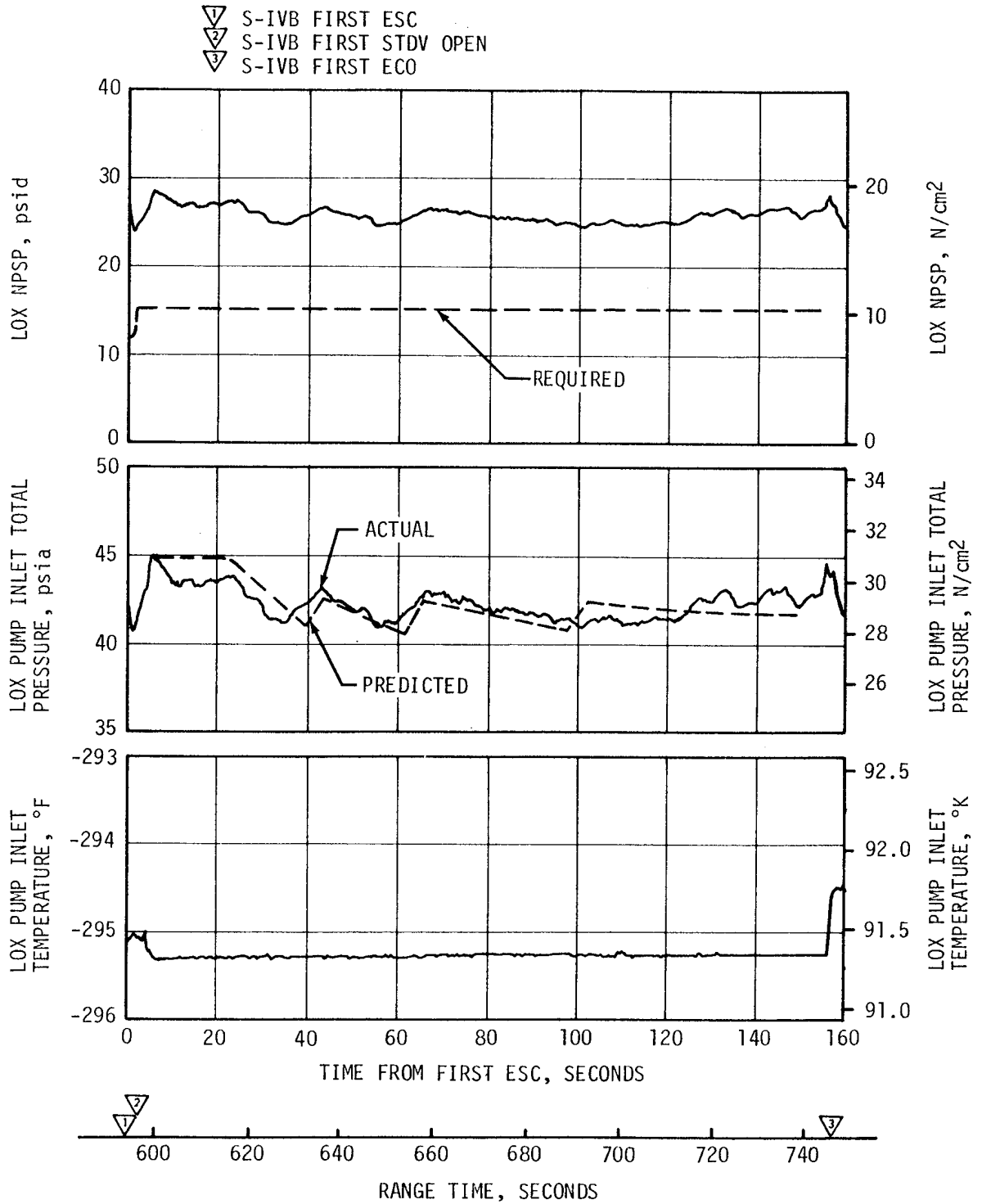


Figure 7-14. S-IVB LOX Pump Inlet Conditions - First Burn

The cold helium supply was adequate to meet all flight requirements. At first burn ESC the cold helium spheres contained 381 lbm of helium. At the end of the second burn, the helium mass had decreased to 175 lbm. Figure 7-16 shows helium supply pressure history.

7.11 S-IVB PNEUMATIC CONTROL SYSTEM

The pneumatic control and purge system performed satisfactorily during all phases of the mission. Pneumatic regulator operation was nominal at all times. The LOX chilldown pump motor container purge pressure was lower than on previous flights. The low pressure was probably due to contamination of the sintered orifices that control the pressure. The lower pressure did not effect LOX chilldown pump performance.

7.12 S-IVB AUXILIARY PROPULSION SYSTEM

The APS demonstrated close to nominal performance throughout its flight and met control system demands out to propellant depletion at approximately 19.5 hours.

The APS propellant supply systems performed as expected during the flight. Propellant temperatures ranged from 71 to 96°F. The propellant usage, as shown in Table 7-4, approximated the nominal prediction out to 12 hours 47 minutes. At this time the APS yaw engines were erroneously fired as a result of the loss of the primary yaw gyro. When the backup yaw gyro took over, the yaw engine firing rate which had built up in magnitude and duration subsided to normal limit cycle pulsing operation. At 13 hours and 42 minutes the APS received an erroneous signal from the IU to return to the TD&E attitude. Following this unscheduled maneuver the APS maintained limit cycle operation until 19 hours and 9 minutes. At this time, more erroneous signals were received from the IU. At 70,150 seconds (19:29:10) a yaw engine in each module went on steady state and the pitch engines were fired in alternating series of pulses until propellant depletion. This APS activity was sufficient to cause a stage velocity change of 7 to 10 ft/s. All the erroneous firing signals received from the IU were after normal stage life time. For an additional discussion of the results of these erroneous firing signals see paragraph 10.4.4.

The APS propellant pressurization was satisfactory throughout the flight. However, Module 1 regulator outlet pressure started to increase at approximately 3 hours and by 7.5 hours the regulator outlet pressure had increased to 203 psia and then reached a maximum of 204.5 psia at 10 hours (Figure 7-17). Examination of the helium bottle temperature and regulator outlet pressure and the vehicle orientation indicates that solar heating was responsible for these pressure changes. A similar thermal effect on the regulator outlet pressure was experienced during the regulator qualification tests and also at approximately 5.5 hours after TLI on the AS-505 flight.

- ▽ S-IVB FIRST ECO
- ▽ START CRYOGENIC REPRESS
- ▽ S-IVB SECOND ESC
- ▽ S-IVB SECOND ECO
- ▽ START COLD HELIUM DUMP, 9716.0

- ▽ END COLD HELIUM DUMP, 10,597.0
- ▽ START COLD HELIUM DUMP, 13,359.4
- ▽ END COLD HELIUM DUMP, 14,196.6
- ▽ START COLD HELIUM DUMP, 16,884.8
- ▽ END COLD HELIUM DUMP, 18,684.4

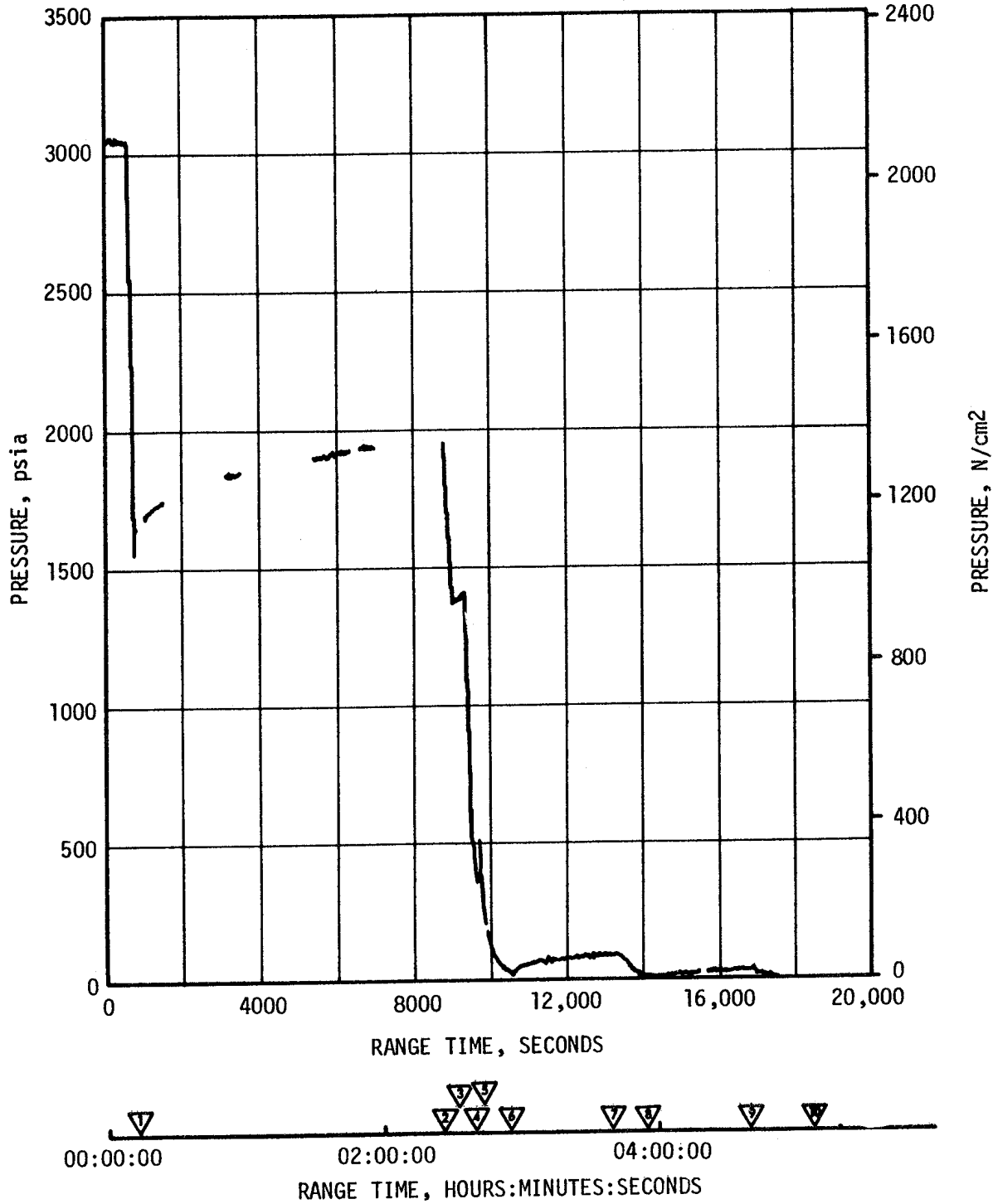


Figure 7-16. S-IVB Cold Helium Supply History

Table 7-4. S-IVB APS Propellant Consumption

TIME PERIOD	MODULE 1		MODULE 2	
	OXIDIZER, LBM	FUEL, LBM	OXIDIZER, LBM	FUEL, LBM
Initial Load	204.8	126.1	204.3	126.1
First Burn (Roll Control)	0.5	0.3	0.5	0.3
ECO to End of First APS Ullage Burn (86.7 sec)	12.9	10.2	12.9	10.2
End of First Ullage Burn to Start of Second Ullage Burn	13.8	8.2	3.5	2.6
Second Ullage Burn (76.7 sec)	11.5	9.1	11.7	9.2
Second Burn (Roll Control)	0.4	0.2	0.4	0.2
ECO to Start of Evasive Ullage Burn	16.0	10.1	14.4	9.0
Evasive Ullage Burn (80 sec)	11.9	9.4	11.9	9.4
From End of Evasive Ullage Burn to Start of Lunar Impact Ullage Burn at 6 Hours	8.1	5.1	12.0	7.5
Lunar Impact Ullage Burn (217 sec)	26.7	22.0	30.7	24.6
From End of Lunar Impact Burn to Loss of Yaw Gyro at Approx. 12 Hours 47 Minutes	17.9	11.2	18.1	11.3
Propellant Usage During Unstable Period During Loss of Yaw Gyro to Repeat of TD&E Maneuver at 13 Hours 42 Minutes	20.1	12.4	19.2	12.0
Propellant Usage From 13 Hours 42 Minutes to 19 Hours 9 Minutes	9.8	6.1	13.3	8.4
From 19 Hours 9 Minutes to Propellant Depletion	55.2	21.8	55.7	21.4

Note: The APS propellant consumption presented in this table was determined from helium bottle conditions (pressure, volume, temperature).

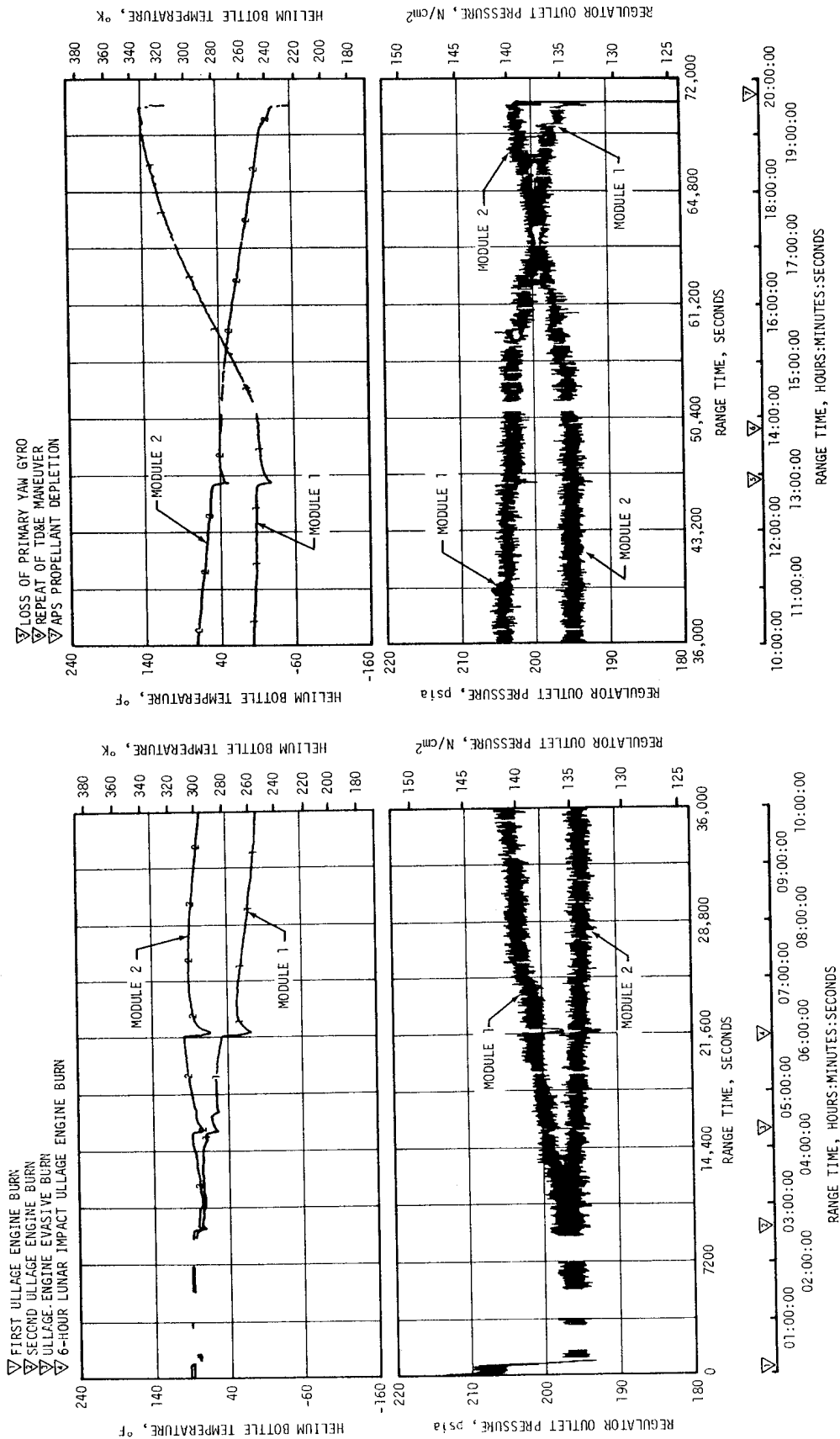


Figure 7-17. APS Helium Bottle Temperature and Regulator Outlet Pressure

Nominal primary regulator operation is 196 ± 3 psig with a lockup of 203 psig. The higher regulator pressure of 204.5 psia observed during this flight does not present any system operation problems. A thermal analysis of the AS-508 flight indicated that the APS regulator temperature was maintained above -10°F for approximately 6.5 hours beyond TLI.

The APS ullage pressures in the propellant ullage tanks ranged from 187 to 202 psia. The helium bottle temperatures ranged from -30 to $+140^{\circ}\text{F}$.

The performance of the attitude control thrusters and the ullage thrusters was satisfactory throughout the mission. The thruster chamber pressures ranged from 95 to 102 psia. The ullage thrusters successfully completed the three sequenced burns of 86.7 seconds, 76.7 seconds and 80.0 seconds as well as the ground commanded 217 second lunar impact burn. The planned ullage burn at 9 hours, to impact the lunar target area, was not required.

7.13 S-IVB ORBITAL SAFING OPERATIONS

The S-IVB high pressure systems were safed following J-2 engine cutoff in order to demonstrate this capability. The thrust developed during the LOX dump was utilized to provide a velocity change for the lunar impact maneuver. The manner and sequence in which the safing was performed is presented in Figure 7-18.

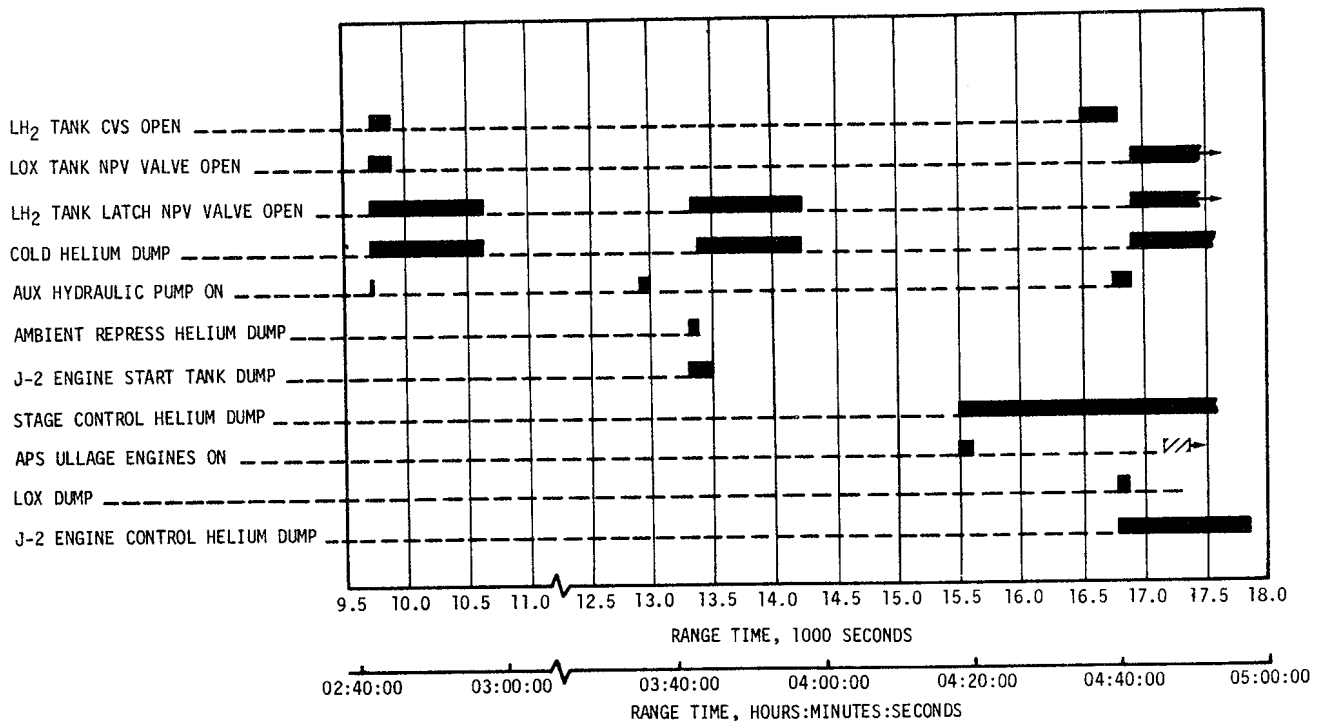


Figure 7-18. S-IVB LOX Dump and Orbital Safing Sequence

7.13.1 Fuel Tank Safing

The LH₂ tank was satisfactorily safed by accomplishing three programmed vents, as indicated in Figure 7-18, utilizing both the Nonpropulsive Vent (NPV) and CVS. The LH₂ tank ullage pressure during safing is shown in Figure 7-9. At second ECO, the LH₂ tank ullage pressure was 32.4 psia and after three vent cycles had decayed to approximately zero. The mass of GH₂ and LH₂ vented agrees with the 2510 lbm of liquid residual and pressurant in the tank at the end of powered flight.

7.13.2 LOX Tank Dump and Safing

Immediately following second burn cutoff, a programmed 150 second vent reduced LOX tank ullage pressure from 38.6 psia to 18.0 psia, as shown in Figure 7-13. Data levels were as expected with 73.6 lbm of helium and 128.9 lbm of GOX being vented overboard. As indicated in Figure 7-13, the ullage pressure then rose gradually due to self-pressurization, to 23.0 psia at the initiation of the TD&E maneuver.

The LOX tank dump was initiated at 16,759.4 seconds (04:39:19.4) and was satisfactorily accomplished. A steady-state liquid flow of 375 gpm was reached within 15 seconds. Gas ingestion did not occur during dump. The LOX residual at the start of dump was 3923 lbm. Calculations indicate that 2330 lbm of LOX was dumped. During dump, the ullage pressure decreased from 23.2 psia to 22.8 psia. LOX dump ended at 16,807.4 seconds (04:40:07.4) as scheduled by closure of the Main Oxidizer Valve (MOV). A steady-state LOX dump thrust of 760 lbf was obtained. The total impulse before MOV closure was 31,000 lbf-s, resulting in a calculated velocity change of 28.5 ft/s. Figure 7-19 shows the LOX dump thrust, LOX flowrate, oxidizer mass, and LOX ullage pressure during LOX dump. The predicted curves provided for the LOX flowrate and dump thrust correspond with the quantity of LOX dumped and the actual ullage pressure.

Seventy-two seconds following termination of LOX dump, the LOX NPV valve was opened and remained open for the duration of the mission. LOX tank ullage pressure decayed from 22.2 psia at 16,880 seconds (04:41:20) to zero pressure at approximately 31,000 seconds (08:36:40).

Sufficient impulse was derived from the LOX dump, LH₂ CVS operation, and APS ullage burn to achieve a successful lunar impact. For further discussion of the lunar impact refer to Section 4A.

7.13.3 Cold Helium Dump

A total of approximately 170 lbm of helium was dumped during the three programmed dumps, which occurred as shown in Figure 7-18.

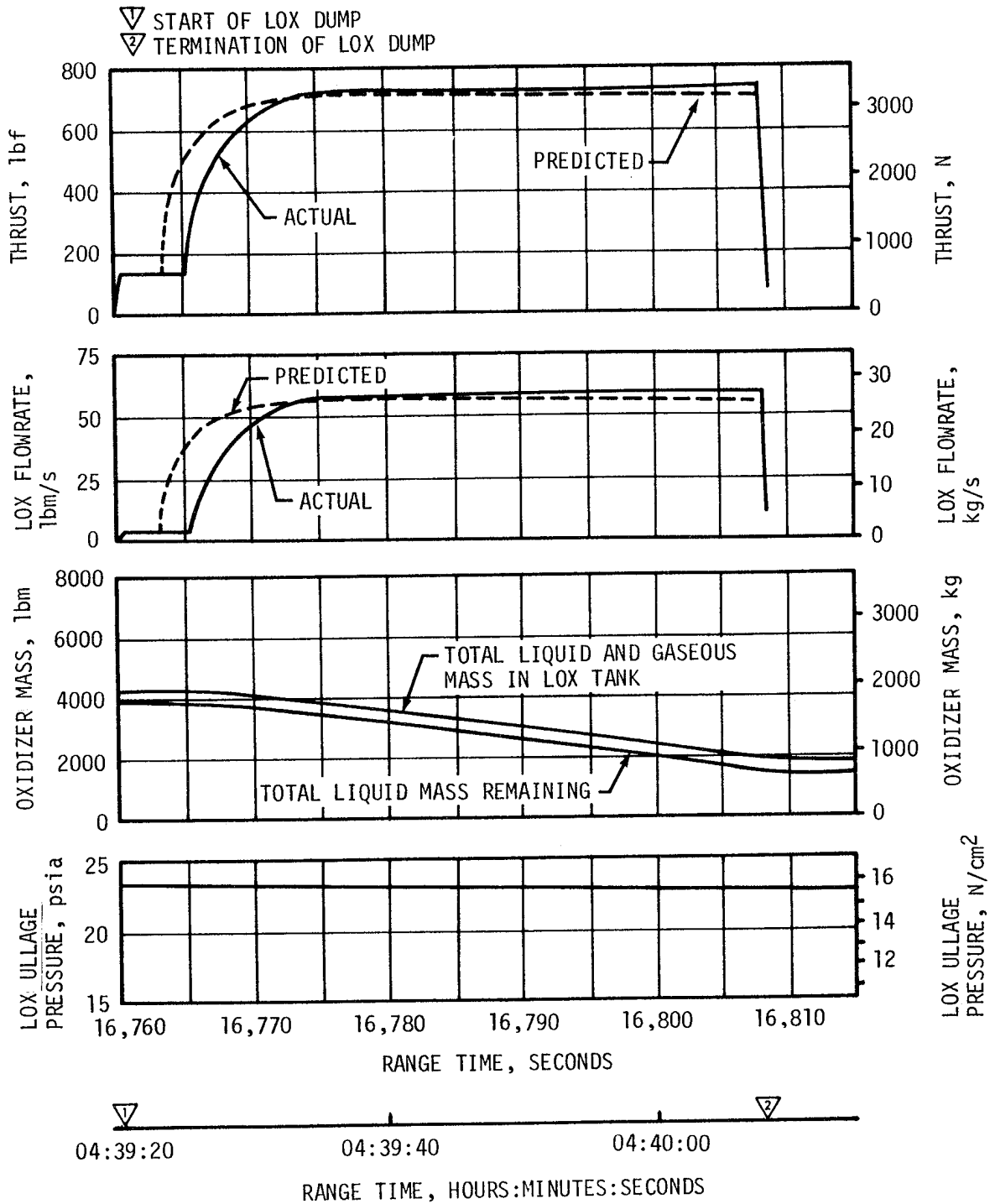


Figure 7-19. S-IVB LOX Dump Parameter Histories

7.13.4 Ambient Helium Dump

Approximately 30.0 lbm of ambient helium in the LOX and LH₂ repressurization spheres was dumped via the fuel tank. The 62 second dump occurred at 13,298.4 seconds (03:41:38.4). The pressure decayed from 3000 to 380 psia.

7.13.5 Stage Pneumatic Control Sphere Safing

The stage pneumatic control sphere was safed by initiating the J-2 engine pump and by flowing helium overboard through the pump seal cavities for 3600 seconds. This activity began at 15,480 seconds (04:18:00) and satisfactorily reduced the pressure in the sphere from 2870 to 1750 psia.

7.13.6 Engine Start Tank Safing

The engine start tank was safed during a period of approximately 150 seconds beginning at 13,298.4 seconds (03:41:38.4). Safing was accomplished by opening the sphere vent valve. Pressure was decreased from 1250 to 10 psia with 4.20 lbm of hydrogen being vented.

7.13.7 Engine Control Sphere Safing

The safing of the engine control sphere began at 16,760 seconds (04:39:20). The helium control solenoid was energized to vent helium through the engine purge system. The initial pressure in the sphere was 3080 psia, and it decayed to about 700 psia in 65 seconds. At this time gaseous helium from the ambient repressurization bottles began flowing to the engine control sphere. Helium from the control sphere and repressurization bottles continued to vent until 17,810 seconds (04:56:50). During this time, the pressure in the repressurization bottles had decayed from 700 to 150 psia. The control sphere pressure had decayed to 130 psia. Subsequent to the closing of the control solenoid, the control sphere repressurized to 170 psia without any noticeable decay in stage ambient repressurization bottle pressure. During the 1050 second safing period, a total of 11.01 lbm of helium was vented overboard.

7.14 HYDRAULIC SYSTEM

The S-IVB hydraulic system performance was satisfactory during its complete mission (S-IC/S-II boost, first and seconds burns of S-IVB, and orbital coast).

SECTION 8

STRUCTURES

8.1 SUMMARY

The structural loads experienced during the S-IC boost phase were well below design values. The maximum Q region bending moment was 69×10^6 lbf-in. at the S-IC LOX tank which was 25 percent of design value. Thrust cutoff transients experienced by AS-508 were similar to those of previous flights. The maximum dynamic transient at the Instrument Unit (IU) resulting from S-IC Center Engine Cutoff (CECO) was ± 0.20 g longitudinal. At Outboard Engine Cutoff (OECO) a maximum dynamic longitudinal acceleration of ± 0.28 g and ± 0.85 g was experienced at the IU and Command Module (CM), respectively. The order of magnitude of the thrust cutoff responses are considered normal.

During S-IC stage boost phase, 4 to 5 hertz oscillations were detected beginning at 100 seconds. The maximum amplitude measured in the IU at 125 seconds was ± 0.04 g. Oscillations in the 4 to 5 hertz range have been observed on previous flights and are considered to be normal vehicle response to flight environment.

AS-508 experienced low frequency (14 to 16 hertz) POGO oscillations during S-II stage boost. Three distinct periods of structural/propulsion coupled oscillations exhibited peaks at 180, 250, and 330 seconds. The third period of oscillations resulted in LOX pump discharge pressure variations of sufficient magnitude to activate the center engine thrust OK pressure switches and shut down the engine 132 seconds early. All oscillations decayed to a normal level following CECO. Analysis of flight data indicates that no structural failure occurred as a result of the oscillations. Flight measurements also show that the oscillations were confined to the S-II stage and were not transmitted up the vehicle.

The structural loads experienced during the S-IVB stage burns were well below design values. During first burn the S-IVB experienced low amplitude, 18 to 20 hertz oscillations. The amplitudes measured on the gimbal block were comparable to previous flights and well within the expected range of values. Similarly, S-IVB second burn produced intermittent low amplitude oscillations in the 12 to 14 hertz frequency range which peaked near second burn cutoff.

Three vibration measurements were made on the S-IVB aft interstage. The maximum vibration levels measured occurred at liftoff and during the Mach 1 to Max Q flight period and were considered normal.

8.2 TOTAL VEHICLE STRUCTURES EVALUATION

8.2.1 Longitudinal Loads

The structural loads experienced during boost were well below design values with the exception of the S-II POGO phenomenon discussed in paragraph 8.2.3. The AS-508 vehicle liftoff occurred at a steady-state acceleration of 1.2 g. Maximum longitudinal dynamic response measured during thrust buildup and release was ± 0.18 g and ± 0.40 g at the IU and CM, respectively, as shown in Figure 8-1. Both values are lower than the respective values of ± 0.25 g and ± 0.55 g measured on AS-507.

The longitudinal loads experienced at the time of maximum bending moment (76 seconds) were as expected and are shown in Figure 8-2. The steady-state longitudinal acceleration for AS-508 was 1.9 g as compared to 2.03 g on AS-507.

Figure 8-2 also shows that the maximum longitudinal loads imposed on the S-IC stage thrust structure, fuel tank, and intertank occurred at CECO (135 seconds) at a longitudinal acceleration of 3.6 g. The maximum longitudinal loads imposed on all vehicle structure above the S-IC intertank occurred subsequent to OECO (164 seconds) at an acceleration of 3.8 g.

8.2.2 Bending Moments

The 1-2-1-1 engine start sequence (see paragraph 5.2) on AS-508 introduced lateral responses similar to those measured on AS-507. The maximum response level at the CM was approximately ± 0.17 g (0.118 Grms) as compared to the AS-507 maximum of approximately ± 0.15 g (0.104 Grms). The ± 0.17 g was 50 percent of the preflight predicted 3-sigma value of ± 0.34 g.

The inflight winds that existed during the maximum dynamic pressure phase of the flight peaked at 108.1 knots at 44,540 feet. As shown in Figure 8-3, the maximum bending moment imposed on the vehicle was 69×10^6 lbf-in. at approximately 76 seconds. This moment loading was approximately 25 percent of design value.

8.2.3 Vehicle Dynamic Characteristics

8.2.3.1 Longitudinal Dynamic Characteristics. During S-IC stage boost phase, the significant vehicle response was the expected 4 to 5 hertz first longitudinal mode oscillations. These oscillations began at approximately 100 seconds and continued until CECO. Maximum amplitudes at the S-IC intertank sensor (A001-118) reached ± 0.03 g at 133 seconds and the IU sensor (A002-603) recorded ± 0.04 g at approximately 125 seconds (Figure 8-4).

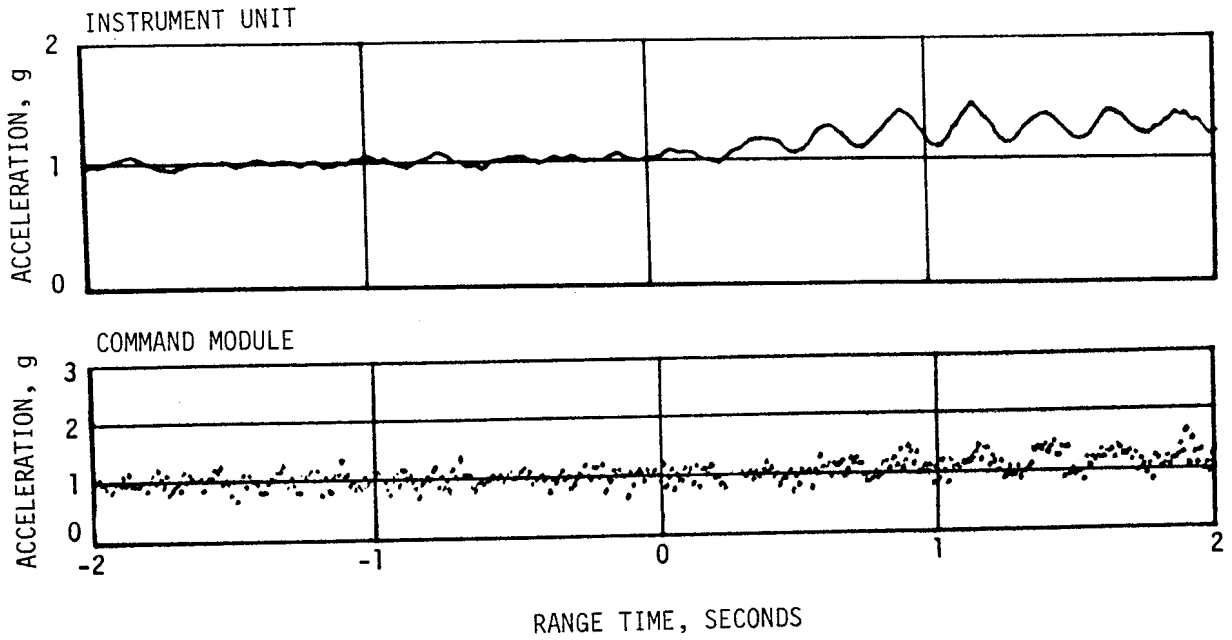


Figure 8-1. Longitudinal Acceleration at CM and IU During Thrust Buildup and Launch

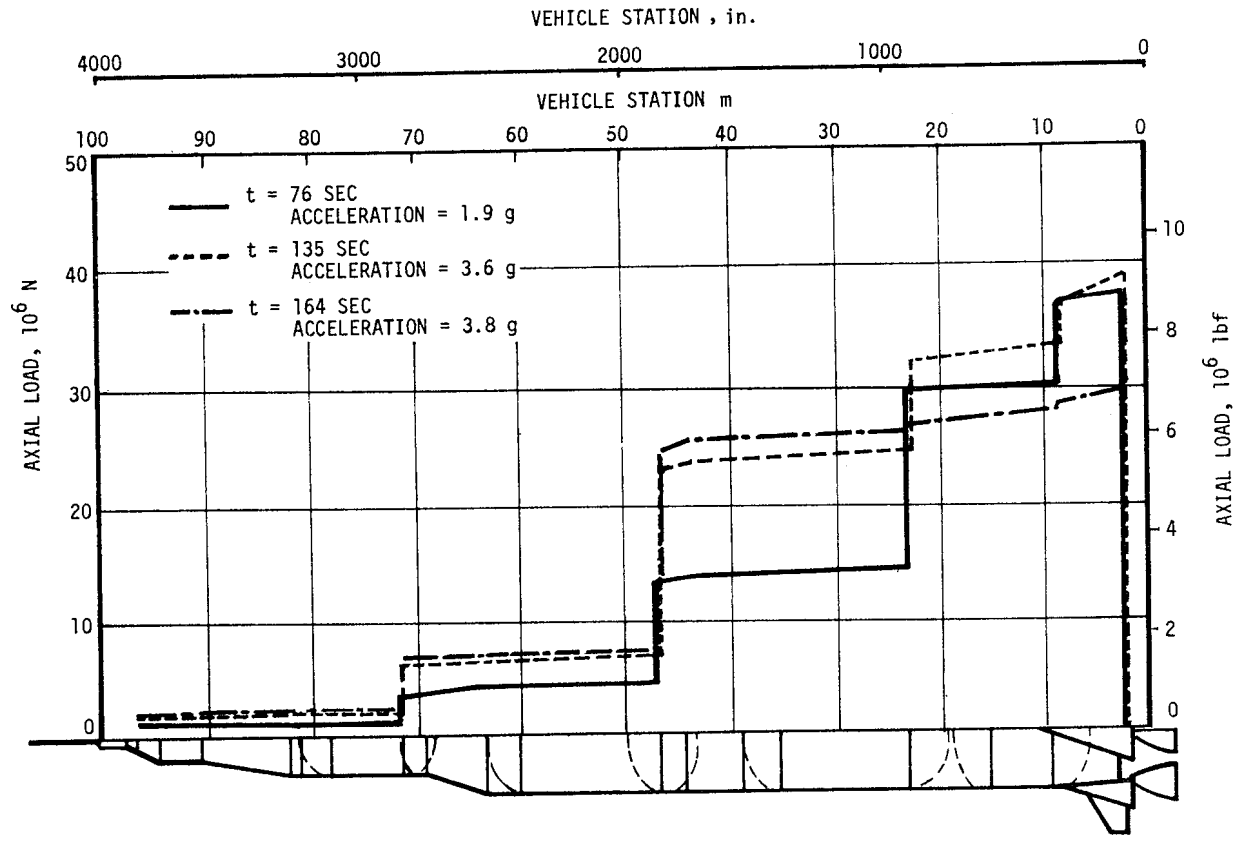


Figure 8-2. Longitudinal Load at Time of Maximum Bending Moment, CECO and OECO

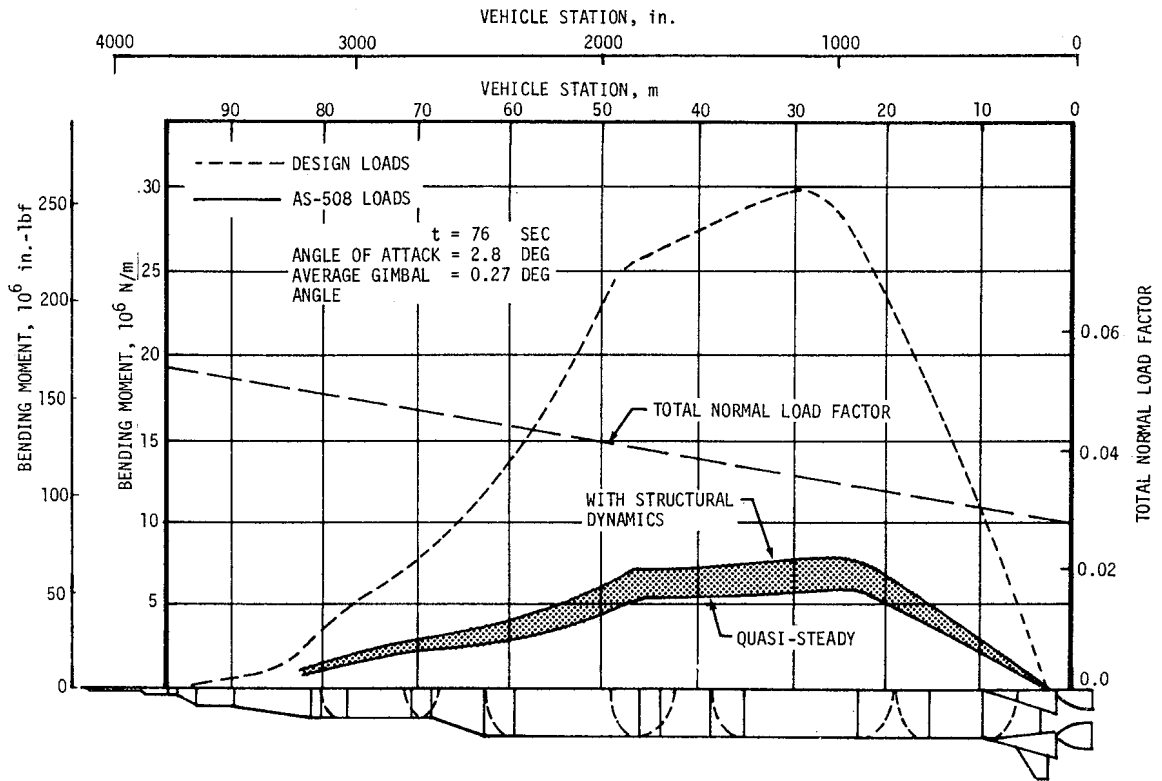


Figure 8-3. Maximum Bending Moment Near Max Q

This is appreciably less than the peak amplitude of ± 0.07 g measured on AS-507. Spectral analysis of chamber pressure measurements show no detectable buildup of structural/propulsion coupled oscillations. POGO did not occur during S-IC boost.

The AS-508 S-IC CECO and OECO transient responses shown in Figure 8-5 were similar to those of previous flights. The maximum dynamics at the IU resulting from CECO was ± 0.20 g. At OECO a maximum dynamic longitudinal acceleration of ± 0.28 g and ± 0.85 g was measured at the IU and CM, respectively.

AS-508 experienced low frequency (14 to 16 hertz) POGO oscillations during S-II stage boost. Three distinct periods of structural/propulsion coupled oscillations exhibited peaks at 180, 250, and 330 seconds. The third period of oscillations resulted in LOX pump discharge pressure variations of sufficient magnitude to activate the center engine thrust OK pressure switches and shut down the engine 132 seconds early. All oscillations decayed to a normal level following CECO.

Analysis shows that the vibration environment observed on AS-508 was similar to AS-507 during S-II stage burn prior to 327 seconds, see Figures 8-6 and 8-7. The oscillations are also apparent in the propulsion parameters as shown in Figures 8-8 and 8-9.

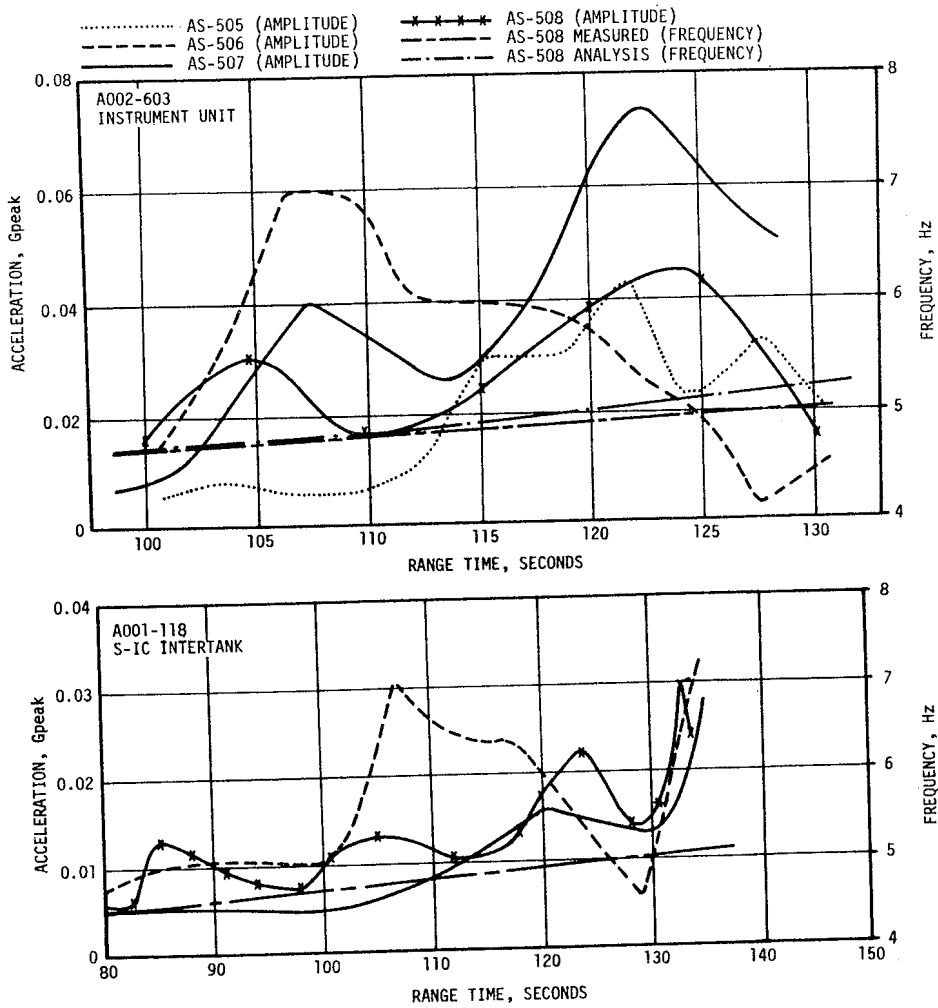


Figure 8-4. Comparison of Longitudinal Responses During S-IC Boost

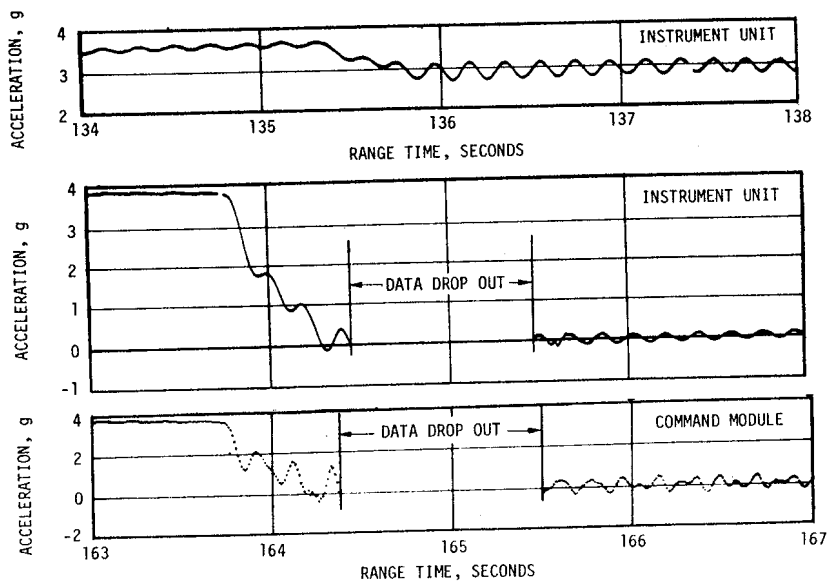


Figure 8-5. Longitudinal Acceleration at CM and IU at S-IC CECO and OECO

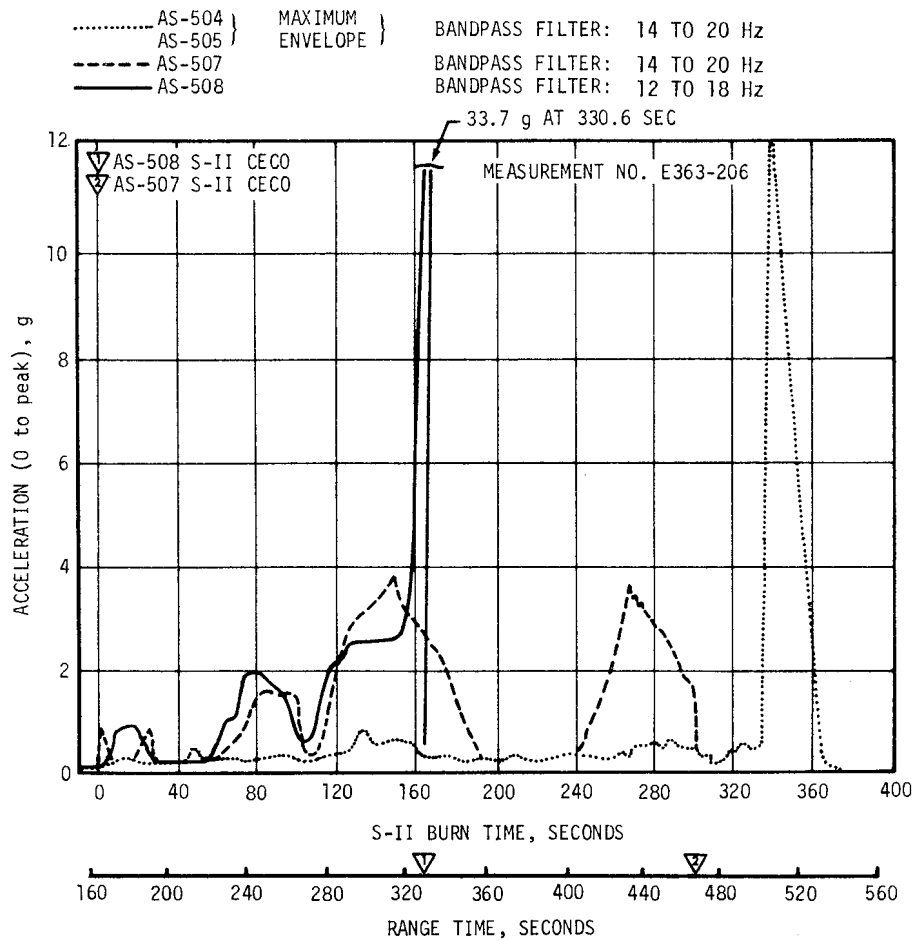


Figure 8-6. Comparison of S-II Engine No. 5 Thrust Pad Acceleration With Previous Flights

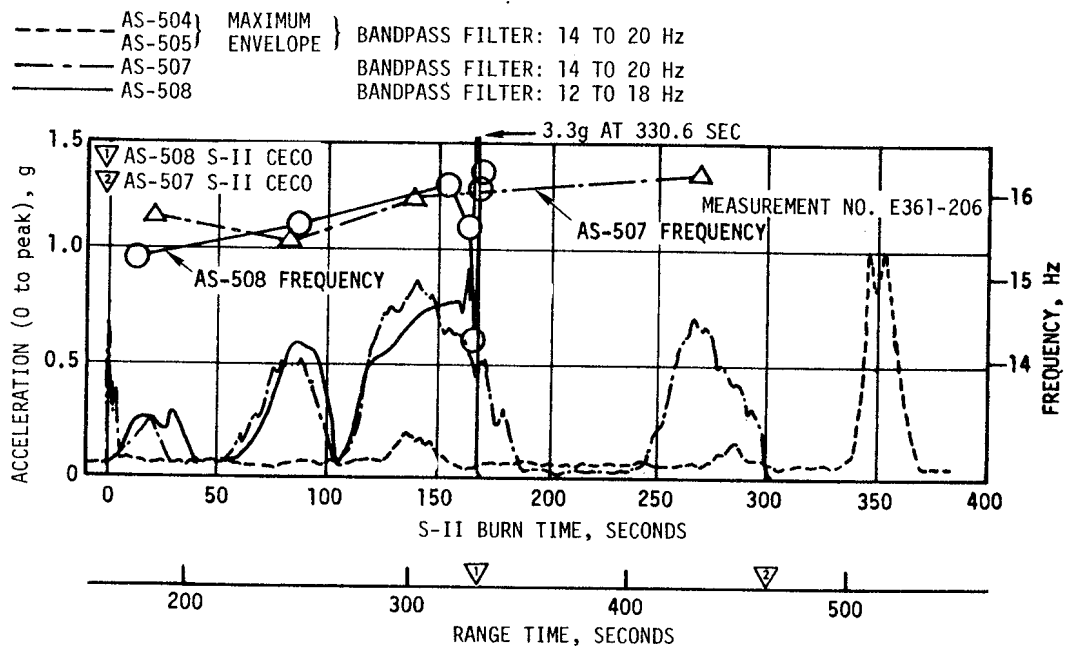


Figure 8-7. Comparison of S-II Engine No. 1 Thrust Pad Acceleration With Previous Flights

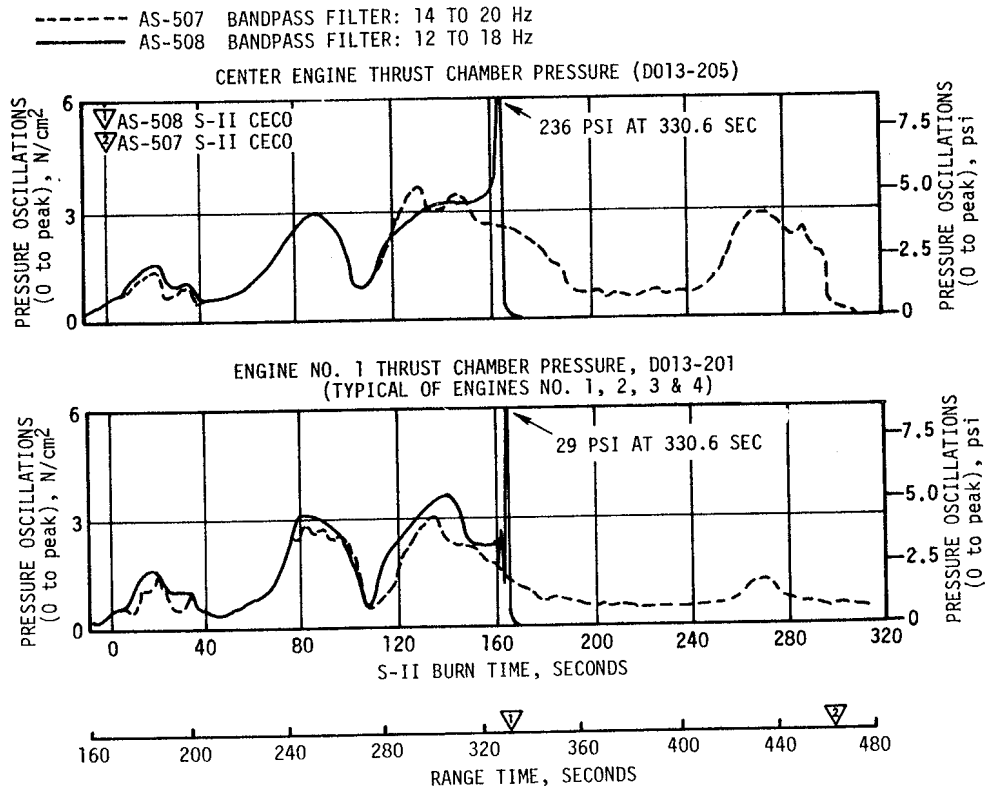


Figure 8-8. S-II Pre-CECO Thrust Chamber Pressure Characteristics

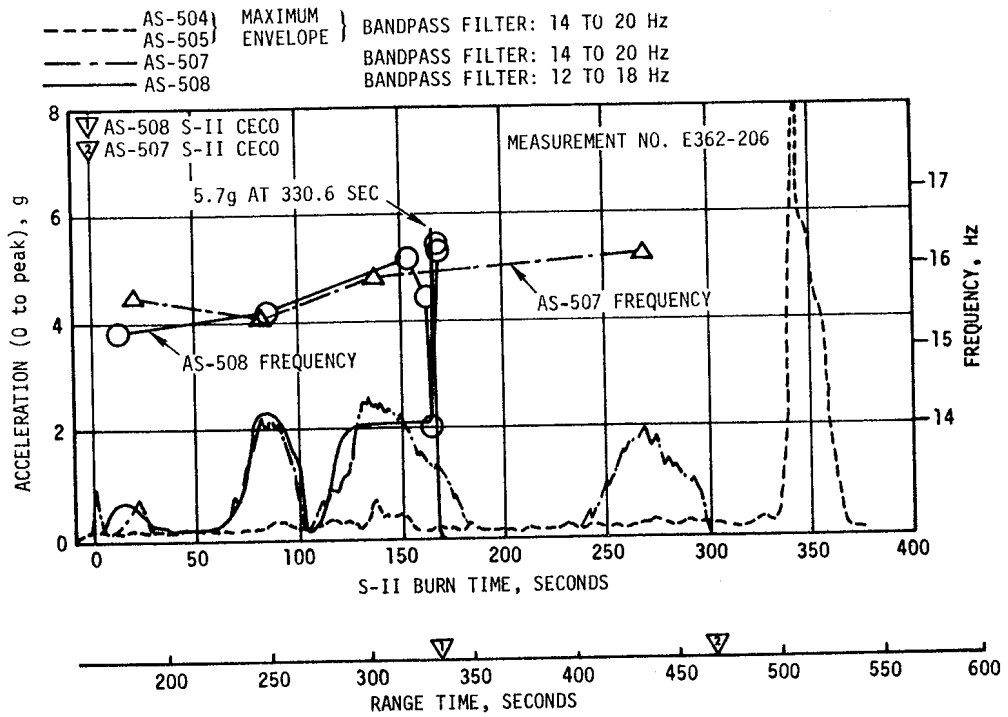


Figure 8-9. Comparison of S-II LOX Sump Acceleration With Previous Flights